DE LA RECHERCHE À L'INDUSTRIE

Magnetic Resonance Image Reconstruction

Philippe Ciuciu
Philippe.ciuciu@cea.fr

IEEE MIC Educational Course

October 31th - November 1st, 2016

Strasbourg, France

www.cea.fr

MRI: A WIDE RANGE OF APPLICATIONS

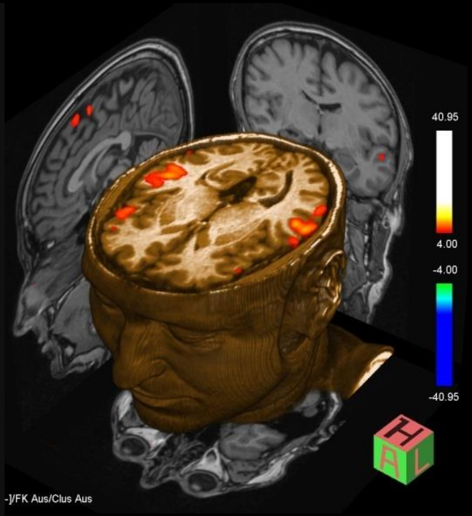

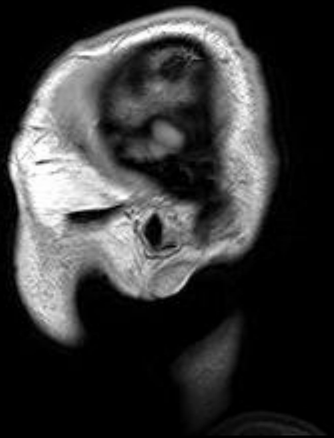

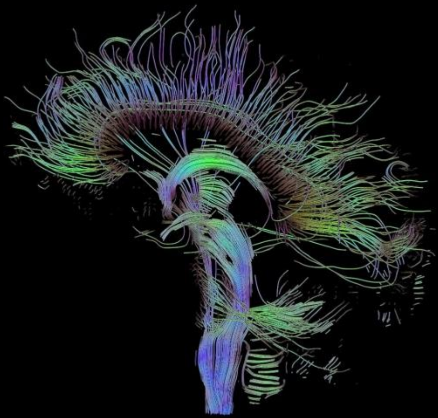

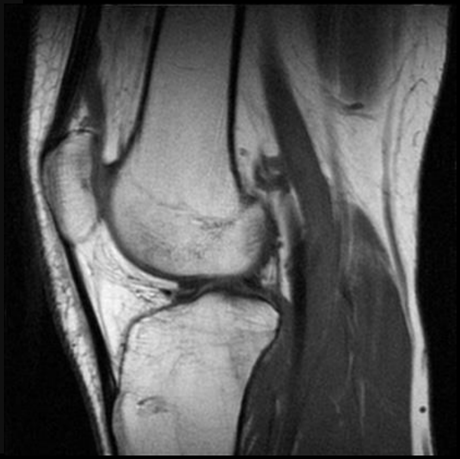

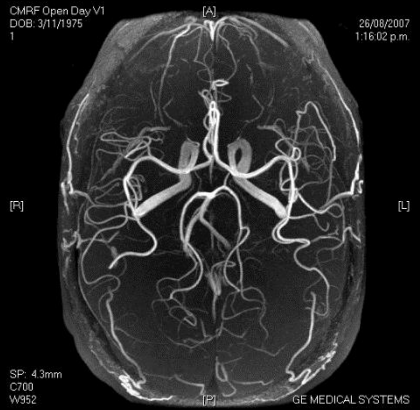

ADVANTAGES OF MAGNETIC RESONANCE IMAGING

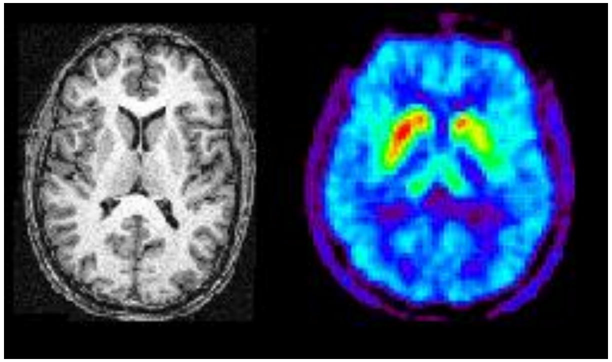

MRI 1 mm PET 5 mm

	X ray CT	SPECT	PET	**MRI**	US	optics
Origin of contrast	Tissue density	biochemical (perfusion)	Biochemical (metabolism)	**Proton density +relaxation times +diffusion coefficients +...**	Speed of sound +density	Light absorption /emission
Spatial Resolution	0.5 to 1 mm	~ 10 mm	2.5 to 5 mm	**< 1 mm**	~1 mm	< 1 µm
Imaging depth	Not limited	Not limited	Not limited	**Not limited**	a few cm	a few mm

INTRODUCTION: HISTORICAL PERSPECTIVE

- 1973: Lauterbur: first MRI image of tubes in an NMR spectrometer
- 1981: First commercial scanners < 0.2T
- 1985: 1.5T MRI
- 1990: first functional MRI (Ogawa) & first diffusion tensor MRI (Moseley)
- 1998: 8T magnet at Ohio State University
- 2004: 9.4T human magnet at Chicago
- 2010: 17T small bore MRI for rodents at NeuroSpin/CEA, France
- **Expected 02/2017**: 11.7 T at NeuroSpin/CEA, France

1977 : First image in Humans (Mansfield et al. Br. J. Radio.)

Nobel prize in Medecine 2003

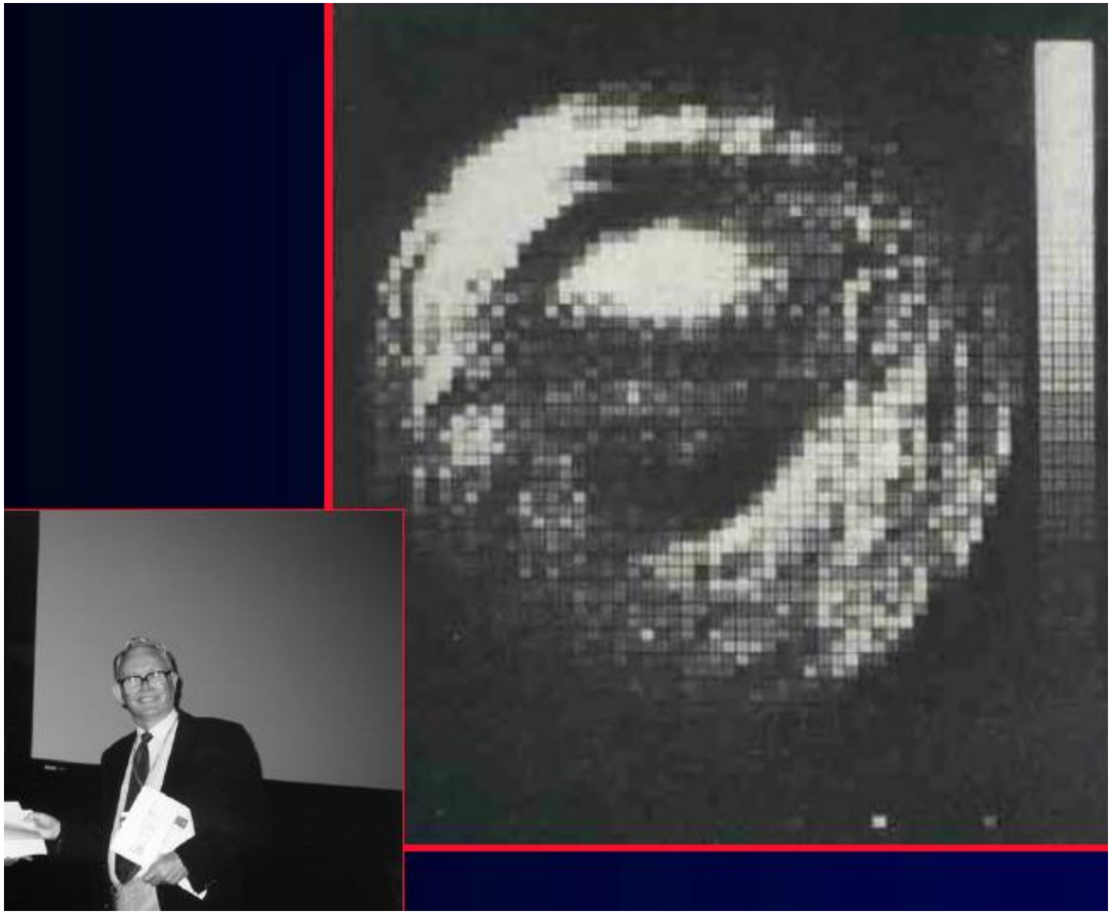

1983 : First images at 1.5T (General Electric)

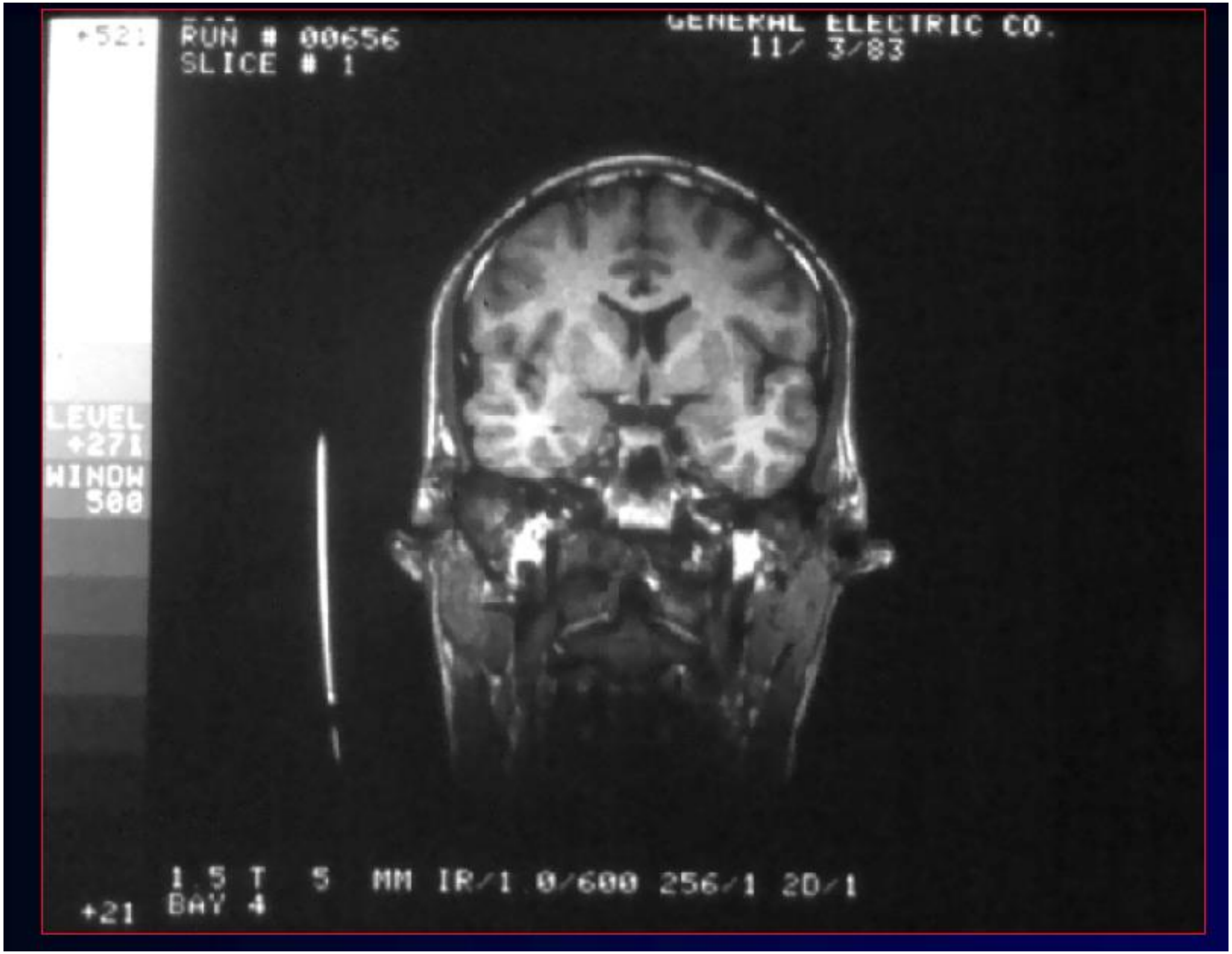

OUTLINE

- Part I: Background in MRI [OPTIONAL]
- Part II: Non-Cartesian MRI reconstruction
- Part III: Iterative model-based reconstruction
- Part IV: Parallel (multi-channel) imaging & reconstruction
- Part V: Compressed Sensing

Part I: Background in Magnetic Resonance Imaging

- MRI scanner
- Sampling k-space & Cartesian reconstruction
- Trajectories and acquisition strategies
- Image reconstruction strategies

DESCRIPTION OF AN MRI SCANNER

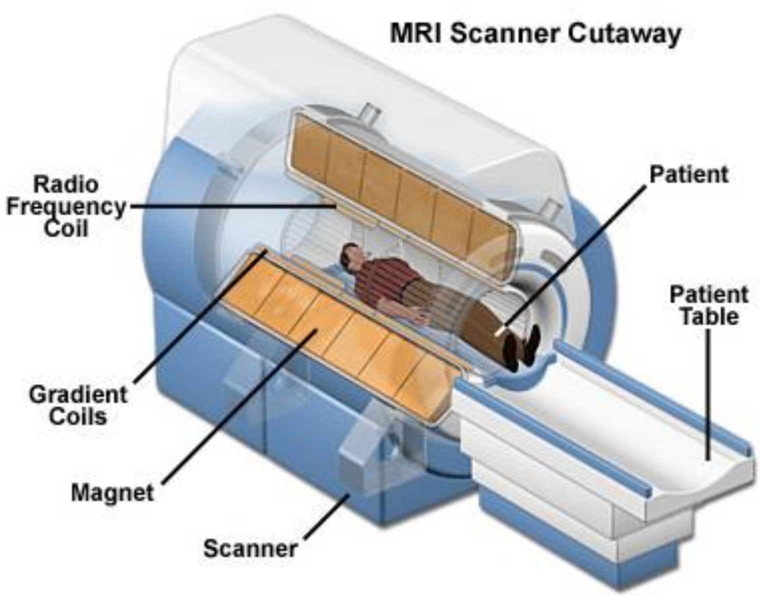

- **A superconductor electro-magnet**

⇒ Create macroscopic magnetization from magnetic moments of spins of certain atomic nuclei

Static B_0: Magnet 1.5T, 3T or 7T (superconductor in liquid Helium)

- **A transmit-receive radiofrequency system (RF coil)**

⇒ Flip the magnetization and record their relaxation to equilibrium state

125 MHz at 3T, 300 MHz at 7T

- **3 gradient coils to add variable magnetic fields along X, Y and Z directions**

⇒ Encode space to localize the signal in 3D

(10 to 80 mT/m)

HOW THE THREE MAGNETIC FIELDS INTERACT

- Primary magnetic field (B_0). Align the spins in the z-direction
- Tip the global magnetization into the transverse (x,y) plane using a RF pulse at Larmor frequency $\omega_0 = \gamma B_0$.
- Release the RF pulse and measure transverse relaxation.
- Gradient magnets. Localize the MR signal.

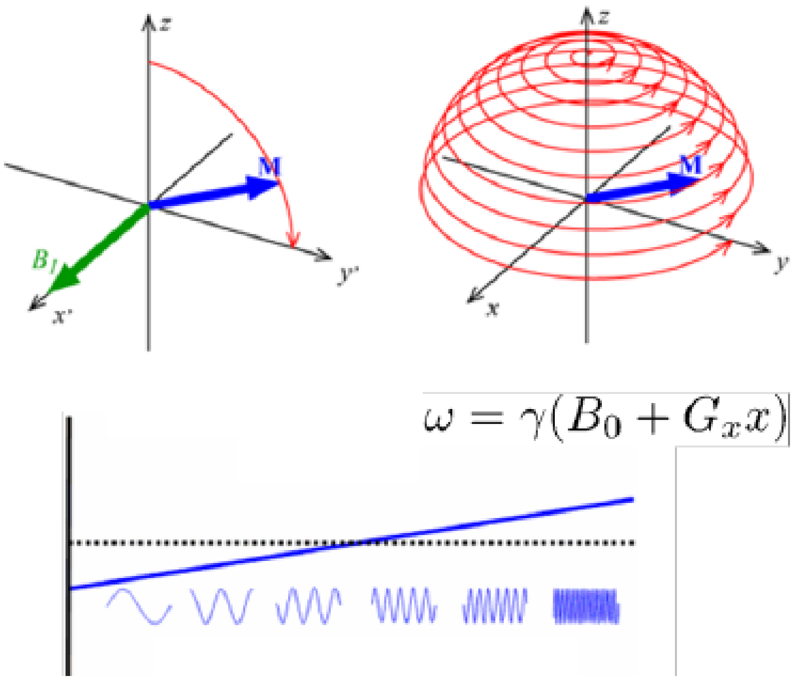

OUTLINE

OPTIONAL SECTION DEPENDING ON THE AUDIENCE

Part I: Background in Magnetic Resonance Imaging

- MRI scanner
- Sampling k-space & Cartesian reconstruction
- Trajectories and acquisition strategies
- Image reconstruction strategies

SAMPLING K-SPACE

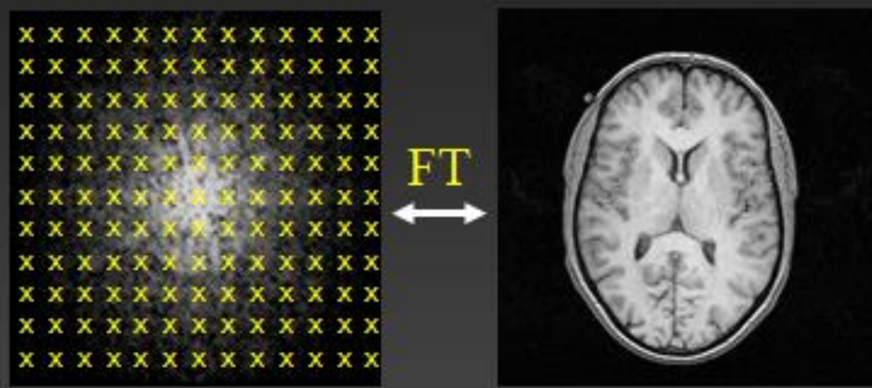

Perfect reconstruction of an object would require measurement of *all* locations in *k*-space (infinite!)

Data is acquired point-by-point in *k*-space (sampling)

SAMPLING K-SPACE

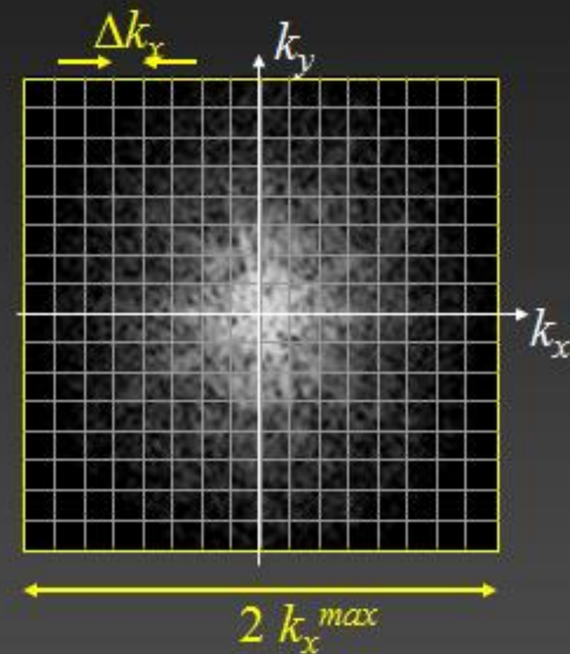

1. What is the highest frequency we need to sample in k-space (k^{max})?
2. How close should the samples be in k-space (Δk)?

FREQUENCY SPECTRUM

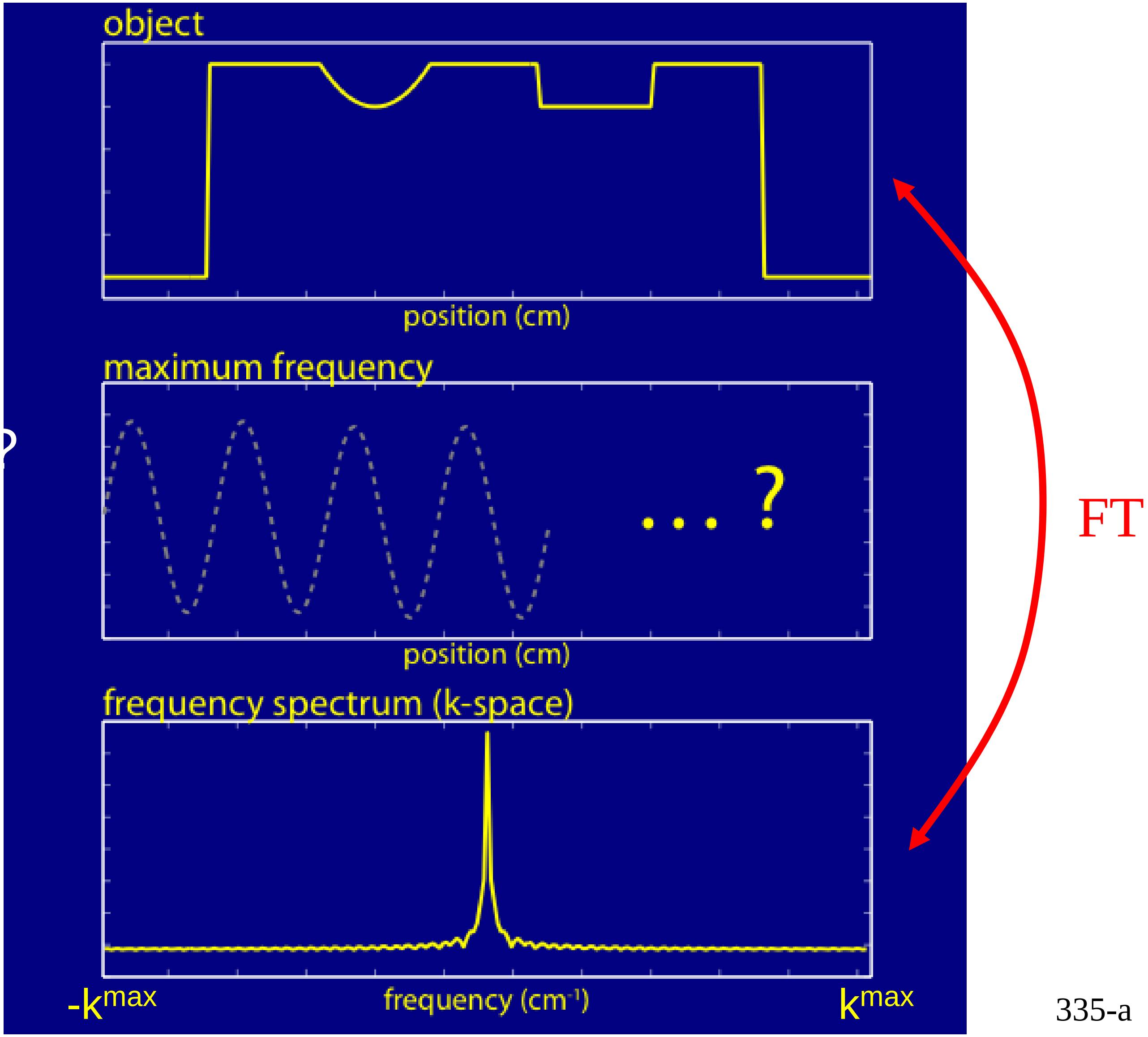

FREQUENCY SPECTRUM

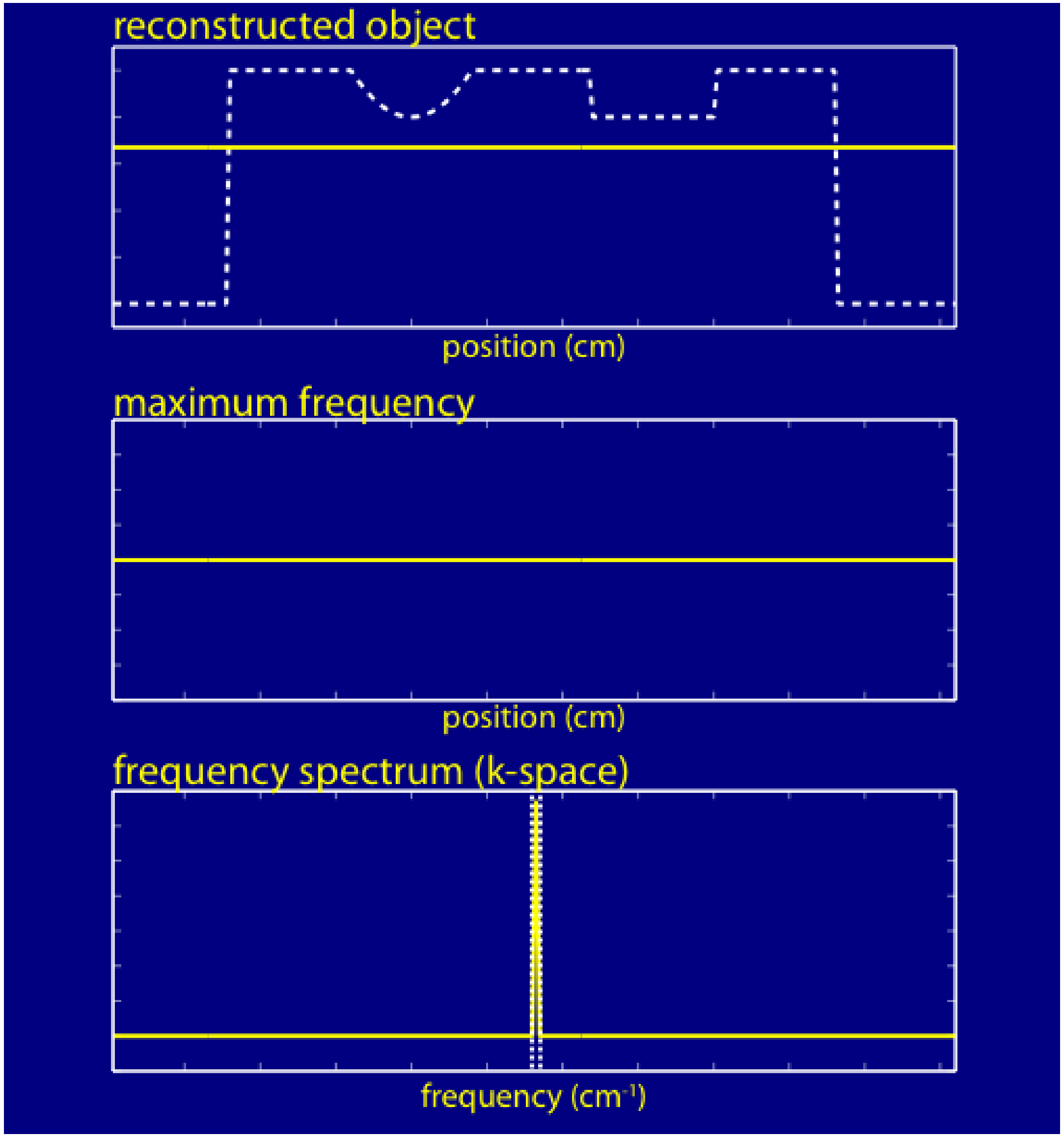

FREQUENCY SPECTRUM

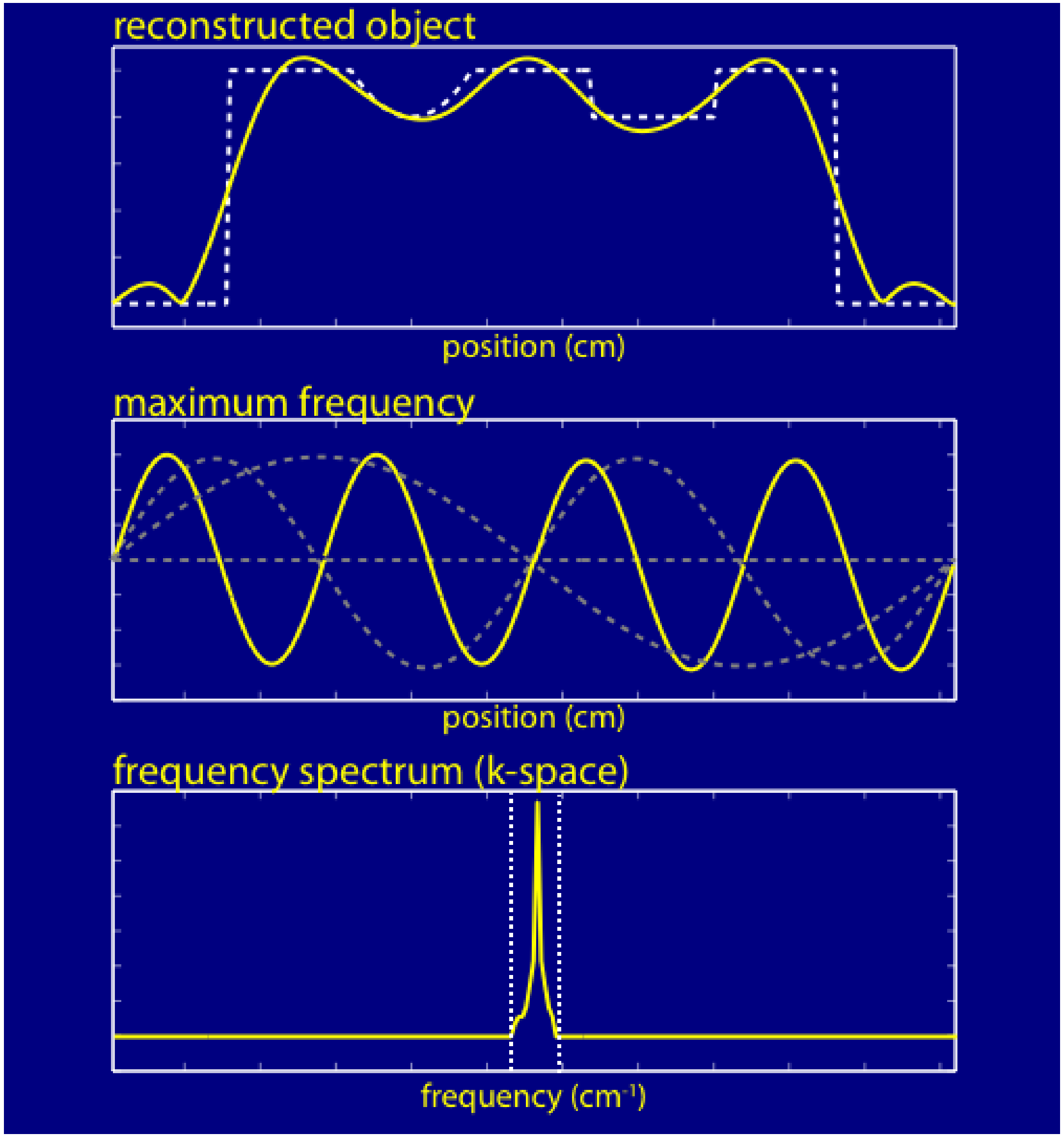

FREQUENCY SPECTRUM

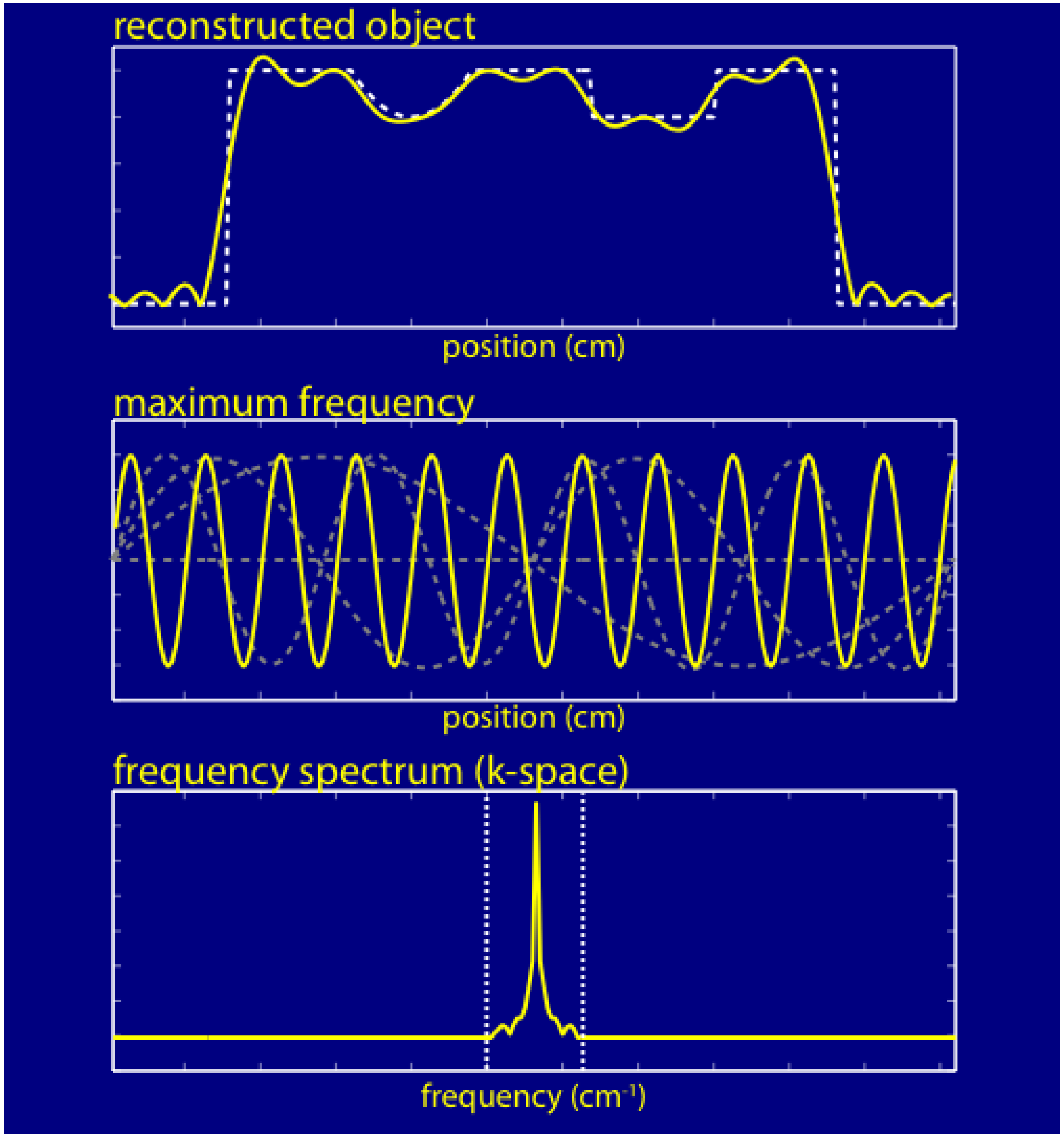

FREQUENCY SPECTRUM

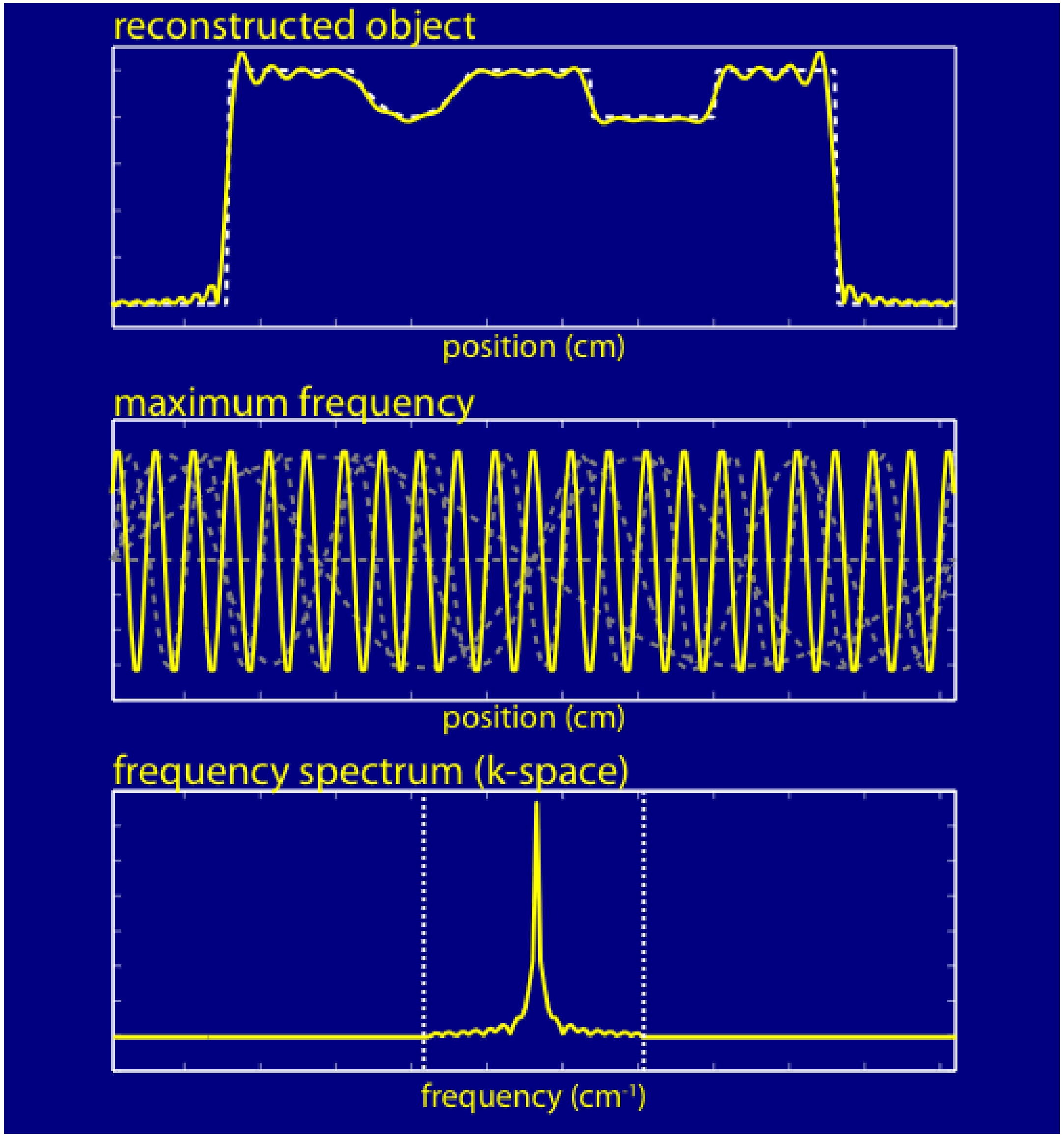

FREQUENCY SPECTRUM

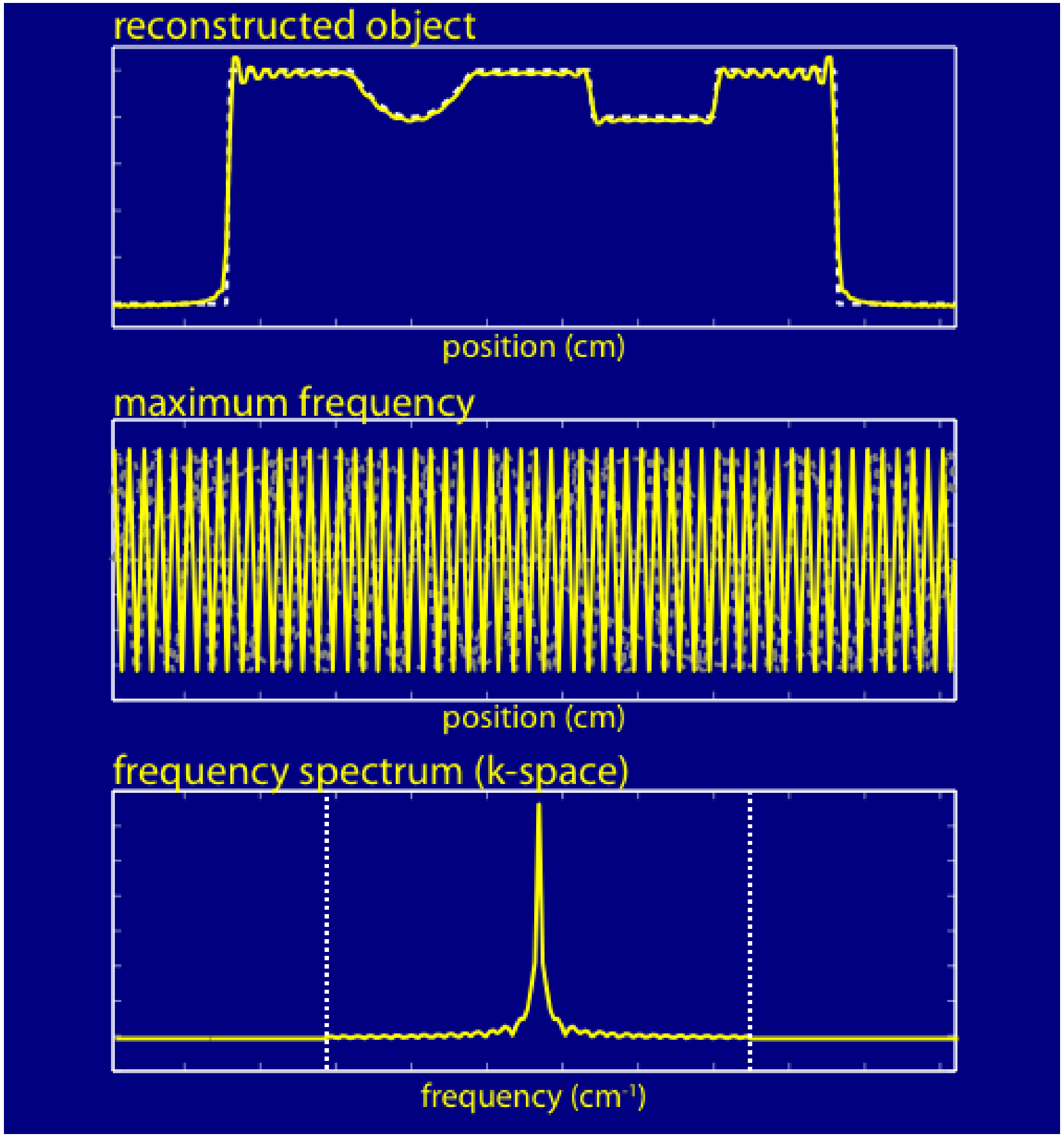

FREQUENCY SPECTRUM

Higher frequencies make the reconstruction look more like the original object!

Large k^{max} increases resolution (allows us to distinguish smaller features)

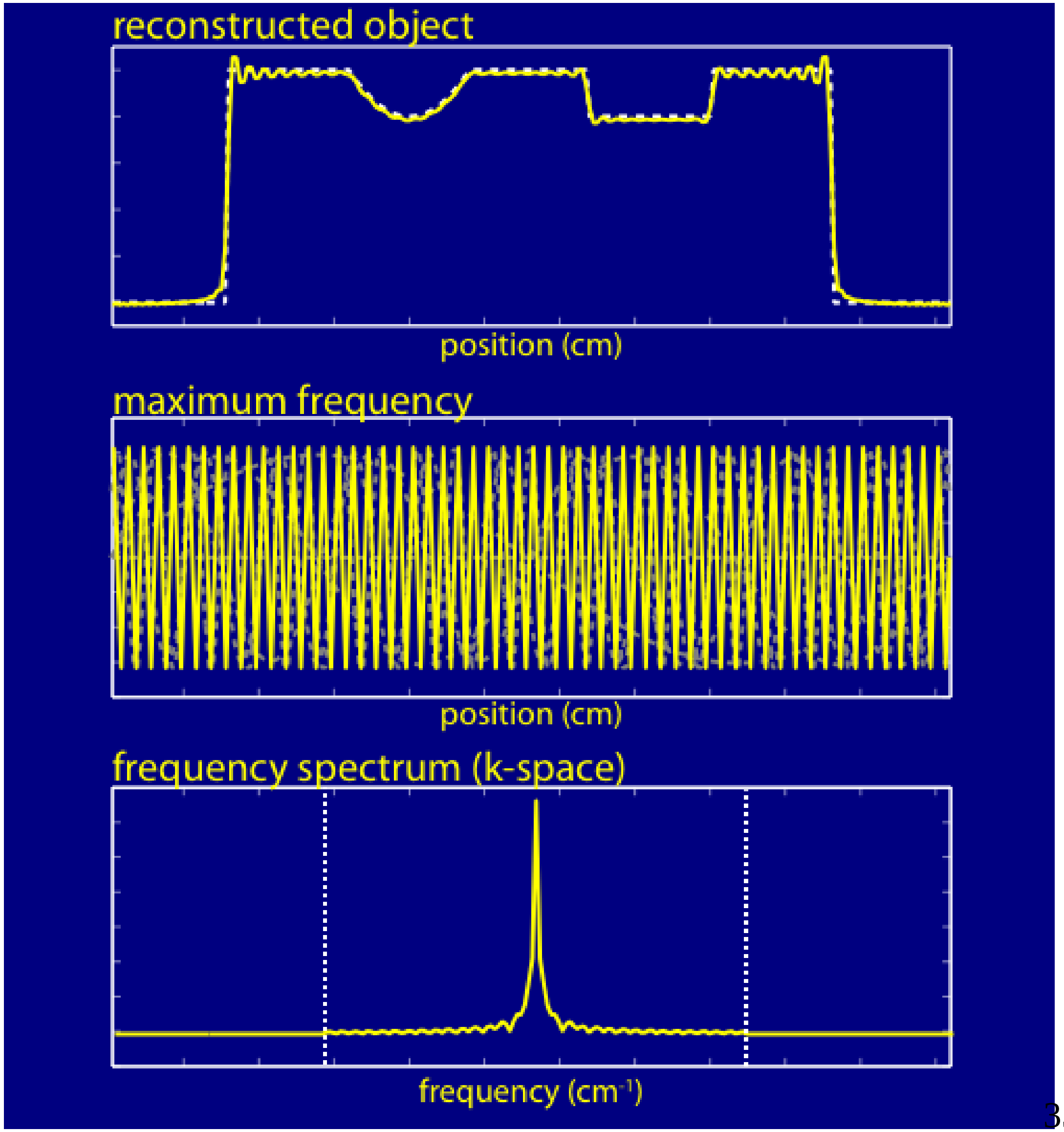

CHOOSING MAXIMAL FREQUENCY

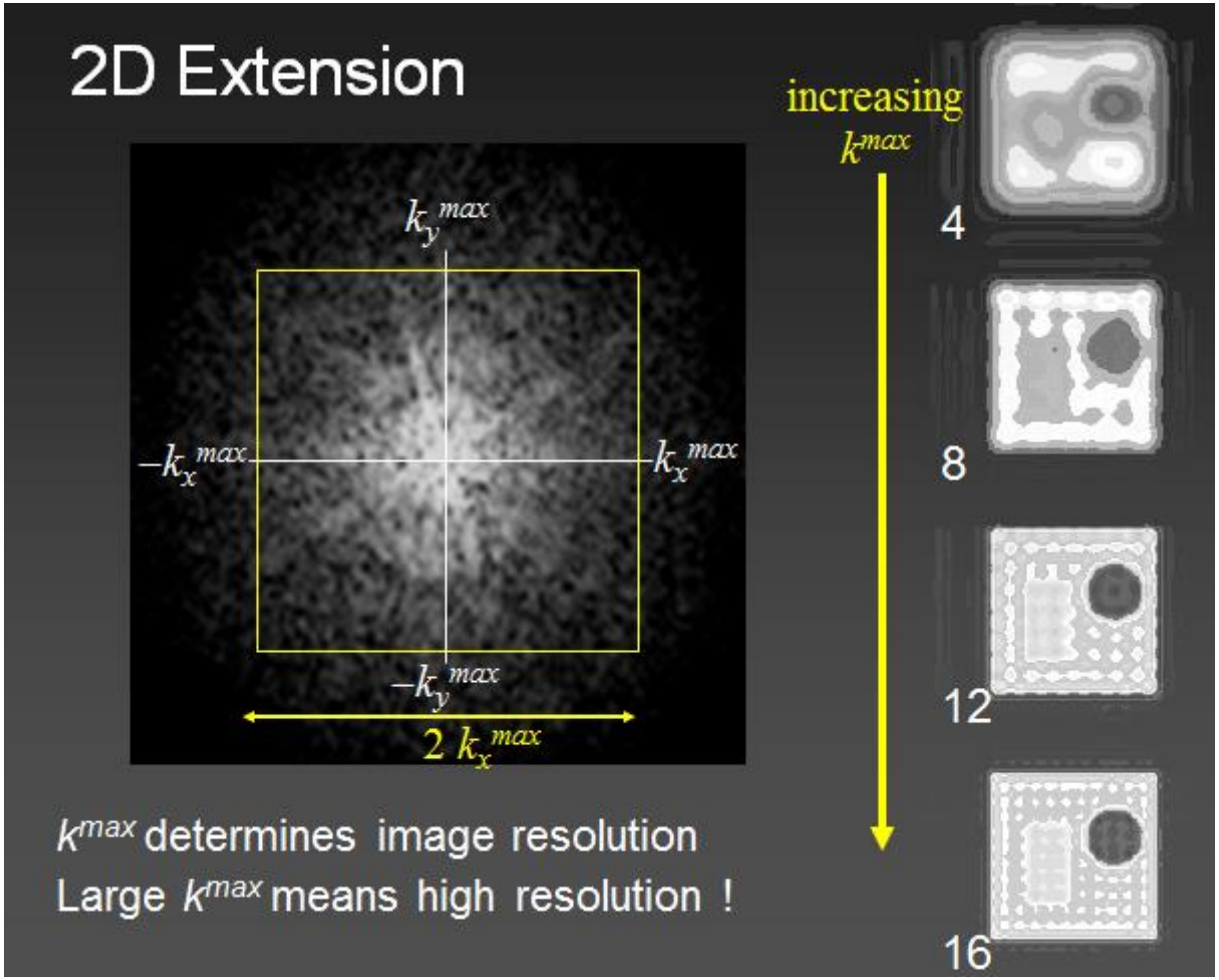

NYQUIST SAMPLING THEOREM

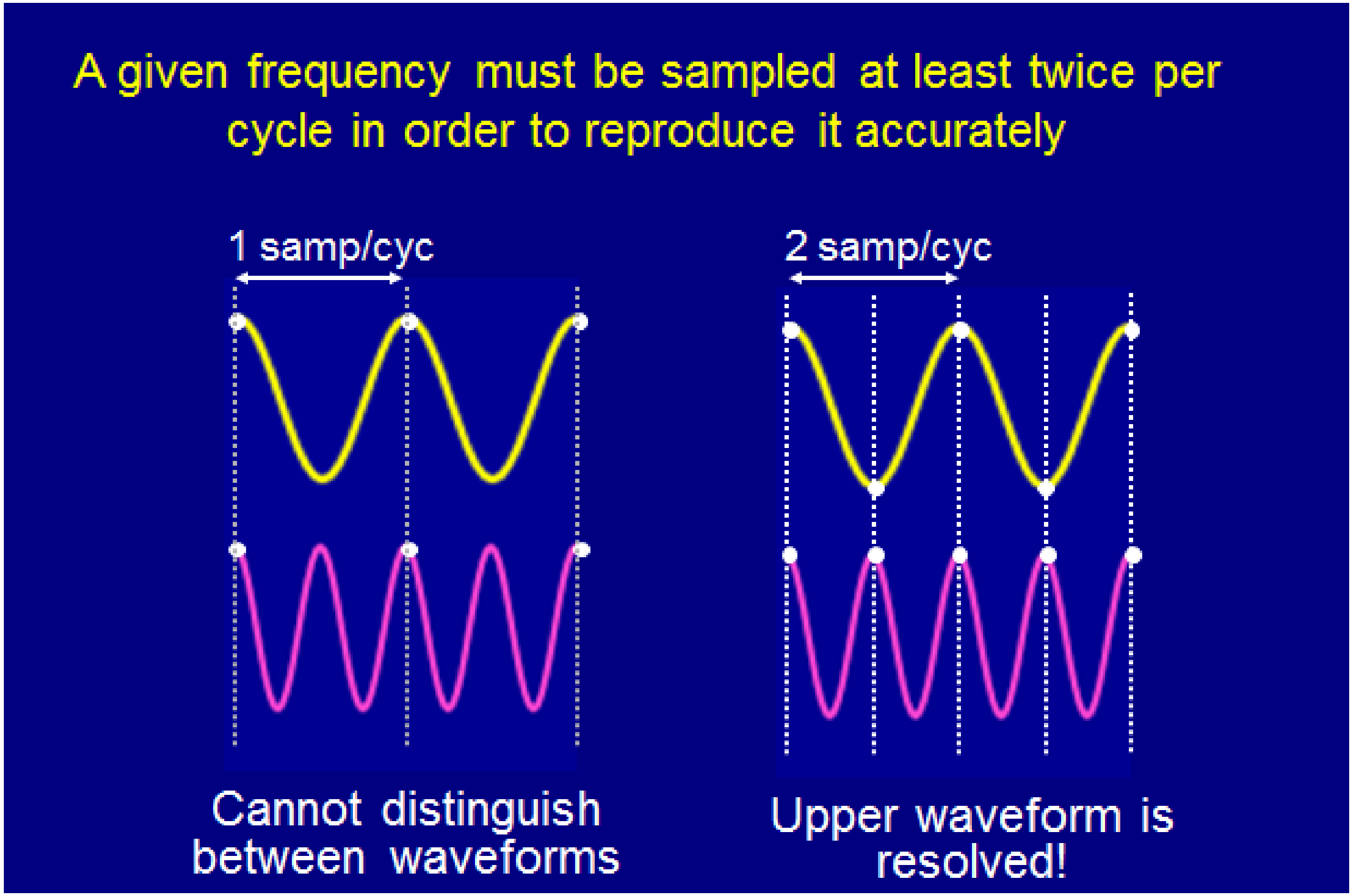

NYQUIST SAMPLING THEOREM

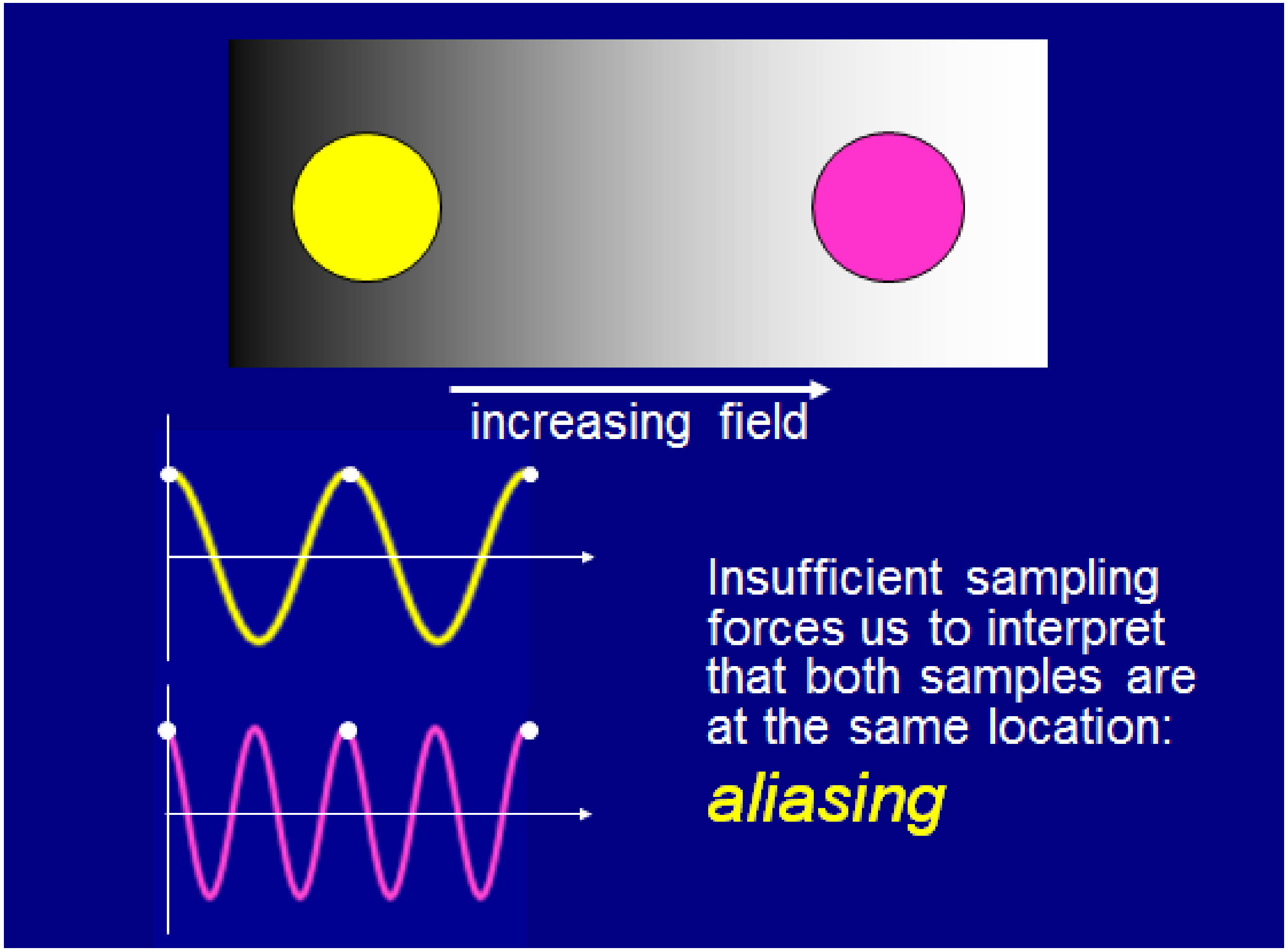

ALIASING ARTIFACT

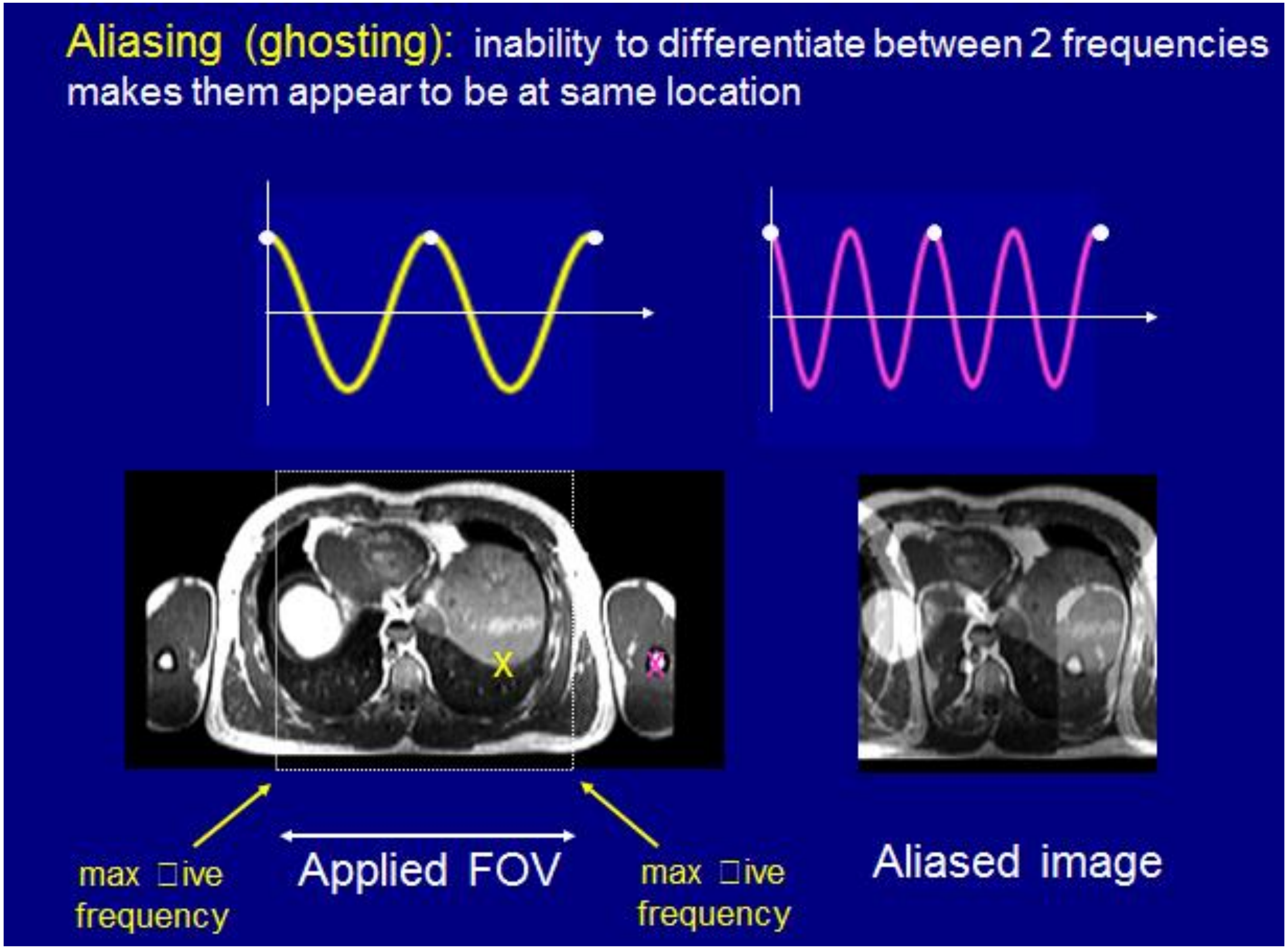

K-SPACE RELATIONS: FOV & RESOLUTION

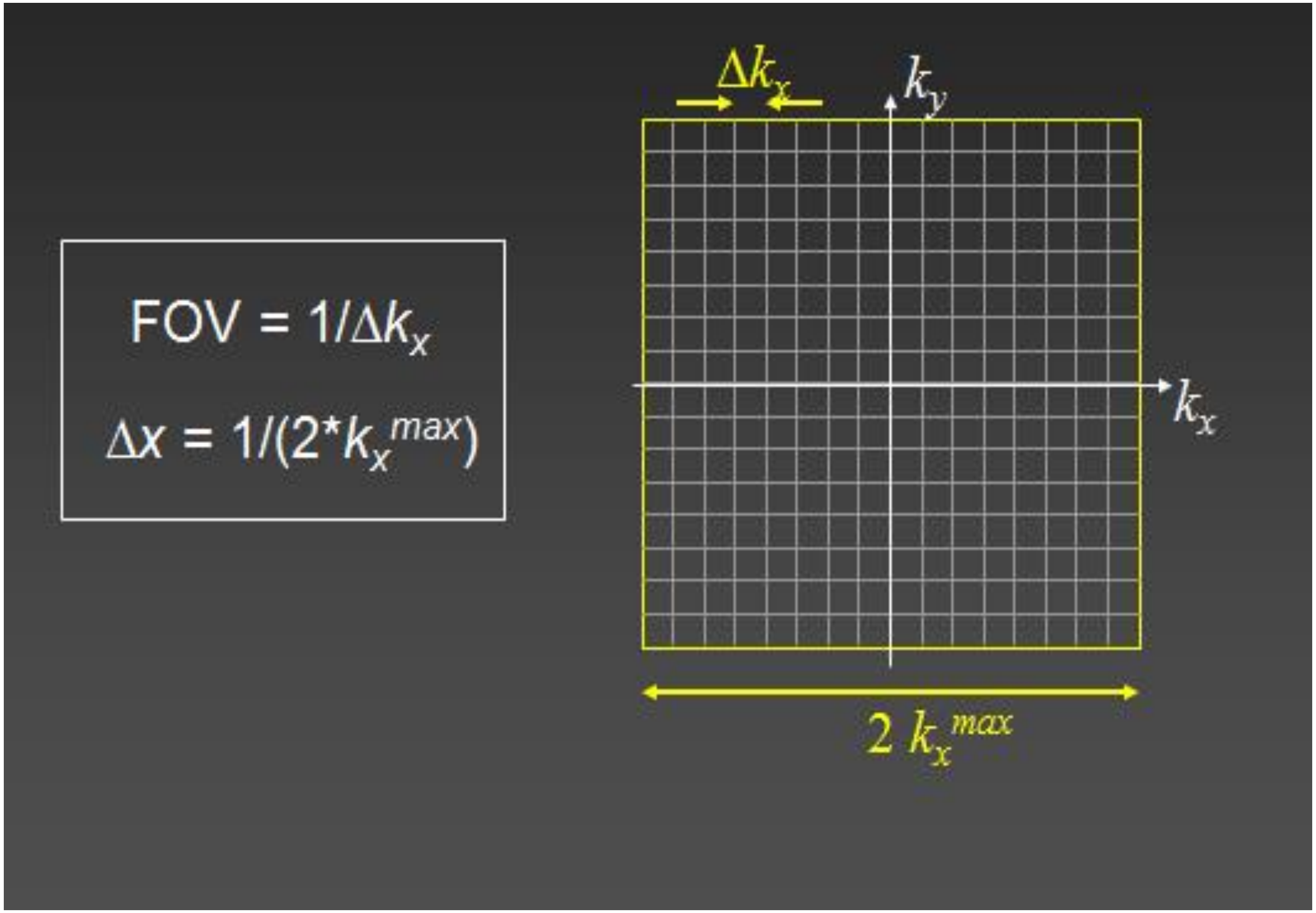

K-SPACE RELATIONS: FOV & RESOLUTION

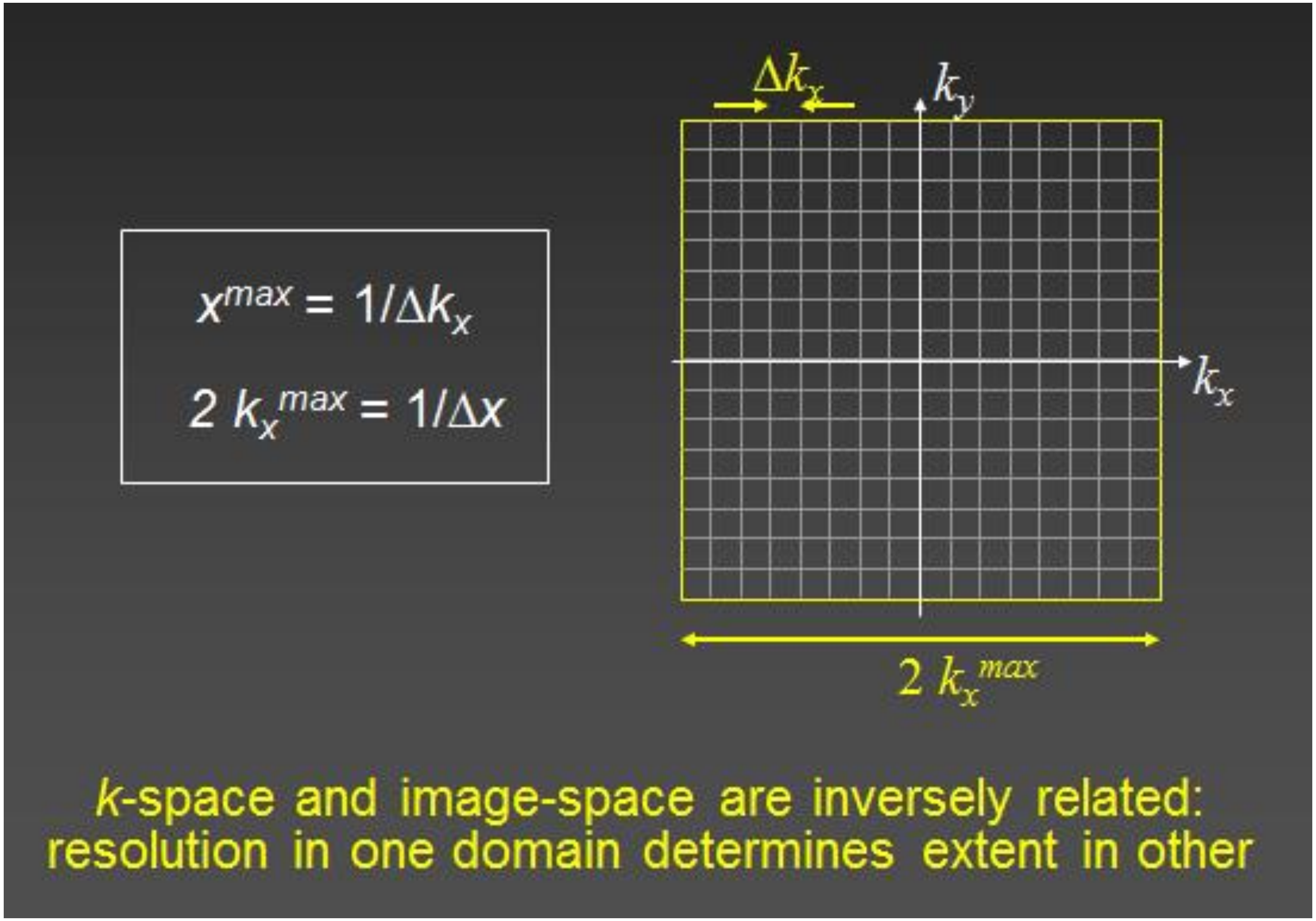

STANDARD MR IMAGE RECONSTRUCTION

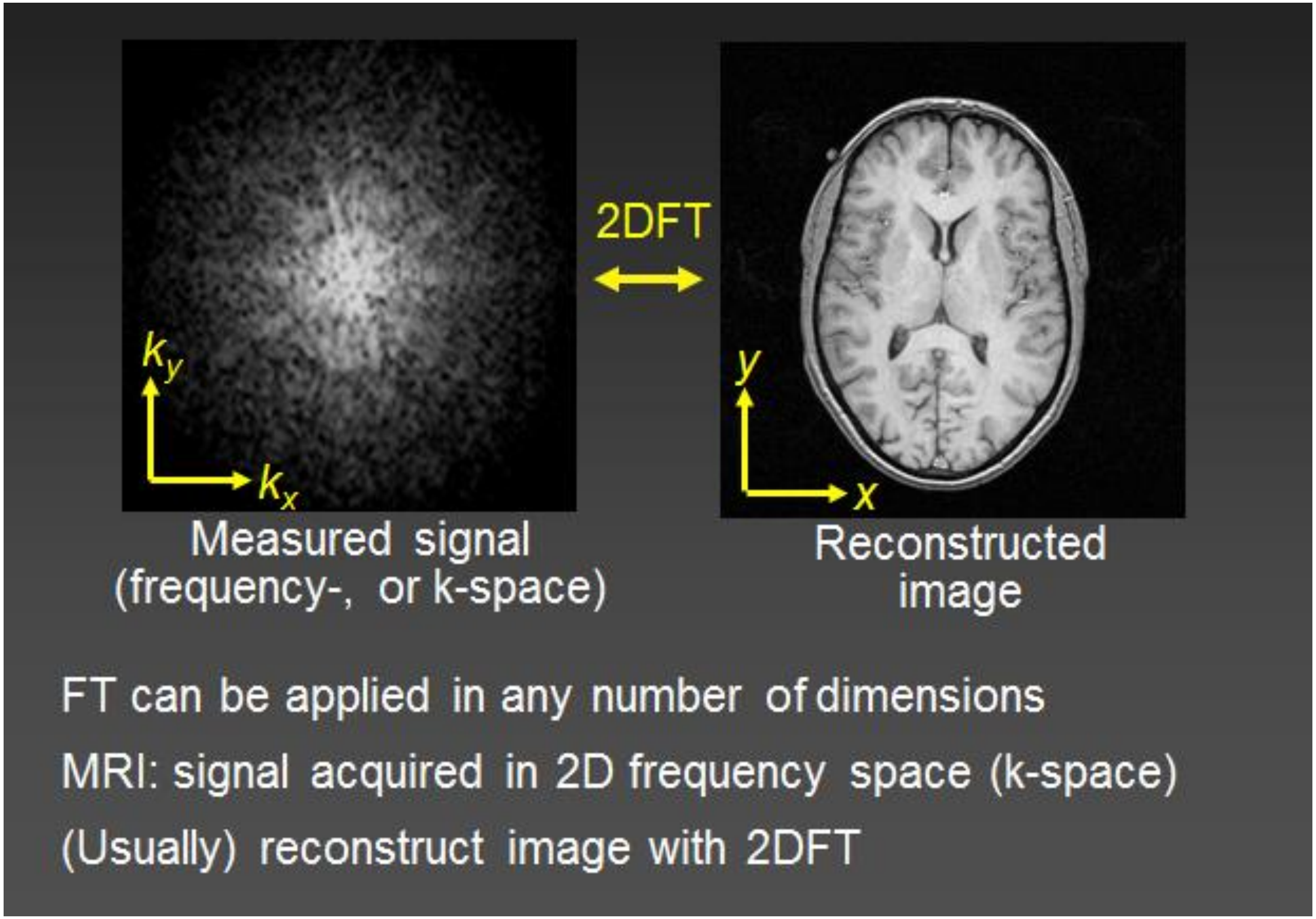

PARTIAL FOURIER

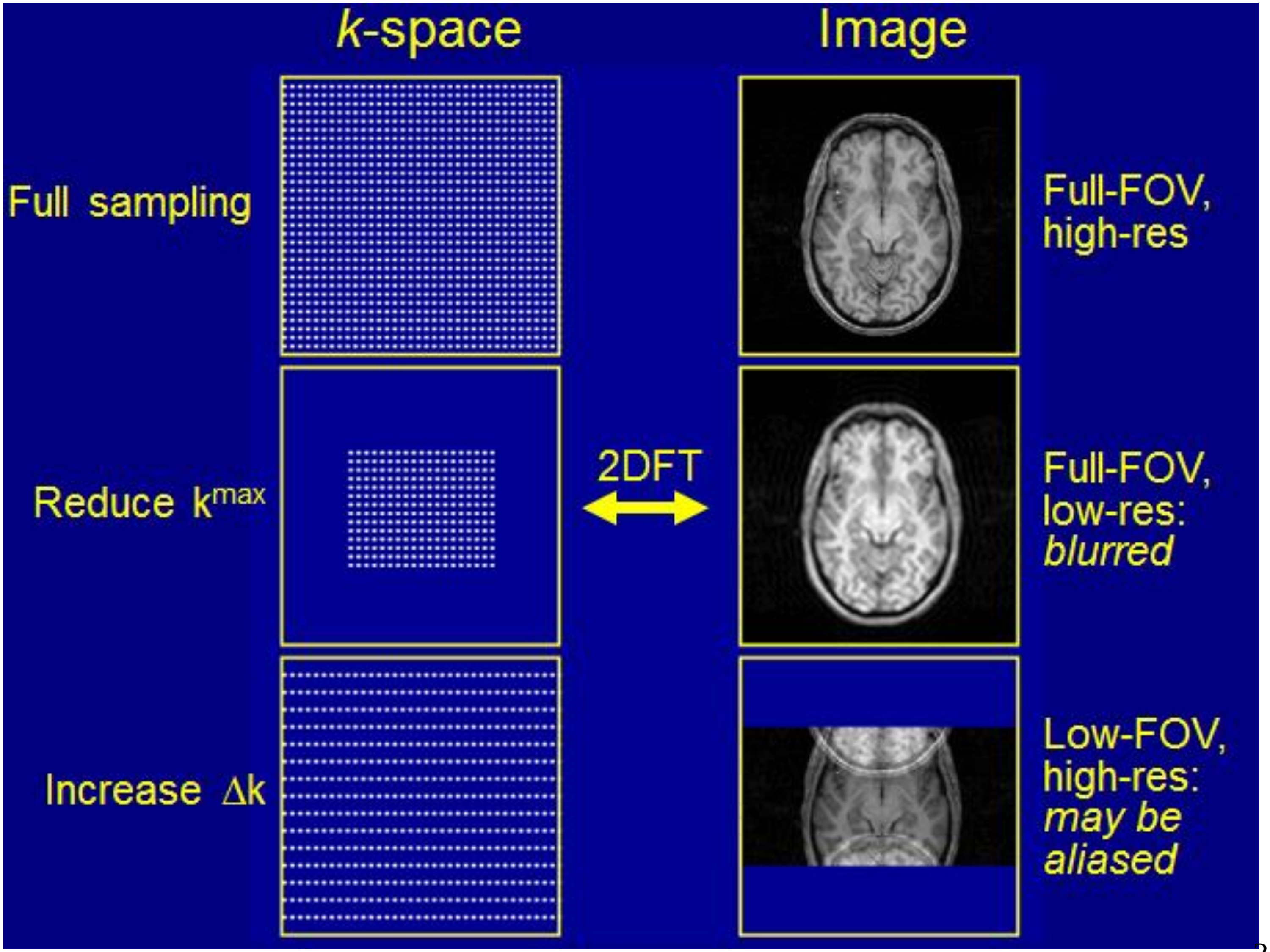

OUTLINE

Part I: Background in Magnetic Resonance Imaging

- MRI scanner
- Sampling k-space & Cartesian reconstruction
- Trajectories and acquisition strategies
- Image reconstruction strategies

K-SPACE TRAJECTORY MODELING

Mathematical modelling:

Let $\vec{\kappa} : [0, T] \rightarrow \mathbb{R}^d$, $(d = 2, 3)$ denote the sampling curve. We have:

$$\vec{\kappa}(t) = \vec{\kappa}(0) + \gamma \int_0^t \vec{G}(\tau) d\tau$$

$$d = 2, \quad \vec{G} = (G_x, G_y), \; \vec{\kappa} = (k_x, k_y)$$

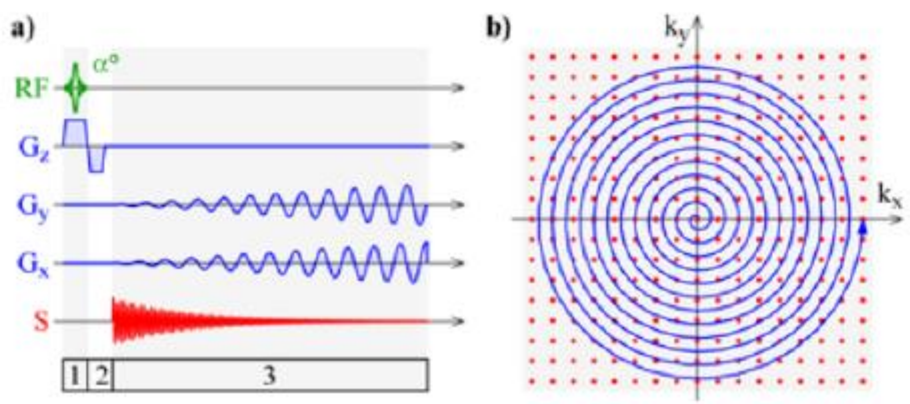

Figure: Spiral imaging: Pulse sequence (Left) and corresponding sampling trajectory (Right).

K-space location is proportional to accumulated area under gradient waveforms

K-SPACE TRAJECTORY CONSTRAINTS

The *gradient encoding* $\vec{G}$ should satisfy: The $\vec{G}$ field is called *gradient encoding*, it should satisfy:

- $\|\vec{G}\|_\infty \leq G_{\text{max}}$: **bounded gradient magnitude**, (eg, 70 mT.m^{-1}).
- $\|\dot{\vec{G}}\|_\infty \leq S_{\text{max}}$: **bounded slew rate**, (eg, 300 T.m^{-1}.s^{-1}).

Admissible sampling curves

An admissible sampling curve in MRI is a curve belonging to the set:

$$\mathcal{S}_{\text{MRI}} = \left\{ \vec{\kappa} \in \left(\mathcal{C}^2([0, T])\right)^d, \|\dot{\vec{\kappa}}\|_\infty \leqslant \alpha = \gamma G_{\text{max}}, \|\ddot{\vec{\kappa}}\|_\infty \leqslant \beta = \gamma S_{\text{max}} \right\}$$

Similar to driving a car on the Fourier plane.

EXAMPLES: RASTER-SCAN 2D DFT ACQUISITION

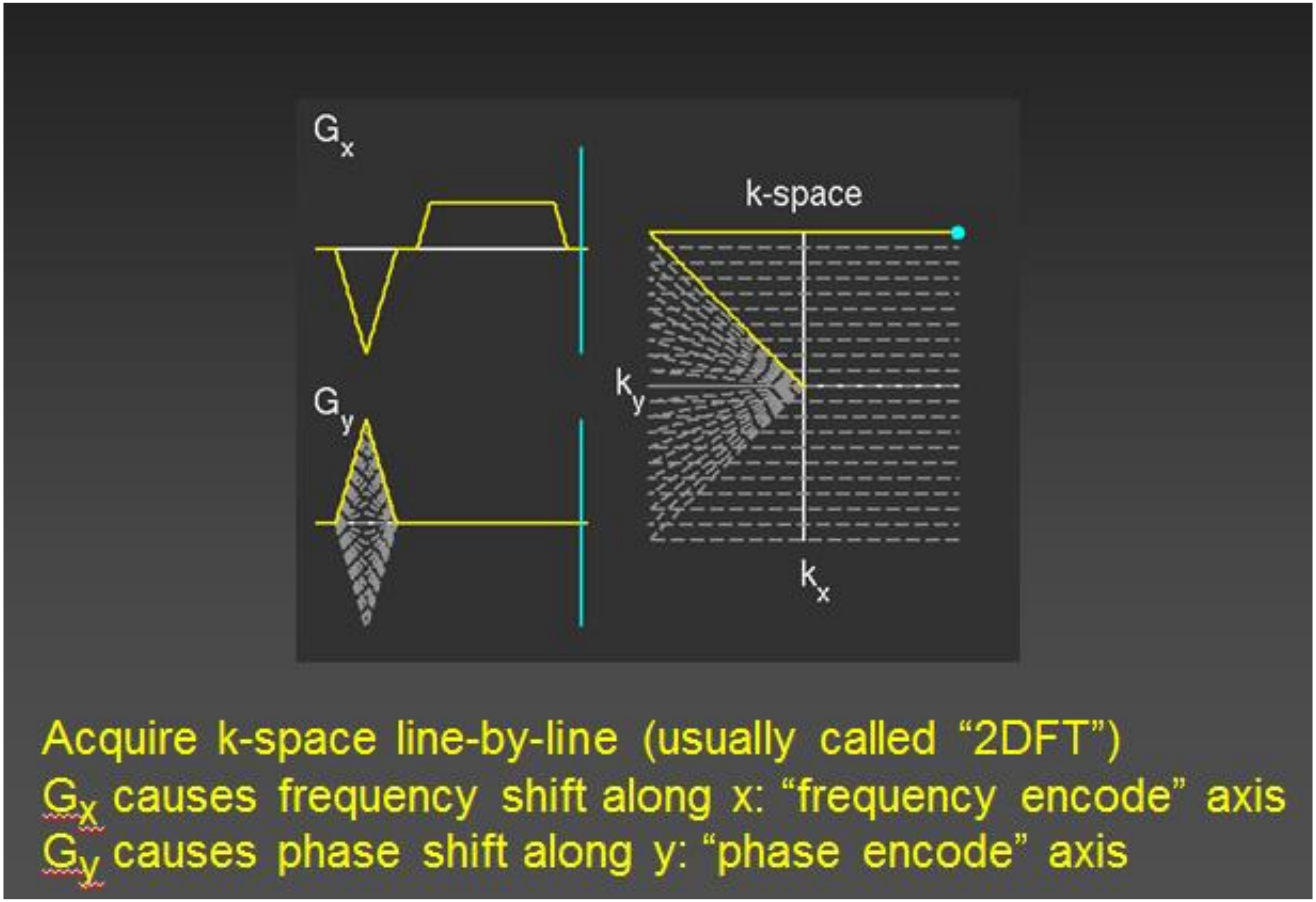

EXAMPLES: ECHO PLANAR IMAGING (EPI) ACQUISITION

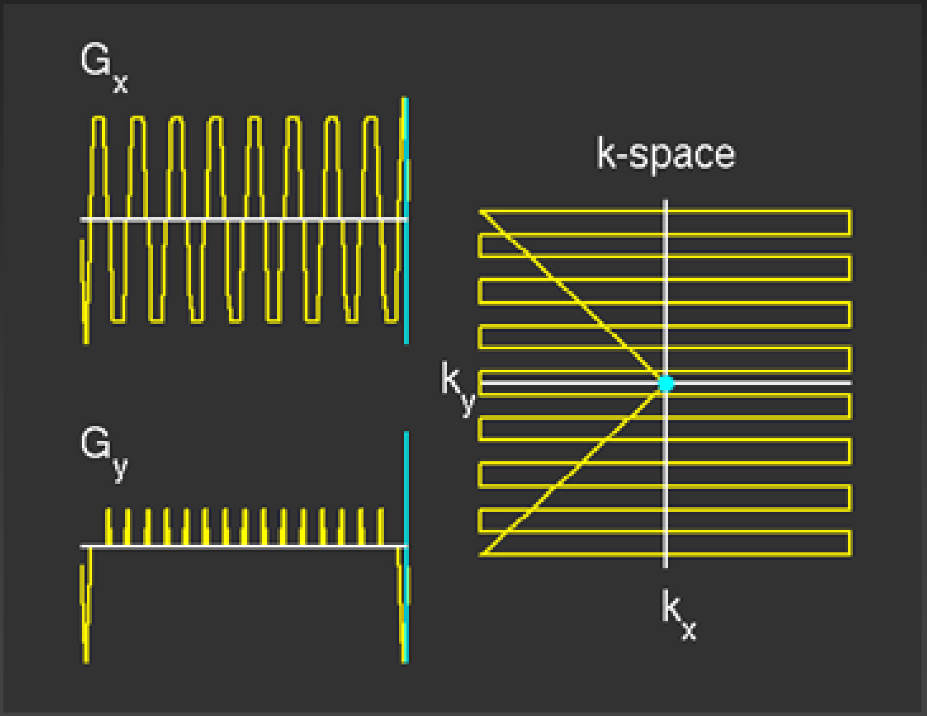

Single-shot (snap-shot): acquire all data at once

IMAGE QUALITY VS. ACQUISITION TIME

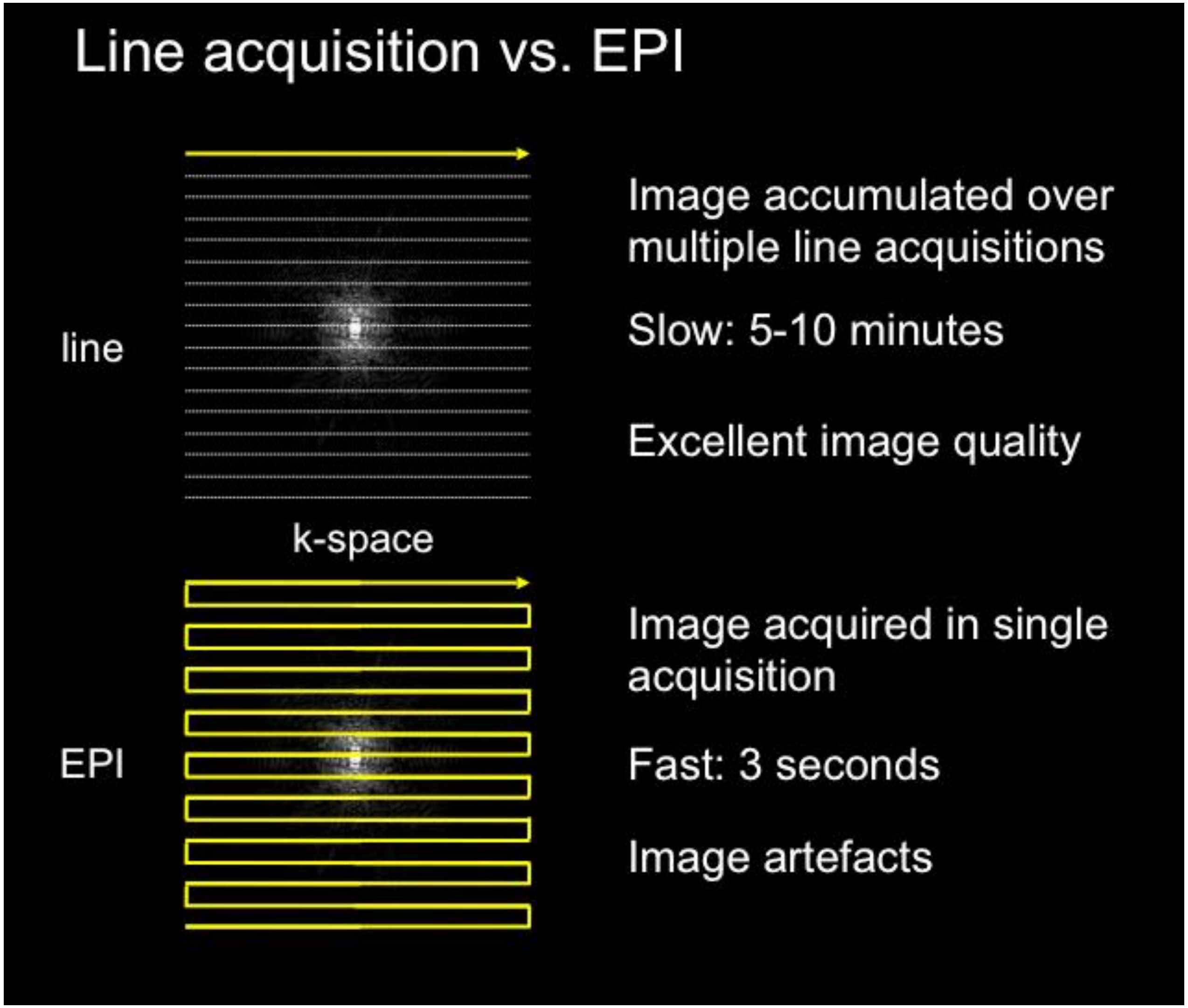

IMAGE QUALITY VS. ACQUISITION TIME

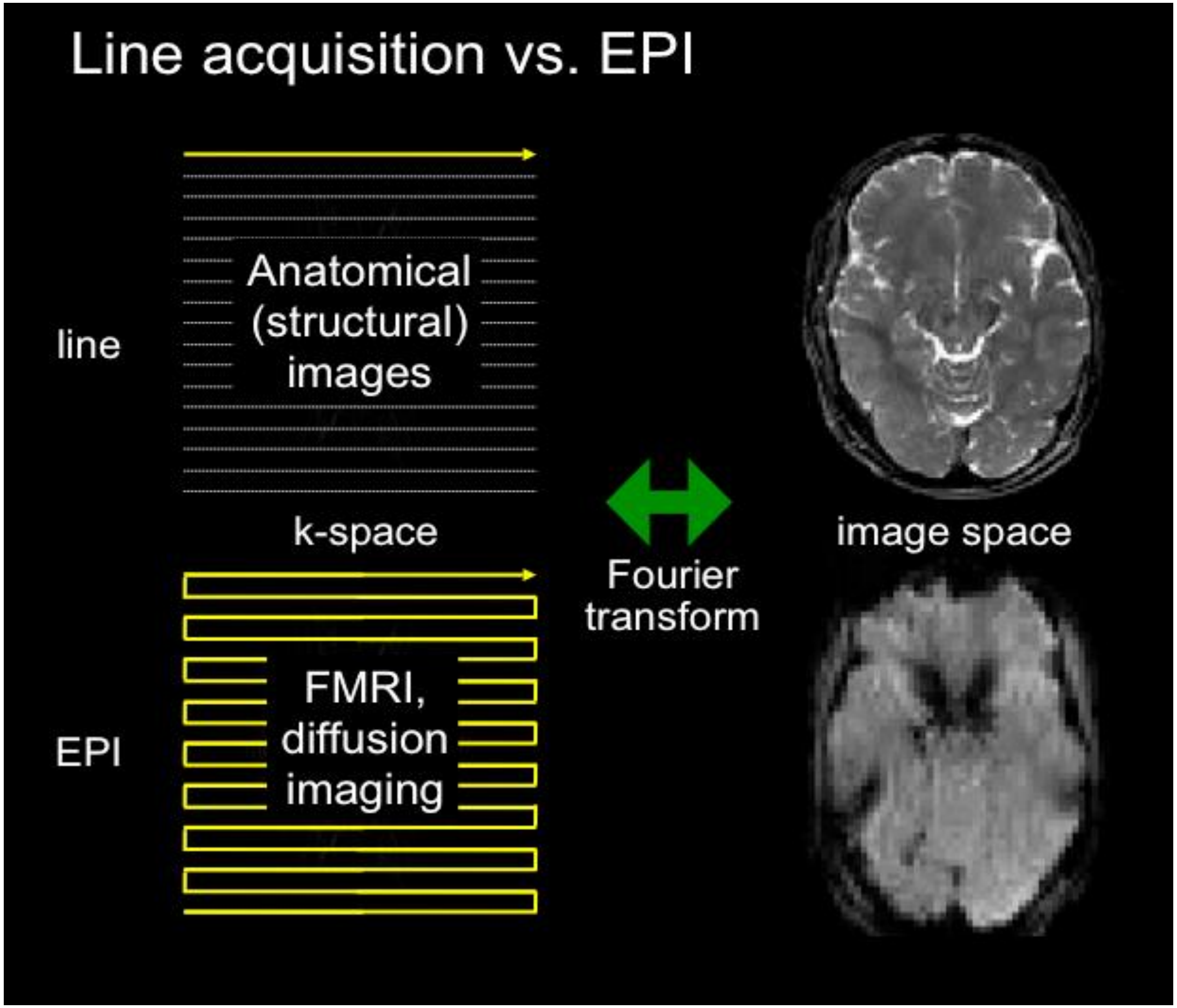

MANY POSSIBLE TRAJECTORIES THROUGH K-SPACE

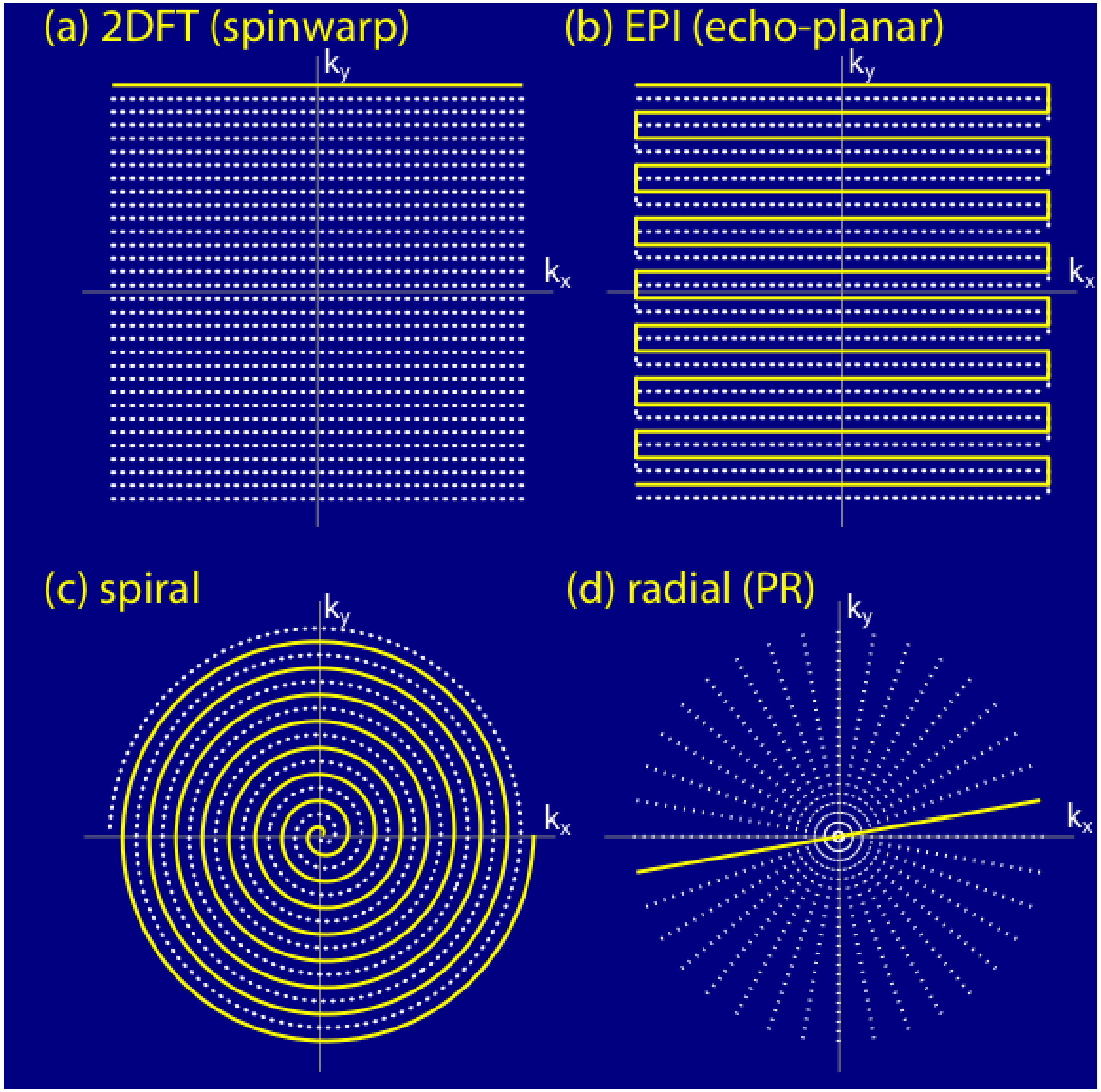

NON-CARTESIAN MR IMAGE RECONSTRUCTION

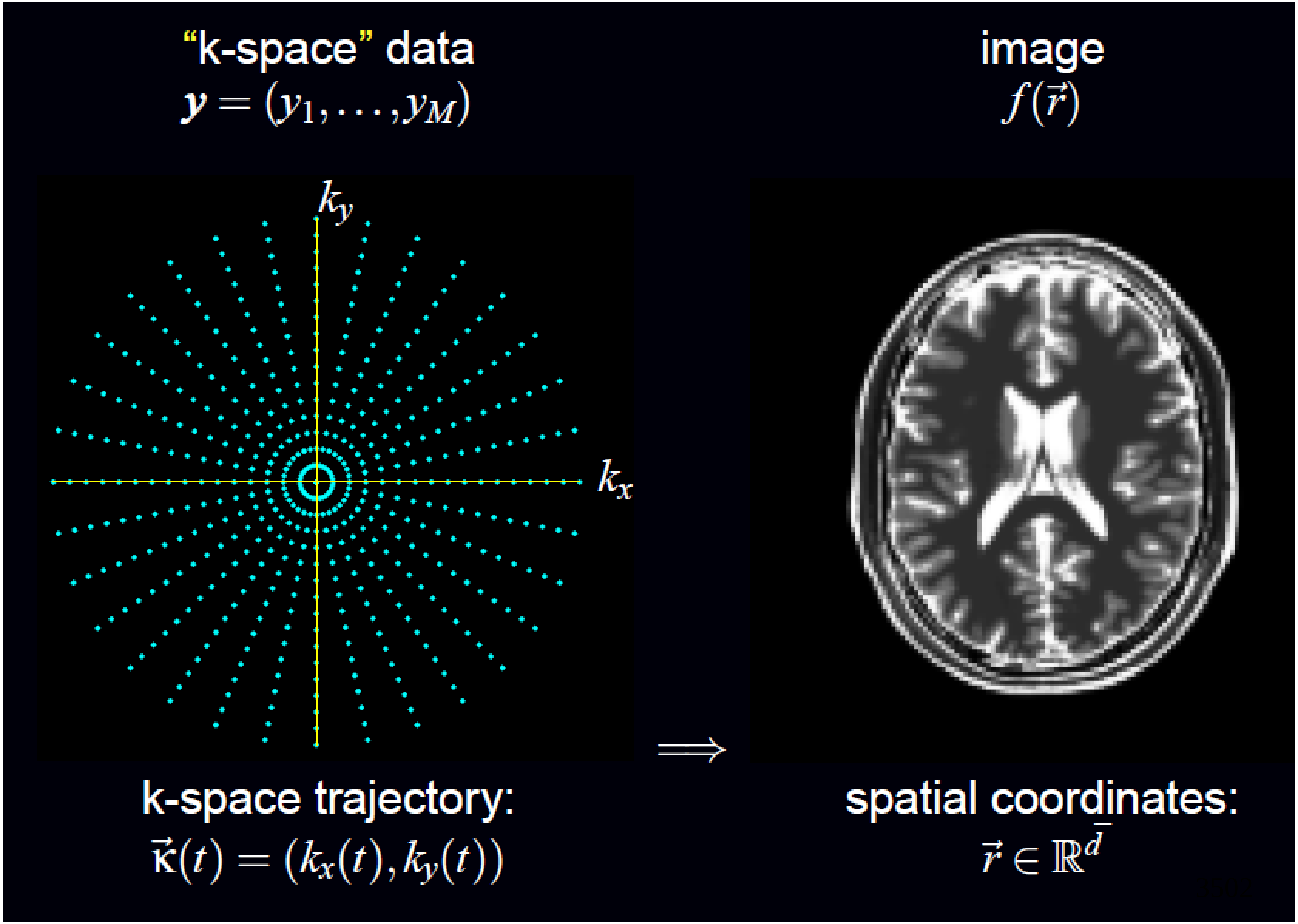

OUTLINE

Part I: Background in Magnetic Resonance Imaging

- MRI scanner
- Sampling k-space & Cartesian reconstruction
- Trajectories and acquisition strategies
- Image reconstruction strategies

TEXTBOOK MRI MEASUREMENT MODEL

- Ignoring *lots* of things, the standard measurement model is:

$$y_i = s(t_i) + n_i \quad i = 1 \ldots m$$

$$s(t) = \int x(\vec{r}) e^{-2\imath\pi\vec{\kappa}(t)\cdot\vec{r}} d\vec{r} = \mathring{x}(\vec{\kappa}(t)).$$

- $\vec{r}$: spatial coordinates
- $\kappa(t)$: k-space trajectory of the MR pulse sequence
- $f(\vec{r})$: object's unknown transverse magnetization
- $\mathring{x}(\vec{\kappa})$: Fourier transform of $x(\vec{r})$. We get noisy samples of this!
- $e^{-2\imath\pi\vec{\kappa}(t)\cdot\vec{r}}$ provides spatial information

- Goal of image reconstruction: find $x(\vec{r})$ from measurements $\{y_i\}_{i=1}^m$

- The unknown object $x(\vec{r})$ is a continuous-space function, but the recorded measurements $\boldsymbol{y} = [y_1, \ldots, y_m]^T$ are finite!
- Under-determined (ill posed) problem $\Longrightarrow$ No canonical solution.

All MR scans provide only "partial" k-space data.

IMAGE RECONSTRUCTION STRATEGIES (1/2)

- **Continuous-continuous** formulation
  - Pretend that a continuum of measurements are available:

$$\mathring{x}(\vec{\kappa}) = \int x(\vec{r}) e^{-2\imath\pi\vec{\kappa}\cdot\vec{r}} \, d\vec{r} \, .$$

  - The "solution" is an inverse Fourier transform:

$$x(\vec{r}) = \int \mathring{x}(\vec{\kappa}) e^{2\imath\pi\vec{\kappa}\cdot\vec{r}} \, d\vec{\kappa} \, .$$

  - Now discretize the integral solution:

$$\widehat{x}(\vec{r}) = \sum_{i=1}^{m} \mathring{x}(\vec{\kappa}_i) e^{2\imath\pi\vec{\kappa}_i\cdot\vec{r}} \approx \sum_{i=1}^{m} y_i w_i e^{2\imath\pi\vec{\kappa}_i\cdot\vec{r}},$$

where w_i values are "sampling density compensation factors". Numerous methods for choosing w_i values in the literature.

  - For Cartesian sampling, $w_i = 1/m \implies$ the summation is an inverse FFT.
  - For non-Cartesian sampling, replace summation with gridding (see Section II).

IMAGE RECONSTRUCTION STRATEGIES (2/2)

- **Continuous-discrete** formulation
  - Use many-to-one linear model:

$$y = \mathcal{H}x + n, \quad \text{where} \quad \mathcal{H} : \mathcal{L}_2(\mathbb{R}^d) \mapsto \mathbb{C}^m.$$

  - Minimum norm solution (cf. "natural pixels")

$$\widehat{x}(\vec{r}) = \arg\min_{x \in \mathcal{L}_2(\mathbb{R}^d)} \|x\|_2^2 \quad \text{subject to} \quad y = \mathcal{H}x$$

$$= \mathcal{H}^*(\mathcal{H}\mathcal{H}^*)^{-1}y = \sum_{i=1}^{m} c_i e^{2\imath\pi\vec{\kappa}_i\cdot\vec{r}}, \text{ where } \quad \mathcal{H}\mathcal{H}^* c = y$$

- **Discrete-discrete** formulation

Assume parametric model for object:

$$x(\vec{r}) = \sum_{j=1}^{n} x_j p_j(\vec{r})$$

  - Estimate parameter vector $x = (x_1, \ldots, x_n)$ from data vector y.

OUTLINE

Part II:Non-Cartesian MRI reconstruction

Prof. John Pauly

NON-CARTESIAN MRI

- K-space trajectory does not fall on a Cartesian grid: Spiral, radial, Lissajou

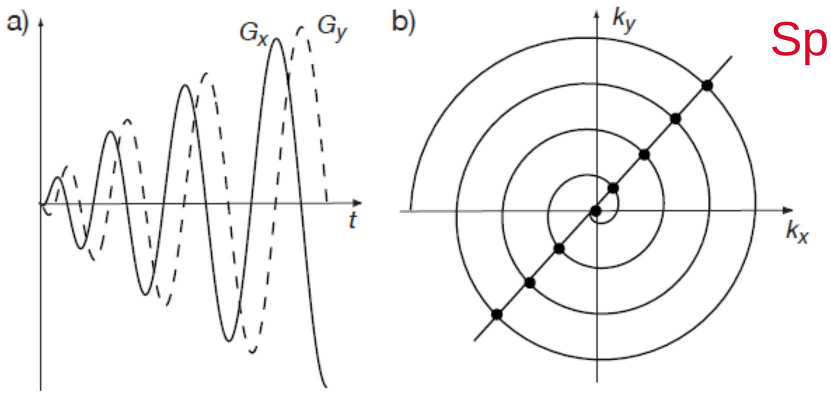

Spiral

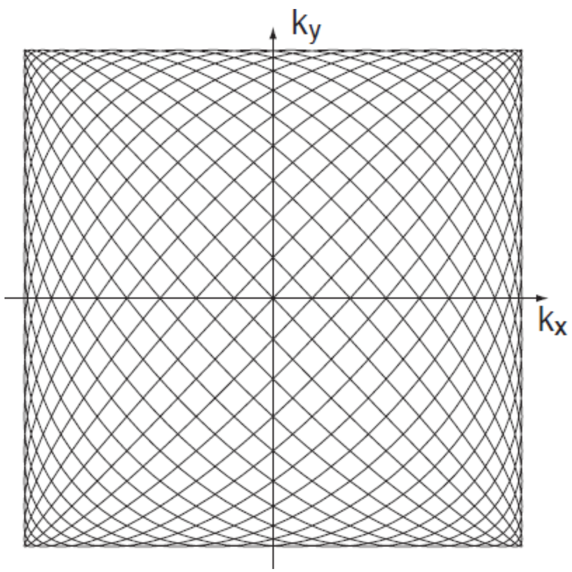

Lissajou

- Faster, more robust to motion than Cartesian MRI

- But reconstruction is more complicated …

RECONSTRUCTION OF NON-CARTESIAN MRI DATA

- Direct FFT won't work
- Radial MRI: backprojection reconstruction, like in CT
- In general:

- Compute the inverse DFT according to the trajectory (slow). Cf **Conjugate Phase reconstruction**.

- **Regridding**: resample the non-Cartesian MRI data onto a 2D Cartesian grid and apply inverse FFT (fast)

K-SPACE RESAMPLING METHODS

- Grid-driven interpolation: estimate the value at each grid point based on the immediately surrounding data

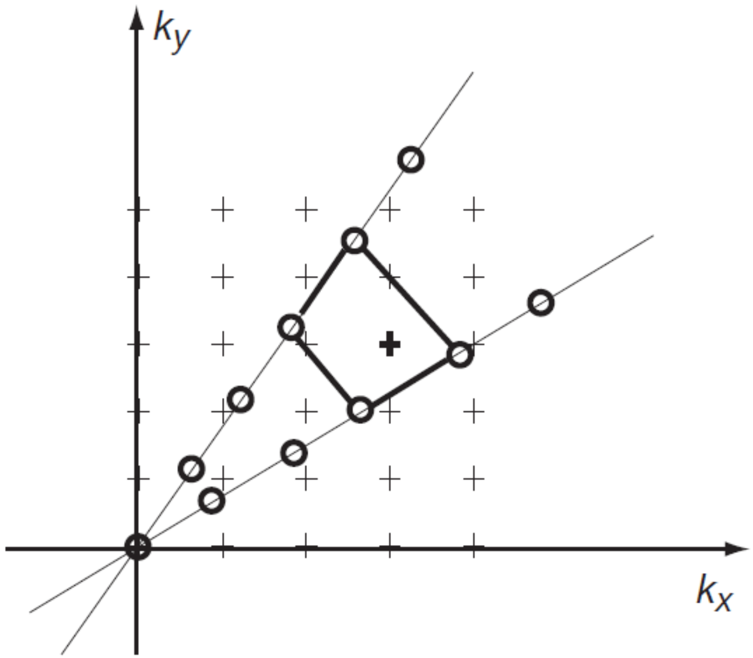

Advantages:

- Easy to implement if the location of neighboring data can be determined analytically
- No density compensation required

Drawbacks:

- Don't use all the input data (less SNR efficient)

\- Quality of image reconstruction is a trade-off between interpolator complexity and k-space oversampling

\- **In practice**: seldom used

- Data-driven interpolation: take each data point and add its contribution to the surrounding grid points

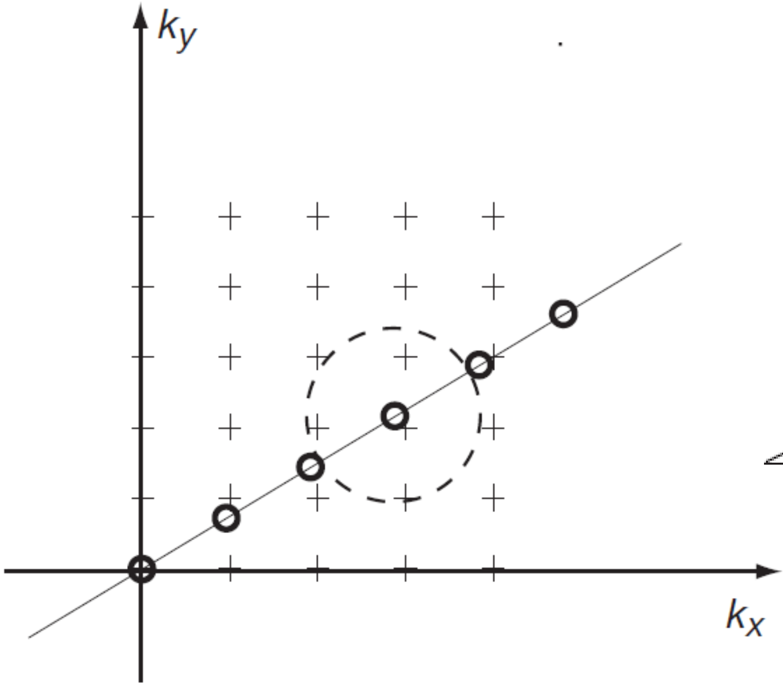

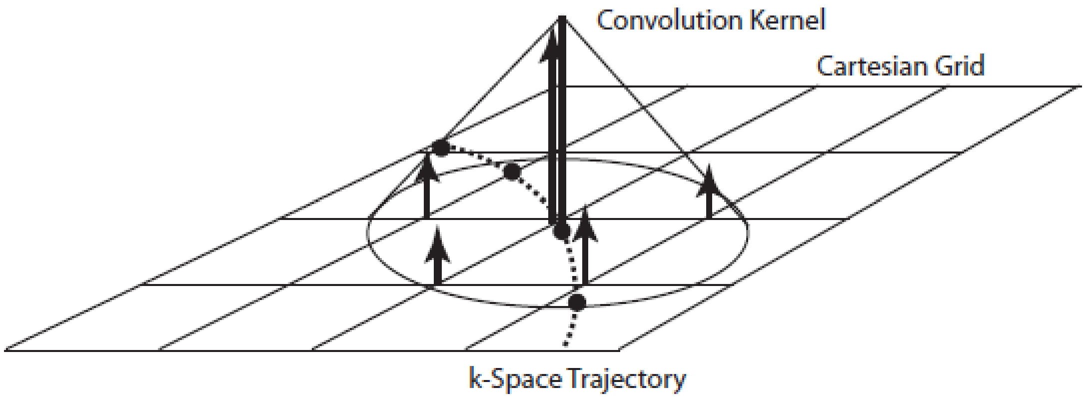

- Convolve with a k-space kernel.
- Evaluate the convolution at the adjacent grid points.

Advantage:

- All data points are used: more SNR efficient

Drawback:

- Require density estimation & compensation

MATHEMATICAL DESCRIPTION OF GRIDDING RECONSTRUCTION

- Non-Cartesian sampling function: $S(k_x, k_y) = \sum_i \delta\left(k_x - k_{x,i}, k_y - k_{y,i}\right)$

- Sampled data: *I*

- Convolution wi
  the Cartesian g

$\hat{M}(k_x, k_y) = \left[\left(M(k\right.\right.$

- After applying t

■ Shah (or Comb) Function:

$$\text{III}(k_x) = \sum_{n=-\infty}^{+\infty} \delta(k_x - n) = \sum_{n=-\infty}^{+\infty} \delta(k_x + n)$$

- Sampling property:

$$\text{III}(k_x)\, f(k_x) = \sum_{n=-\infty}^{+\infty} f(n)\delta(k_x - n)$$

- Replicating property:

$$\text{III}(k_x) \star f(k_x) = \sum_{n=-\infty}^{+\infty} f(k_x - n)$$

$$\hat{m}(x, y) = \left[\left(m(x, y) * s(x, y)\right)c(x, y)\right] * III\left(\frac{x}{FOV_x}, \frac{y}{FOV_y}\right)$$

EFFECTS OF REGRIDDING OPERATIONS

1D Illustration

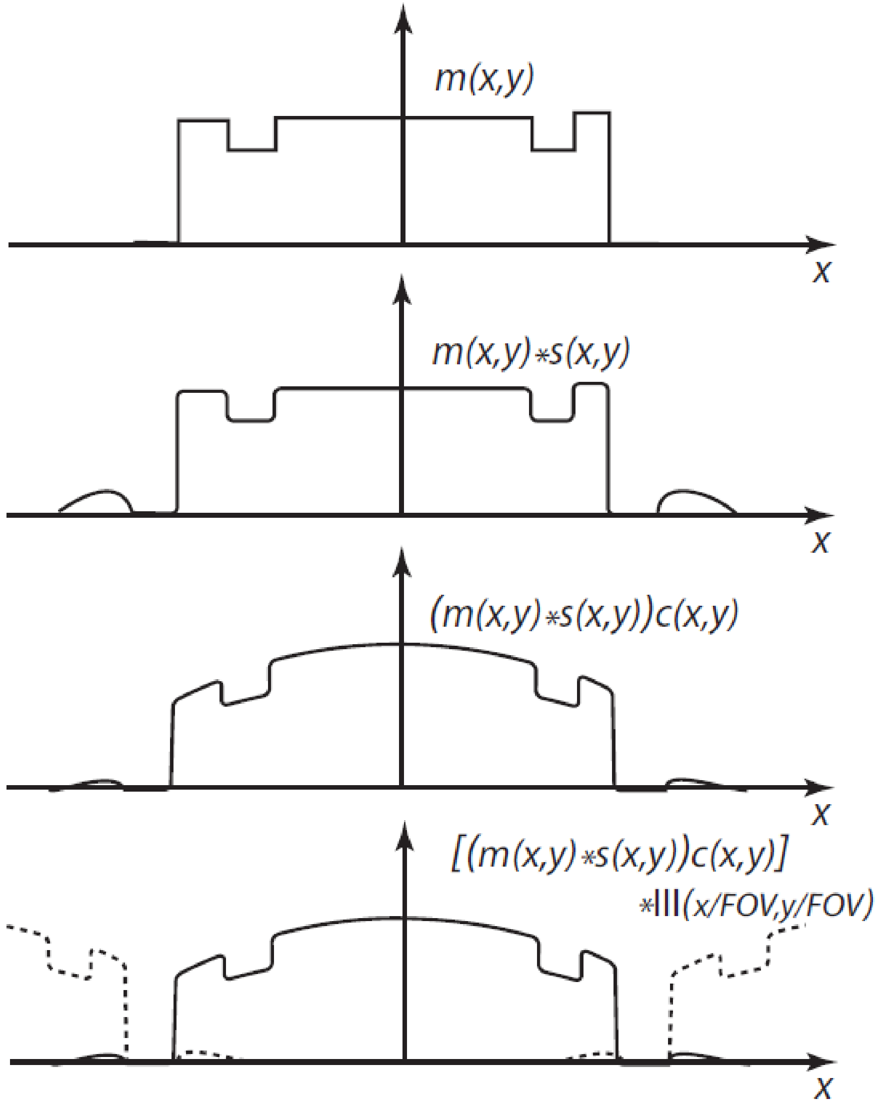

Original signal

Blurring + side lobes

Apodization

Replication

SIMPLE REGRIDDING

- 5 point triangular kernel

Radial k-space
200x200 grid

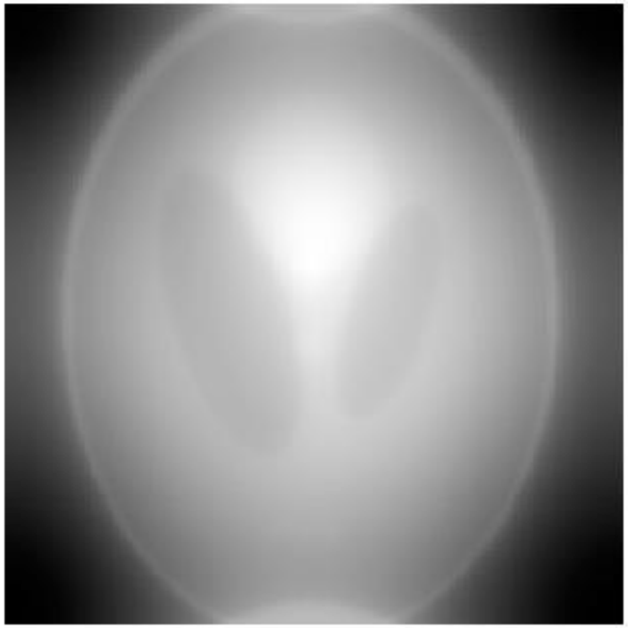

Spiral k-space
128x128 grid

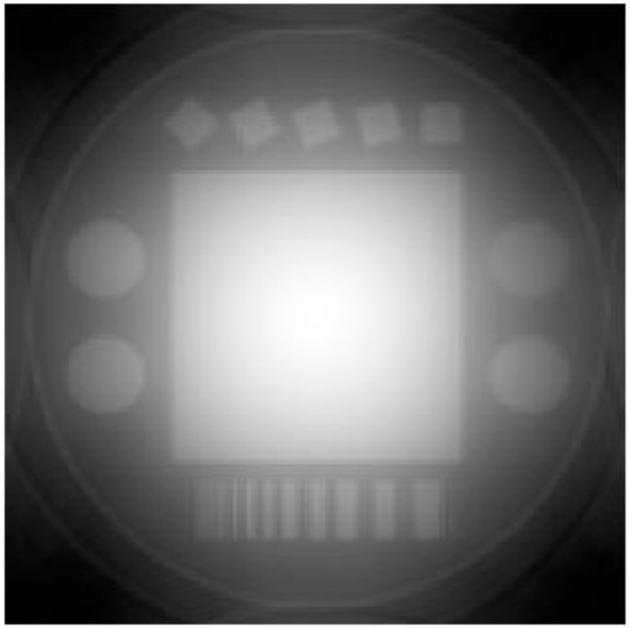

Without density compensation, low frequency artifacts dominate

REGRIDDING DESIGN CONSIDERATIONS

- Non-Cartesian sampling trajectory
  - ✓ Sampling pattern (PSF) & sidelobes
  - ✓ Density compensation

- Convolution kernel
  - ✓ Apodization
  - ✓ Aliasing
  - ✓ Computation time

- Oversampling
  - ✓ Aliasing
  - ✓ Apodization

VARIABLE DENSITY SAMPLING (1/2)

- Non-Cartesian trajectories perform a variable-density sampling of k-space

Radial $S(k_x, k_y)$ Spiral

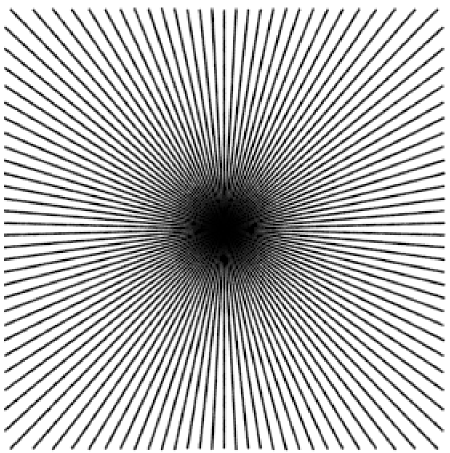

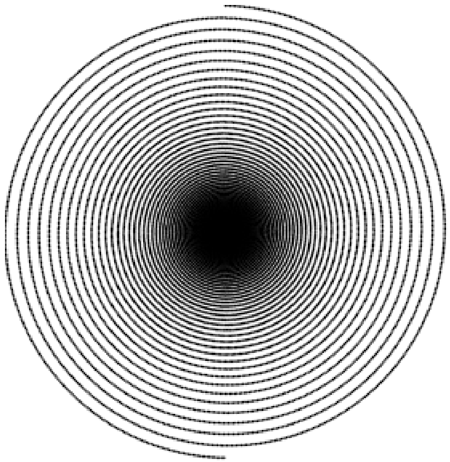

Variable Density

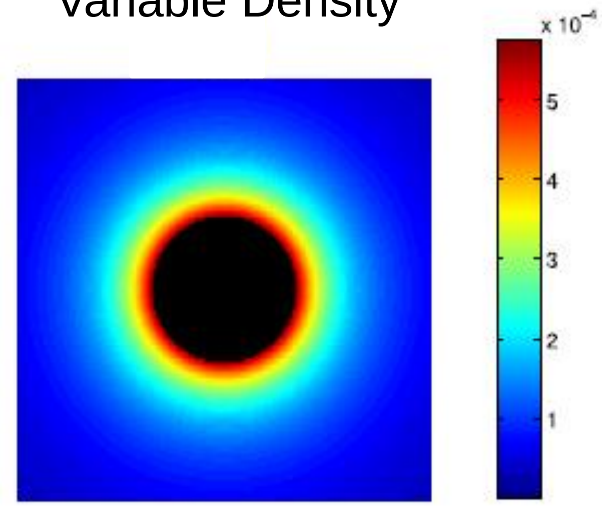

Radial: The central point is acquired N times (# the number of spokes)

Non-uniform k-space weighting

VARIABLE DENSITY SAMPLING (2/2)

- Non-Cartesian trajectories perform a variable-density sampling of k-space

Lissajou

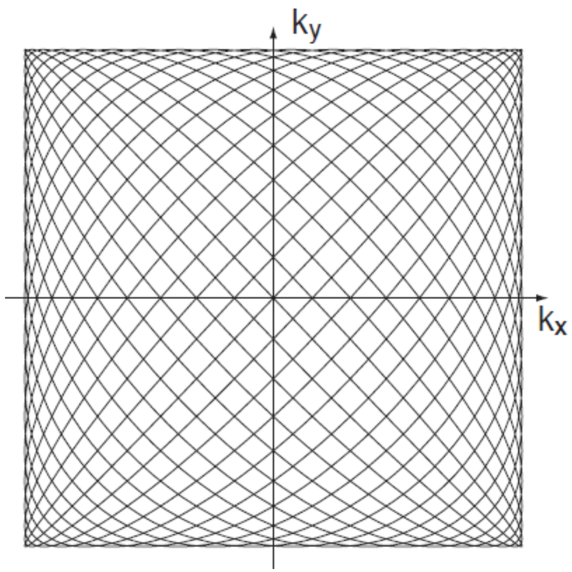

PSF 2D: $s(x,y) = \mathcal{F}^{-1}\{S(k_x, k_y)\}$

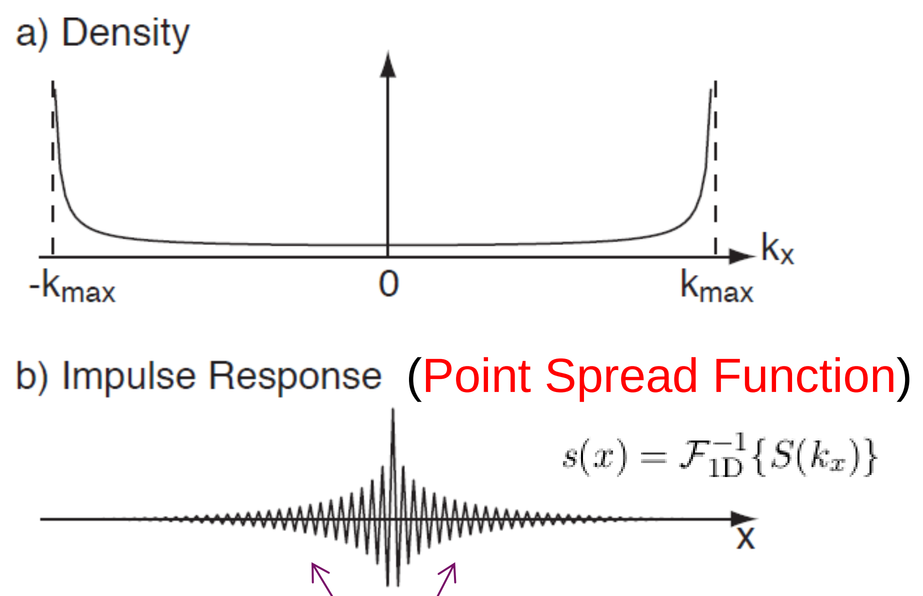

Sidelobes:
Not perfect localization

Ideally the PSF should be an impulse but it is not in practice!

SAMPLING DENSITY COMPENSATION (1/4)

- Pre-compensation (ideal)
  - Sampling density (ρ) must be pre-computed

$$\hat{M}(k_x,k_y) = \left[\left(\frac{M(k_x,k_y)}{\rho(k_x,k_y)} S(k_x,k_y)\right) * C(k_x,k_y)\right] \times III\left(\frac{k_x}{\Delta k_x}, \frac{k_y}{\Delta k_y}\right)$$

  - Using geometry

For radial MRI:

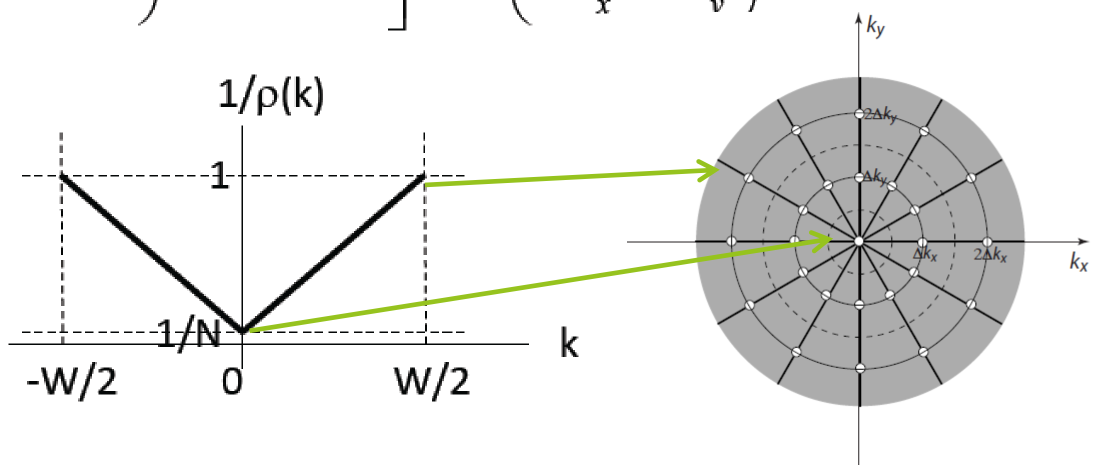

$$w_0 = \frac{1}{N}\pi\left(\frac{\Delta k_r}{2}\right)^2 = \frac{2\pi}{N}(\Delta k_r)^2\frac{1}{8}$$

$$w_n = \frac{2\pi}{N}(\Delta k_r)^2 n, \quad n \geqslant 1.$$

  - Assign an area to each k-space sample (numerical method)
    - E.g. Voronoi diagram

SAMPLING DENSITY COMPENSATION: VORONOI DIAGRAM (2/4)

[Rasche et al, IEEE TMI 1999]

Nine-interleave k-space spiral

Voronoi diagram

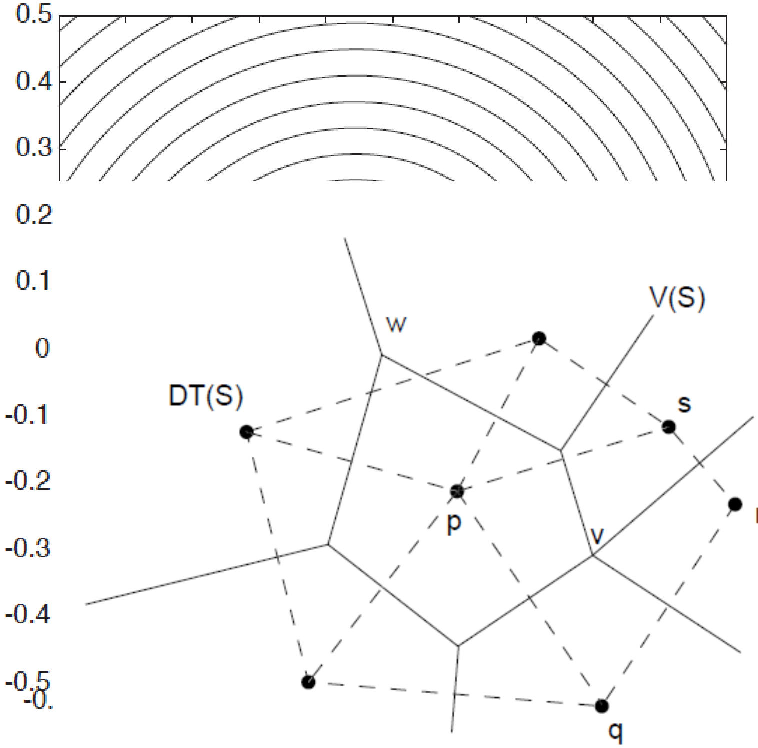

Region for a given sample

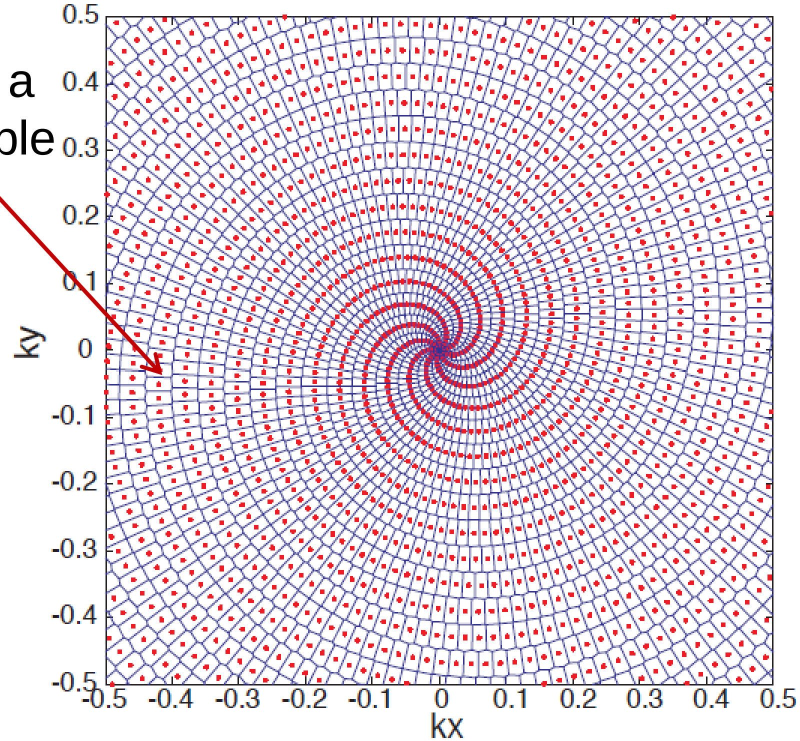

Density approximated as the inverse of the area of these regions

SAMPLING DENSITY COMPENSATION (3/4)

- Post-compensation (after the gridding operation)

$$\hat{M}(k_x,k_y) = \frac{1}{\rho(k_x,k_y)}\left[\left(M(k_x,k_y)S(k_x,k_y)\right)*C(k_x,k_y)\right]\times III\left(\frac{k_x}{\Delta k_x},\frac{k_y}{\Delta k_y}\right)$$

- Find ρ by regridding $M(k_x,k_y)$=1

$$\rho(k_x,k_y) = \left[\left(M(k_x,k_y)S(k_x,k_y)\right)*C(k_x,k_y)\right]\times III\left(\frac{k_x}{\Delta k_x},\frac{k_y}{\Delta k_y}\right)$$

- It works well if the sampling pattern does not change too rapidly
- The gridding convolution kernel blurs the effect of rapid density changes

EFFECT OF DENSITY COMPENSATION ON MR IMAGE RECONSTRUCTION (4/4)

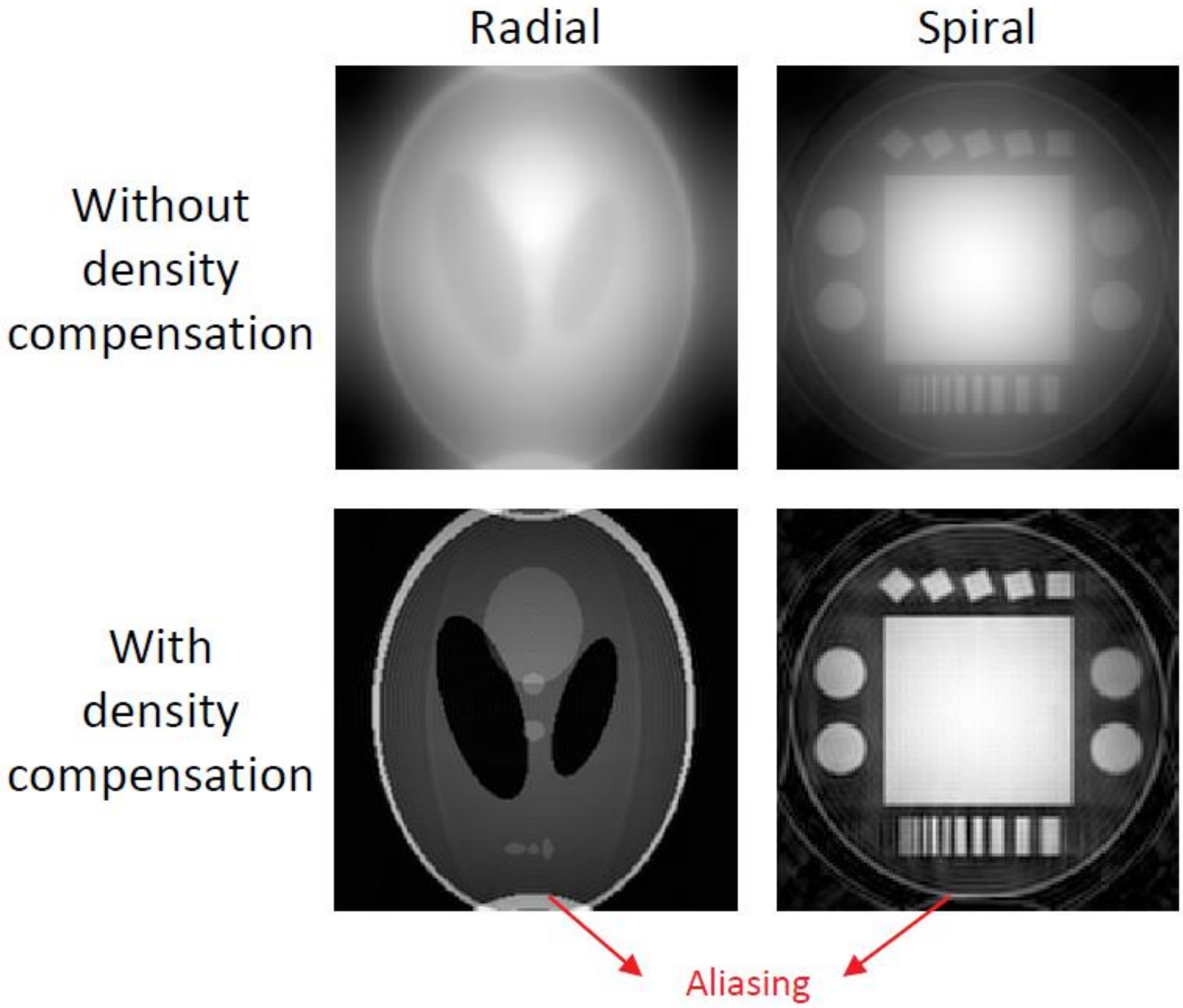

CONVOLUTION KERNEL (1/3)

- The ideal kernel would be an infinite sinc (impractical)

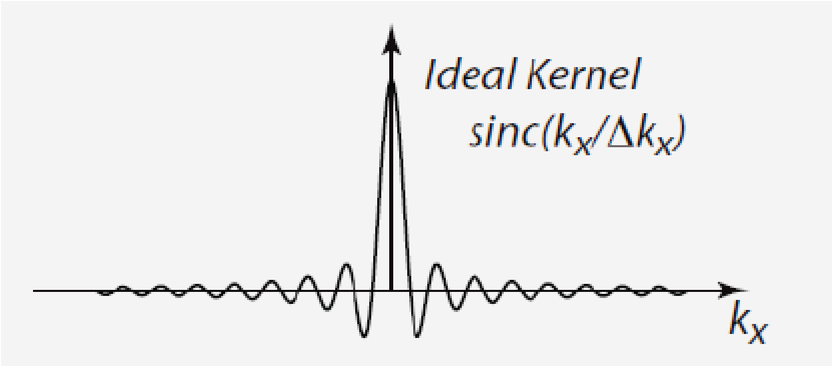

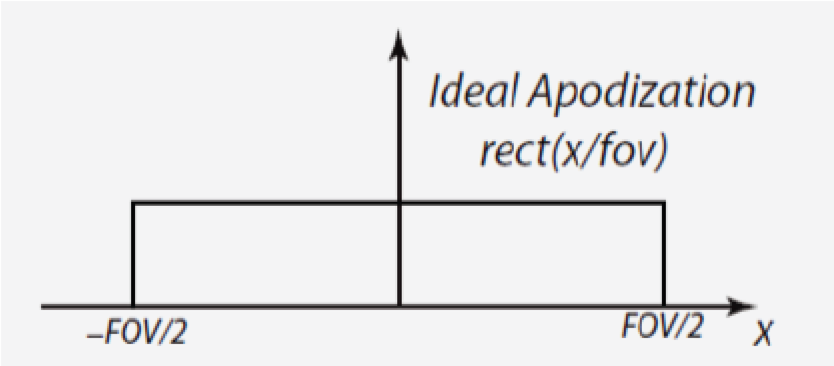

Infinite support!

- Windowed sinc

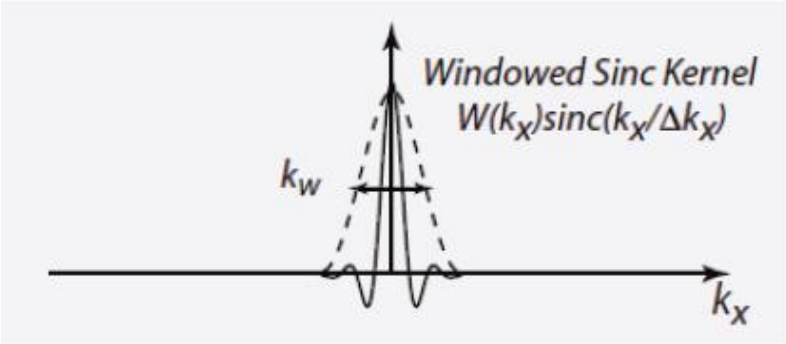

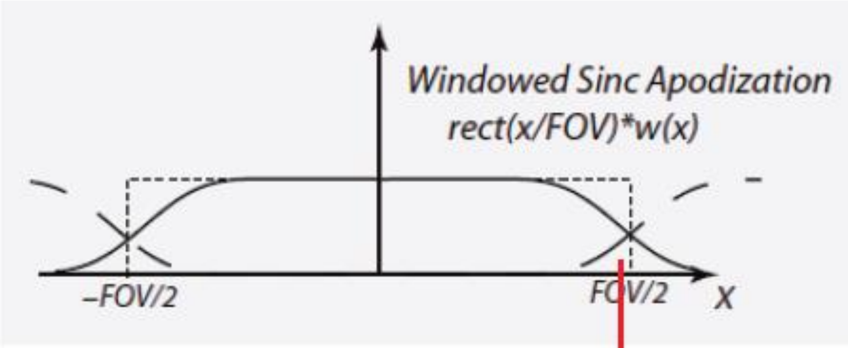

$$x_{tw} \approx \frac{1}{k_w} = \frac{1}{n\Delta k_x} = \frac{1}{n} FOV$$

Aliasing

CONVOLUTION KERNEL (2/3)

- Small kernels: Save computing time

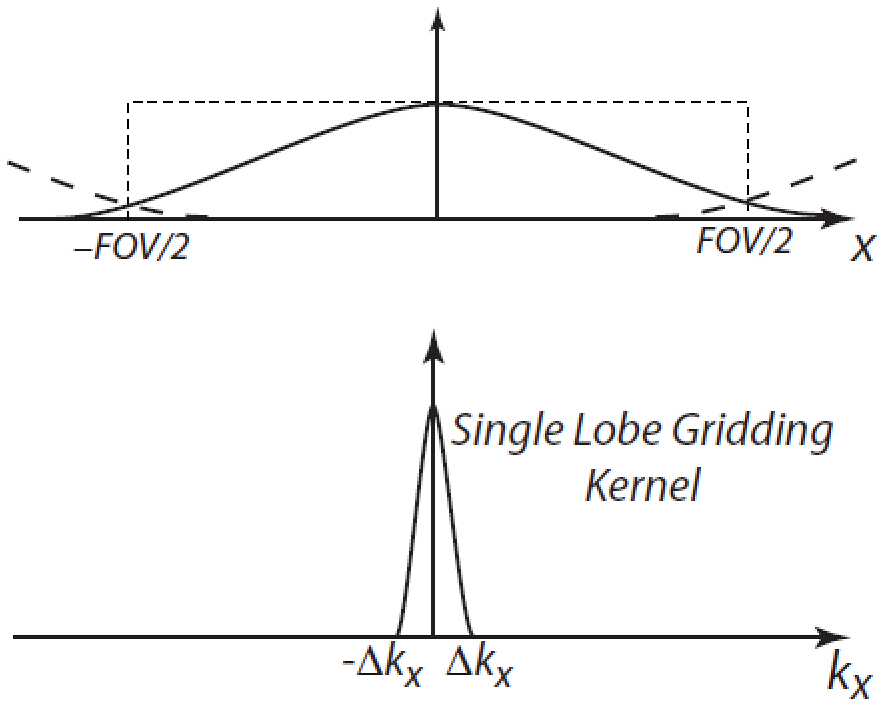

- If the kernel width is wider than that of the *windowed sinc*, the corresponding apodization function is narrower in space

⇒ Aliasing reduced at the cost of FOV

CONVOLUTION KERNEL (3/3)

- Kaiser-Bessel function: smooth lowpass filter
  - ✓ Best kernel (by consensus)

[Jackson et al, IEEE TMI 1991]

$$C(k) = \frac{1}{W} I_0\left(b\left(1 - 2\frac{k}{W}\right)^2 \right) rect\left(\frac{2k}{W}\right)$$

I_0: zero-order modified Bessel function of the first kind

W: width of the kernel

b: scaling parameter

– Inverse Fourier transform

$$c(x) = \frac{\sin\left(\sqrt{\pi^2 W^2 x^2 - b^2}\right)}{\sqrt{\pi^2 W^2 x^2 - b^2}}$$

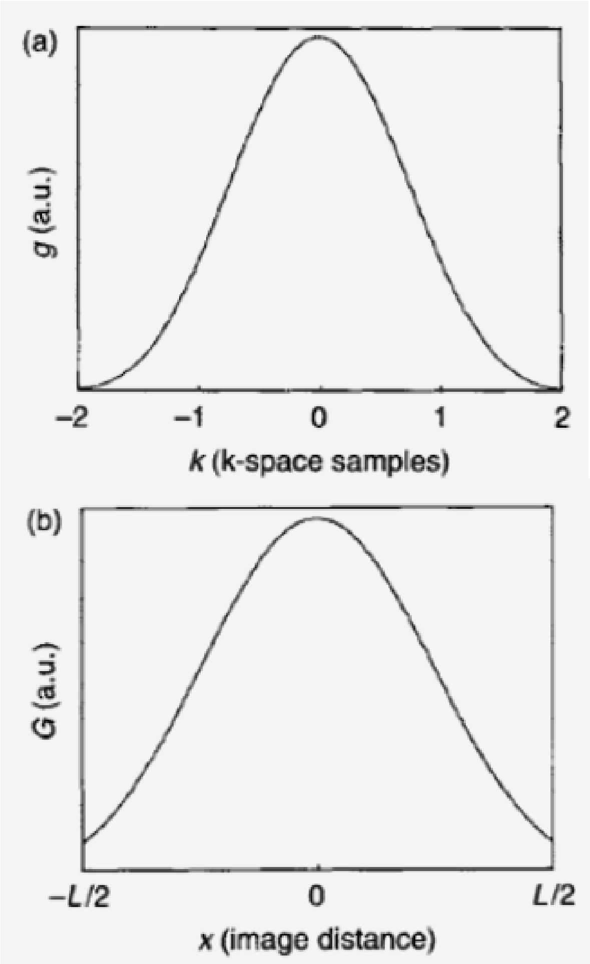

OVERSAMPLING THE CARTESIAN GRID

- Removes aliasing
- Reduces apodization

[O'Sullivan, IEEE TMI 1985]

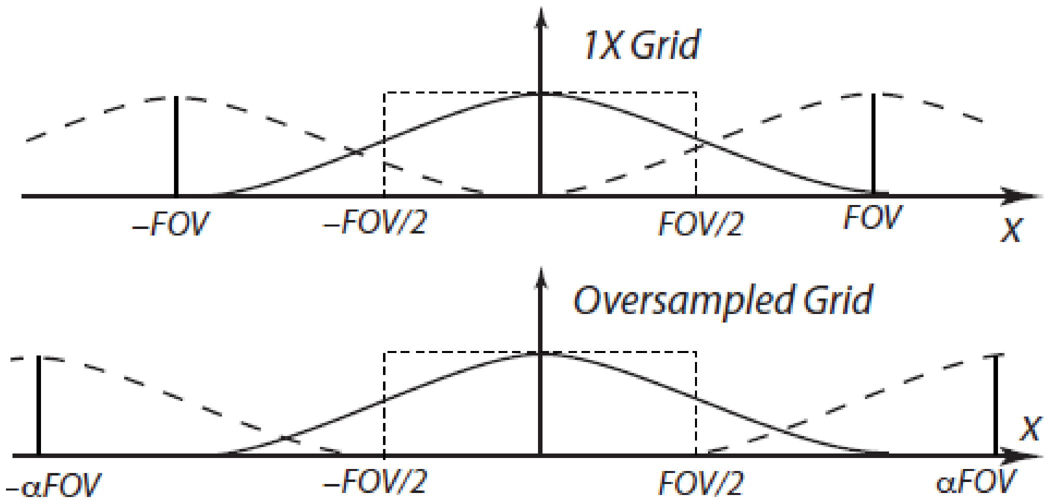

$$\alpha > 1, \quad \left(\frac{\Delta k_x}{\alpha}, \frac{\Delta k_y}{\alpha}\right) \Longrightarrow \hat{m}(x,y) = [(m(x,y) * s(x,y))\, c(x,y)] * \mathrm{III}\left(\frac{x}{\alpha FOV_x}, \frac{y}{\alpha FOV_y}\right)$$

(Deapodization neglected)

OVERSAMPLING THE CARTESIAN GRID

2X grid

Radial

Crop in the image domain

Spiral

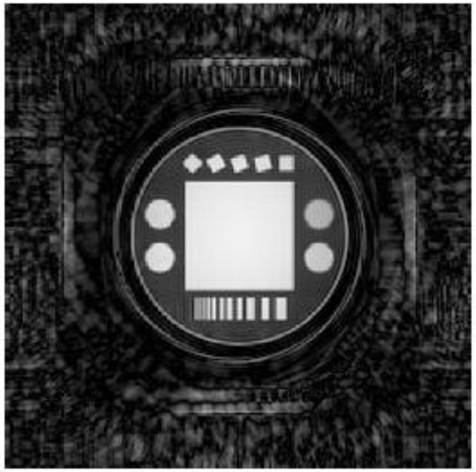

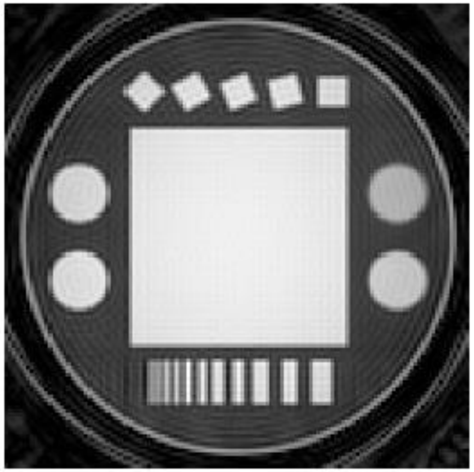

DEAPODIZATION

- Divide the reconstructed image by the inverse Fourier transform of the regridding kernel

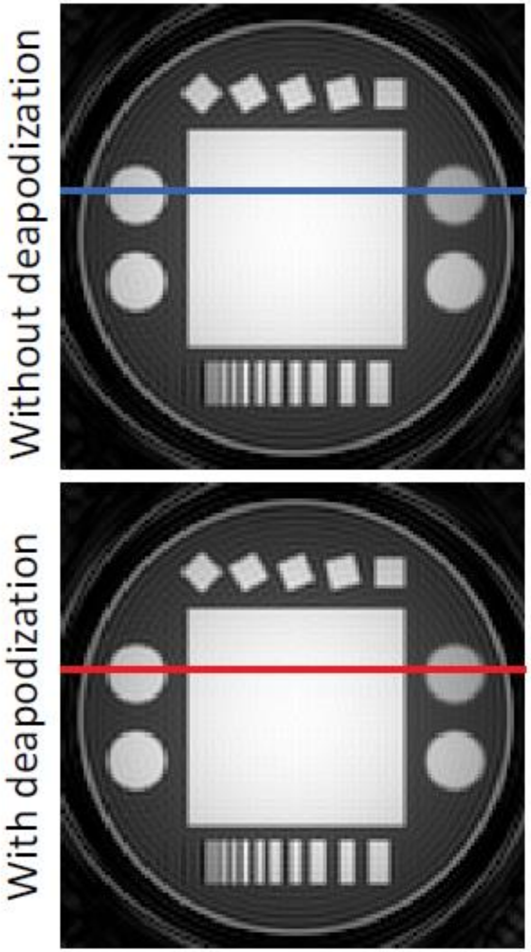

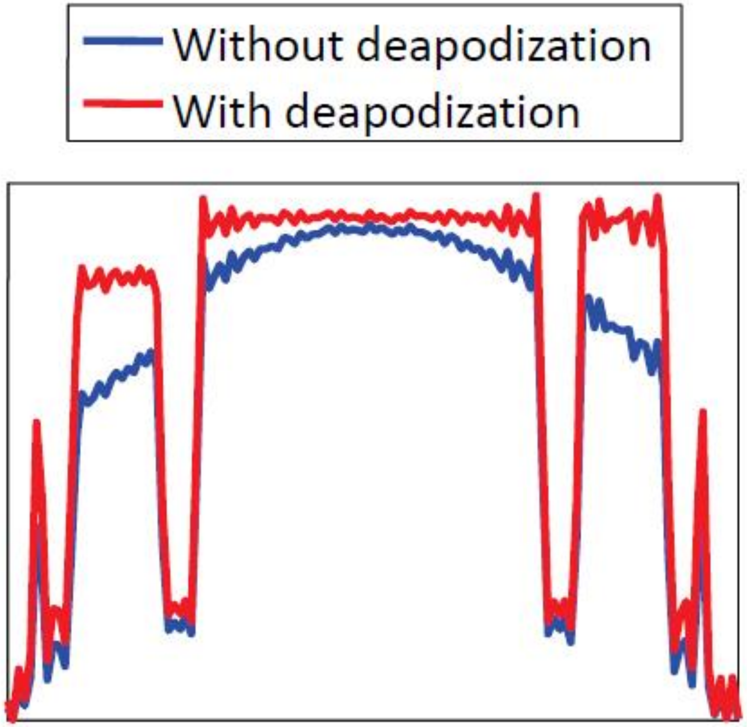

WHY THE KAISER-BESSEL KERNEL IS PREFERRED?

- Lower oversampling factor (save memory)

[Beatty et al, IEEE TMI 2005]

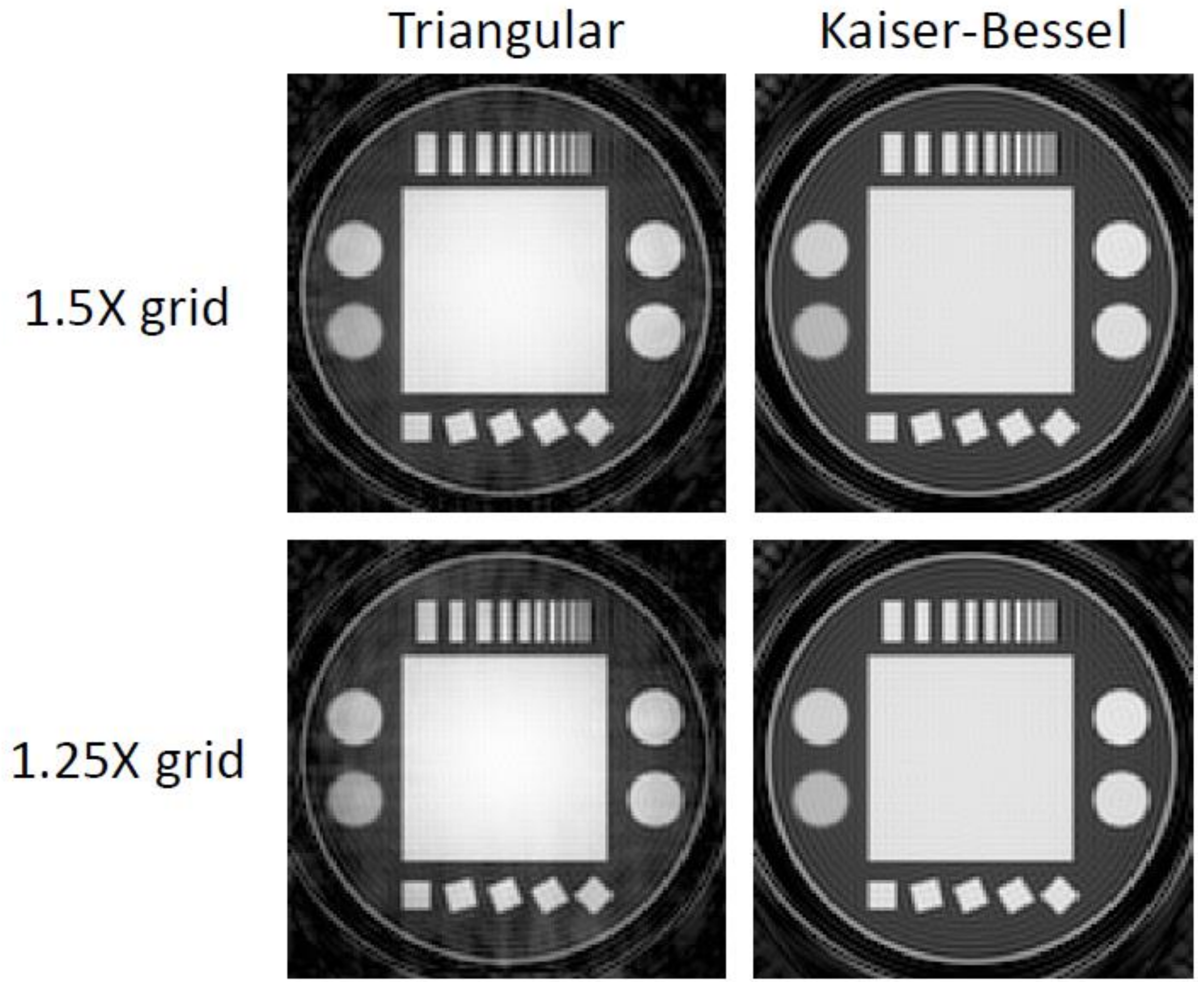

FFTW package: fftw.org

Fast implementations of FFT for a whole range of lengths

SUMMARY OF REGRIDDING RECONSTRUCTION

- Compute the non-Cartesian sampling pattern
- Choose the regridding kernel (e.g. Kaiser-Bessel)
- Density pre-compensation (if possible)
- Convolve the pre-compensated data with the regridding kernel and evaluate the convolution at the oversampled Cartesian grid
- Apply inverse 2D FFT
- Apply the deapodization function
- Apply post-density post-compensation (optional)
- Remove the oversampling by cropping the image

OUTLINE

Part III: Iterative Model-based image reconstruction

- Least squares solution
- Regularized Least Squares
- Beyond quadratic regularization

Prof. Jeff Fessler

Why Iterative Image Reconstruction?

- "Non-Fourier" physical effects such as field inhomogeneity (ΔB_0)
- Incorporate prior information, *e.g.*:
  - Support constraint
  - Piecewise smoothness
  - Phase constraints
- No density compensation needed
- Statistical modeling may reduce noise

Primary Drawbacks of Iterative Methods?

- Algorithm speed
- Complexity, *e.g.* choosing regularization parameter(s)

BASIC SIGNAL MODEL

$$y_i = s(t_i) + n_i, \quad \mathrm{E}[y_i] = s(t_i) = \int x(\vec{r}) e^{-2\imath\pi\vec{\kappa}_i\cdot\vec{r}}\, d\vec{r}.$$

- Goal: Reconstruct $x(\vec{r})$ from $\boldsymbol{y} = (y_1, \ldots, y_M)$.
  - Series expansion of unknown object: $x(\vec{r}) \approx \sum_{j=1}^{n} x_j\, p(\vec{r} - \vec{r}_j)$
    $\longrightarrow$ Usually $p(\cdot)$ 2D rect functions.
  - Substituting into signal model yields:

$$\mathrm{E}[y_i] = \int \sum_{j=1}^{n} x_j\, p(\vec{r} - \vec{r}_j) e^{-2\imath\pi\vec{\kappa}_i\cdot\vec{r}}\, d\vec{r} = \sum_{j=1}^{n} \left[\int p(\vec{r} - \vec{r}_j) e^{-2\imath\pi\vec{\kappa}_i\cdot\vec{r}}\, d\vec{r} \right] x_j$$

$$= \sum_{j=1}^{n} h_{ij}\, x_j, \quad h_{ij} = \mathring{p}(\vec{\kappa}_i) e^{-2\imath\pi\vec{\kappa}_i\cdot\vec{r}_j}, \quad p(\vec{r}) \overset{FT}{\Longleftrightarrow} \mathring{p}(\vec{\kappa})$$

- Discrete-discrete measurement model with system matrix $\boldsymbol{H} = \{h_{ij}\}$:

$$\boxed{\boldsymbol{y} = \boldsymbol{H}\boldsymbol{x} + \boldsymbol{n}}$$

- Goal: estimate coefficients (pixel values) $\boldsymbol{x} = (x_1, \ldots, x_n)$ from $\boldsymbol{y}$.

LEAST SQUARES ESTIMATION

- Estimate object by minimizing a simple cost function:

$$\widehat{\boldsymbol{x}} = \underset{\boldsymbol{x} \in \mathbb{C}^n}{\arg\min}\, \mathcal{J}(\boldsymbol{x}), \quad \mathcal{J}(\boldsymbol{x}) = \|\boldsymbol{y} - \boldsymbol{H}\boldsymbol{x}\|^2$$

  - Data fidelity term $\|\boldsymbol{y} - \boldsymbol{H}\boldsymbol{x}\|^2$ corresponds to negative log-likelihood of Gaussian distribution
  - Equivalent to Maximum likelihood (ML) estimation under white noise assumptions

- Issues:
  - Computing minimizer rapidly
  - Stopping iteration
  - Image quality

ITERATIVE MINIMIZATION BY CONJUGATE GRADIENTS

- CG Algorithm:

Data: $\boldsymbol{y}$
Result: Reconstructed MR image $\widehat{\boldsymbol{x}}$
Choose initial guess $\boldsymbol{x}^{(0)}$ (e.g., by gridding)
for $k \leftarrow 1$ **to** K_{iter} **do**

$$\boldsymbol{g}^{(k)} = \nabla\mathcal{J}(\boldsymbol{x}^{(k)}) = \boldsymbol{H}^*(\boldsymbol{H}\boldsymbol{x}^{(k)} - \boldsymbol{y}) \quad \text{(Gradient)}$$
$$\boldsymbol{p}^{(k)} = \boldsymbol{P}\boldsymbol{g}^{(k)} \quad \text{(Preconditioning)}$$
$$\gamma_k = \begin{cases} 0, & k = 0 \\ \dfrac{\left\langle \boldsymbol{g}^{(k)}, \boldsymbol{p}^{(k)} \right\rangle}{\left\langle \boldsymbol{g}^{(k-1)}, \boldsymbol{p}^{(k-1)} \right\rangle} & k > 0 \end{cases}$$
$$\boldsymbol{d}^{(k)} = -\boldsymbol{p}^{(k)} + \gamma_k \boldsymbol{d}^{(k-1)} \quad \text{(Search direction)}$$
$$\boldsymbol{v}^{(k)} = \boldsymbol{H}\boldsymbol{d}^{(k)}$$
$$\alpha^{(k)} = \left\langle \boldsymbol{d}^{(k)}, -\boldsymbol{g}^{(k)} \right\rangle / \|\boldsymbol{v}^{(k)}\|^2 \quad \text{(Stepsize)}$$
$$\boldsymbol{x}^{(k+1)} = \boldsymbol{x}^{(k)} + \alpha_k \boldsymbol{d}^{(k)} \quad \text{(Update)}$$

- Bottlenecks: Computing $\boldsymbol{H}\boldsymbol{x}(k)$ and $\boldsymbol{H}^*\boldsymbol{r}$:
  - $\boldsymbol{H}$ is too large to be stored explicitly (not sparse)
  - Even if $\boldsymbol{H}$ were stored, directly computing $\boldsymbol{H}\boldsymbol{x}$ is $O(mn)$ per iteration whereas FFT is only $O(m \log m)$.

COMPUTING THE FORWARD PROBLEM RAPIDLY

- Computing $\boldsymbol{H}\boldsymbol{x}$ rapidly

$$[\boldsymbol{H}\boldsymbol{x}]_i = \sum_{j=1}^{n} h_{ij} x_j = \mathring{p}(\vec{\kappa}_i) \sum_{j=1}^{n} e^{-2\imath\pi\vec{\kappa}_i \cdot \vec{r}_j} x_j, \quad i = 1, \ldots, m$$

- Pixel locations $\{\vec{r}_j\}$ are uniformly spaced
- k-space locations $\{\vec{\kappa}_i\}$ are unequally spaced

$\Longrightarrow$ needs nonuniform fast Fourier Transform (NUFFT or NFFT) [Fessler and Sutton, 2003, Potts and Steidl, 2003].

NUFFT (TYPE 2)

- Compute over-sampled FFT of equally spaced signal samples
- Interpolate onto desired unequally-spaced frequency locations
- [Dutt and Rokhlin, 1993]: Gaussien bell interpolator
- [Fessler and Sutton, 2003]: Min-max interpolator and min-max optimized Kaiser-Bessel interpolator.
  - NUFFT toolbox: `https://www.eecs.umich.edu/f̃essler/code/`
  - NFFT toolbox: `https://www-user.tu-chemnitz.de/ p̃otts/nfft/`

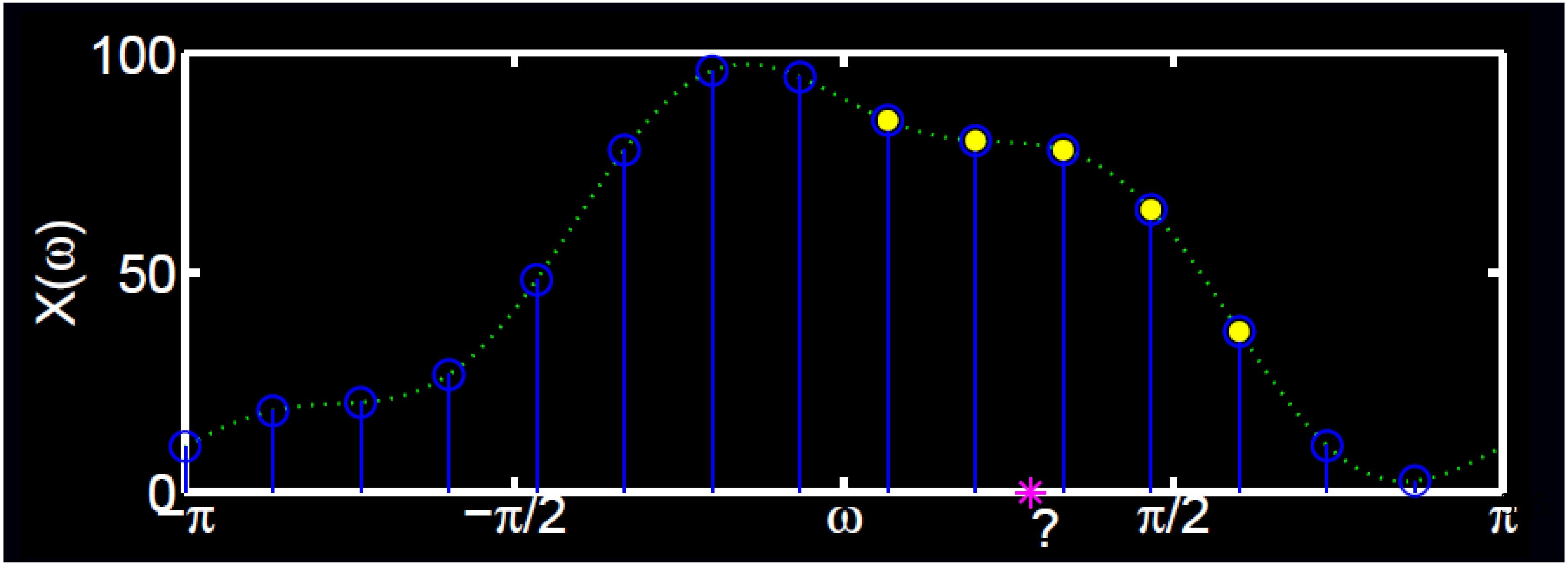

FURTHER ACCELERATION USING TOEPLITZ MATRICES

- Cost function gradient:

$$g^{(k)} = \boldsymbol{H}^*(\boldsymbol{H}\boldsymbol{x}^{(k)} - \boldsymbol{y}) = \boldsymbol{T}\boldsymbol{x}^{(k)} - \boldsymbol{b}$$

$$\text{where} \quad \boldsymbol{T} \triangleq \boldsymbol{H}^*\boldsymbol{H}, \quad \boldsymbol{b} = \boldsymbol{H}^*\boldsymbol{y}.$$

- In the absence of field inhomogeneity, the Gram matrix $\boldsymbol{T}$ is Toeplitz:

$$[\boldsymbol{T}]_{j\ell} = \sum_{i=1}^{m} |\mathring{p}(\vec{\kappa}_i)|^2 e^{-2\imath\pi\vec{\kappa}_i \cdot (\vec{r}_j - \vec{r}_\ell)}.$$

- Computing $\boldsymbol{T}\boldsymbol{x}^{(k)}$ requires an ordinary (2× oversampled) FFT [Chan and Ng, 1996] by embedding $\boldsymbol{T}$ in a $2n \times 2n$ circulant matrix $\boldsymbol{C} = \begin{bmatrix} \boldsymbol{T} & \boldsymbol{B} \\ \boldsymbol{B} & \boldsymbol{T} \end{bmatrix}$.
  - In 2D, block Toeplitz matrix with Toeplitz blocks (BTTB).
  - Precomputing the first column of $\boldsymbol{T}$ and $\boldsymbol{b}$ requires a couple of NUFFT [Eggers et al., 2002, Liu et al., 2005].
- This formulation seems ideal for "hardware" MRI systems.

UNREGULARIZED EXAMPLE: SIMULATED DATA

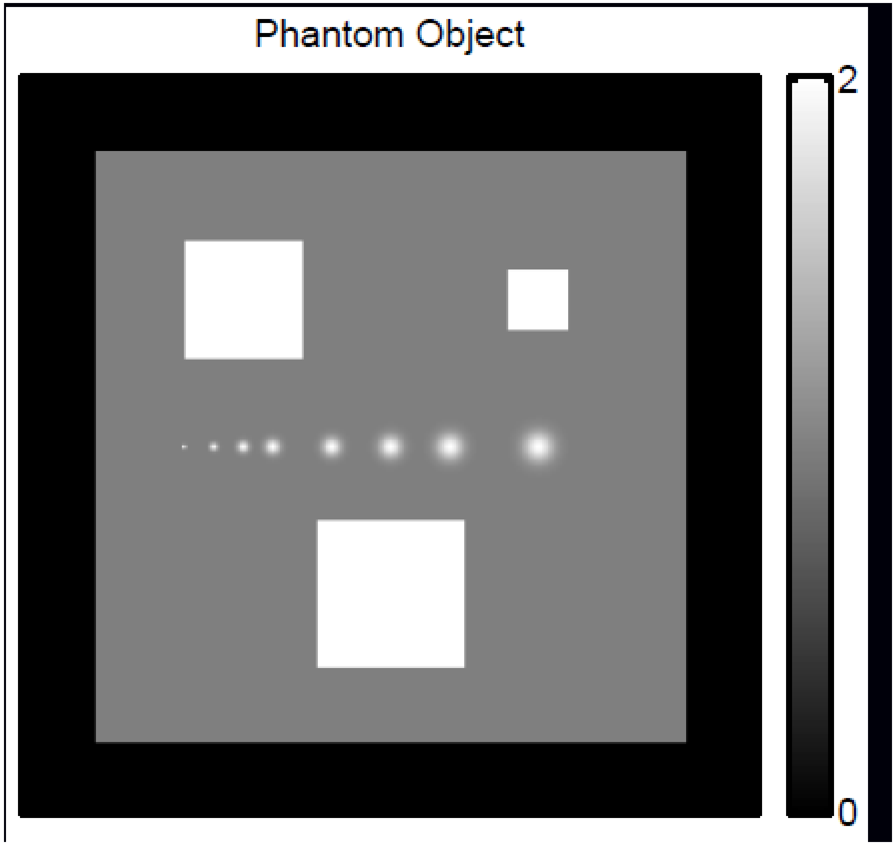

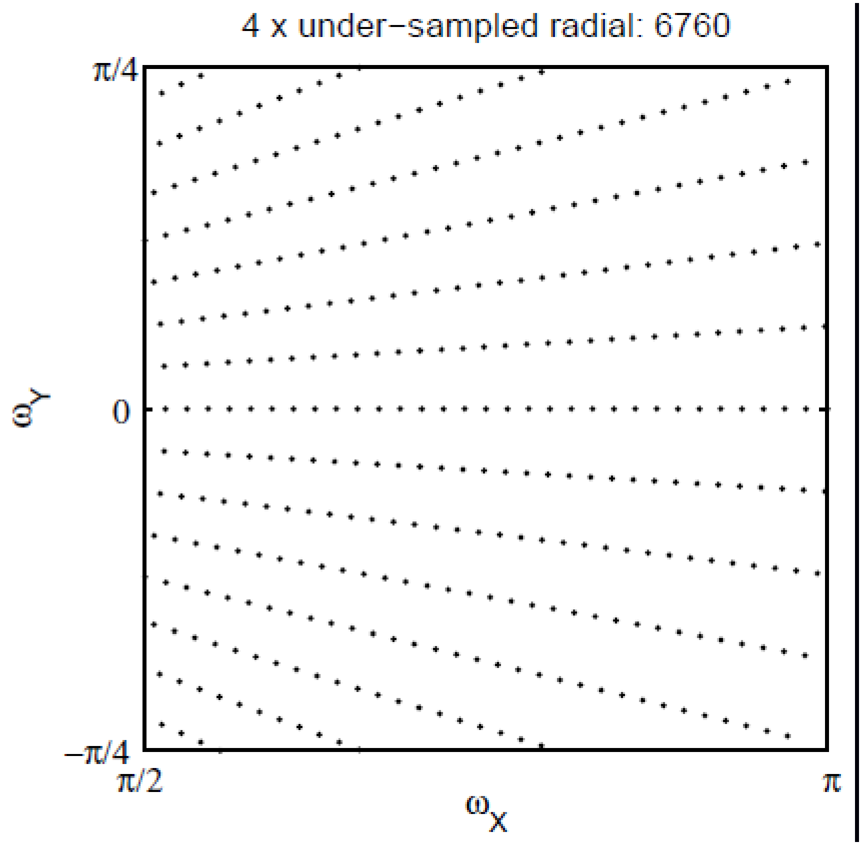

- 4x undersampled radial k-space data
- Analytical k-space generation

UNREGULARIZED EXAMPLE: IMAGES

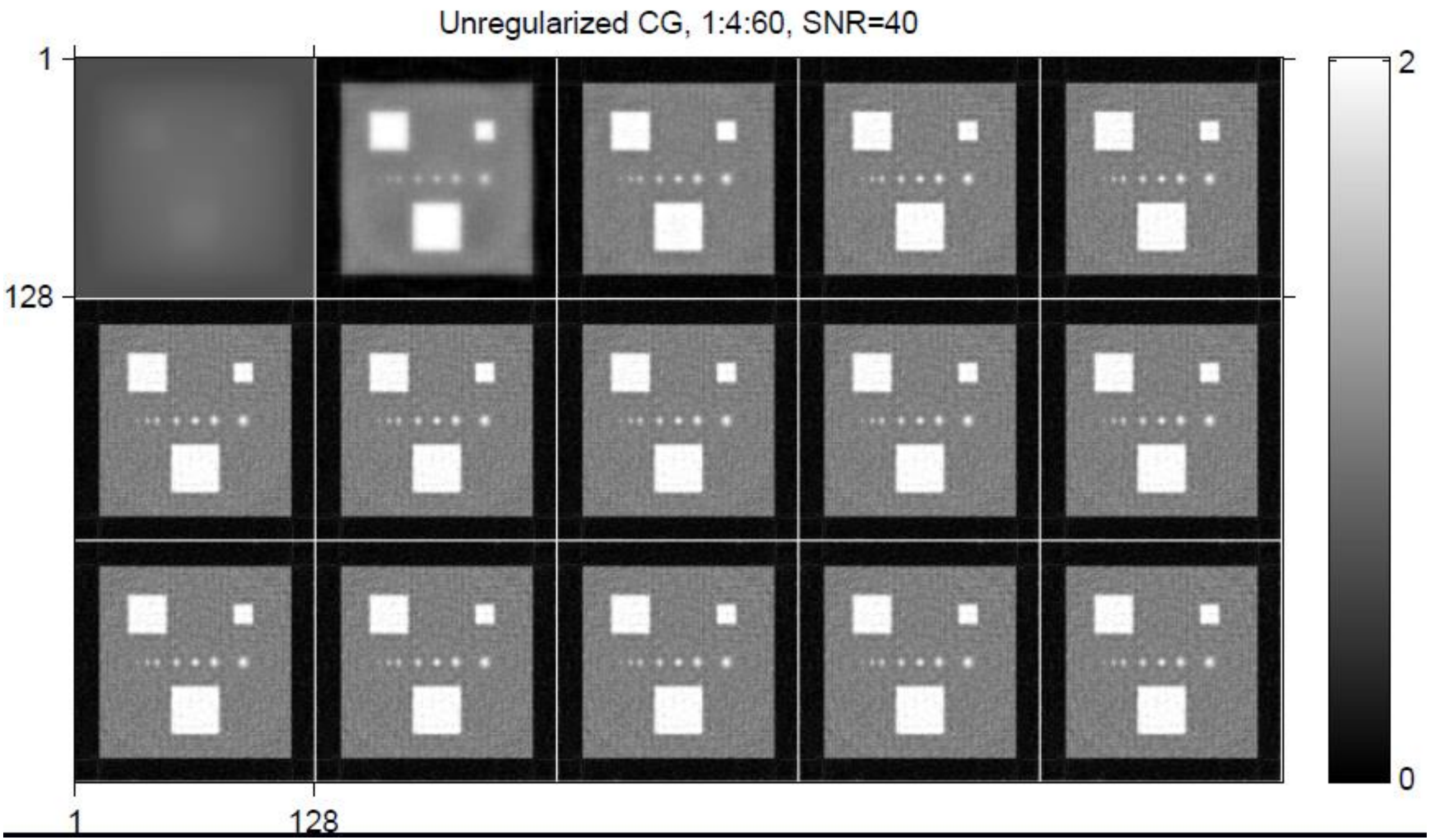

- Iterations: 1:4:60 of unregularized CG reconstruction

UNREGULARIZED EXAMPLE: RMS ERROR

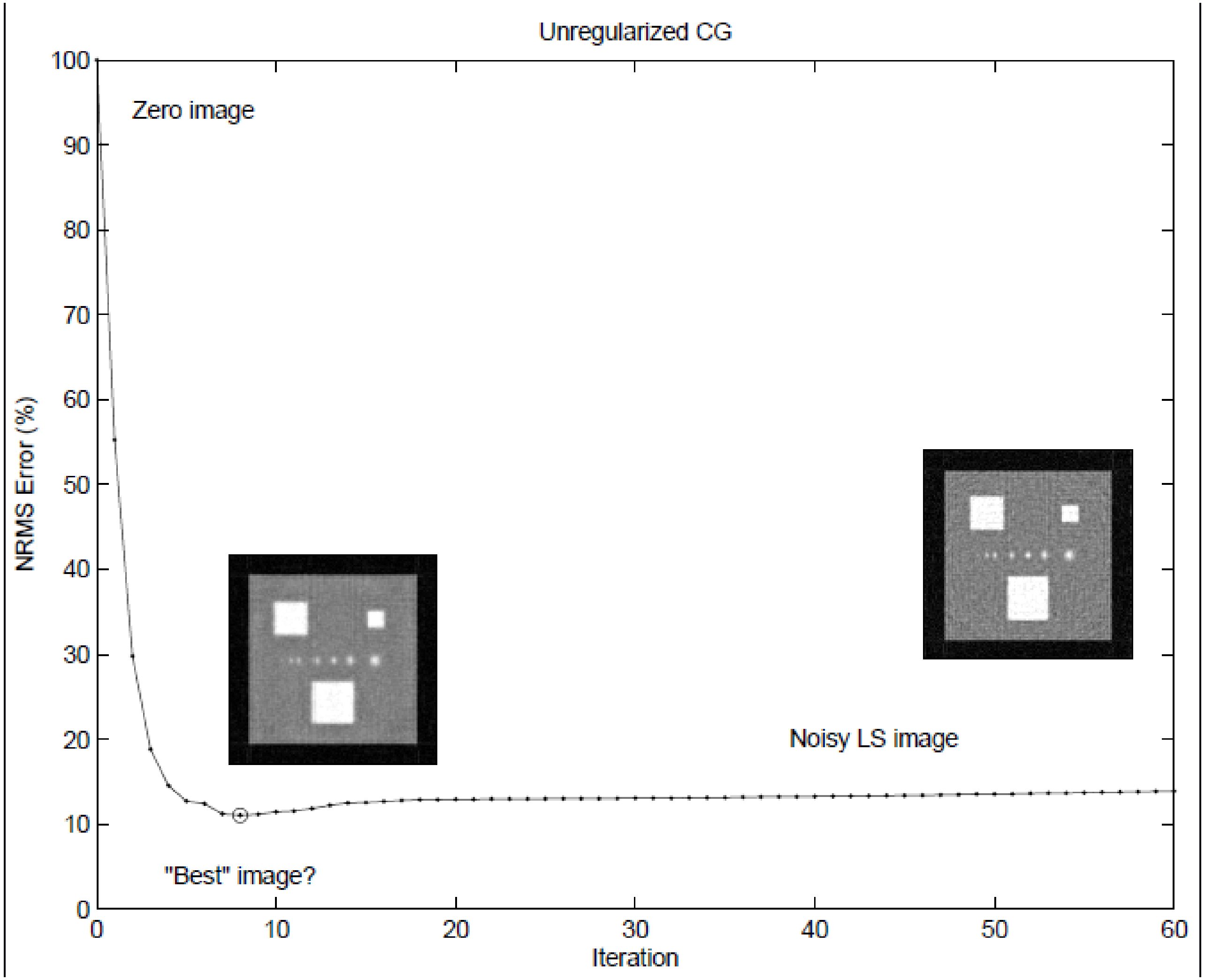

- Complexity: When to stop → A solution: regularization

UNREGULARIZED EIGENSPECTRUM

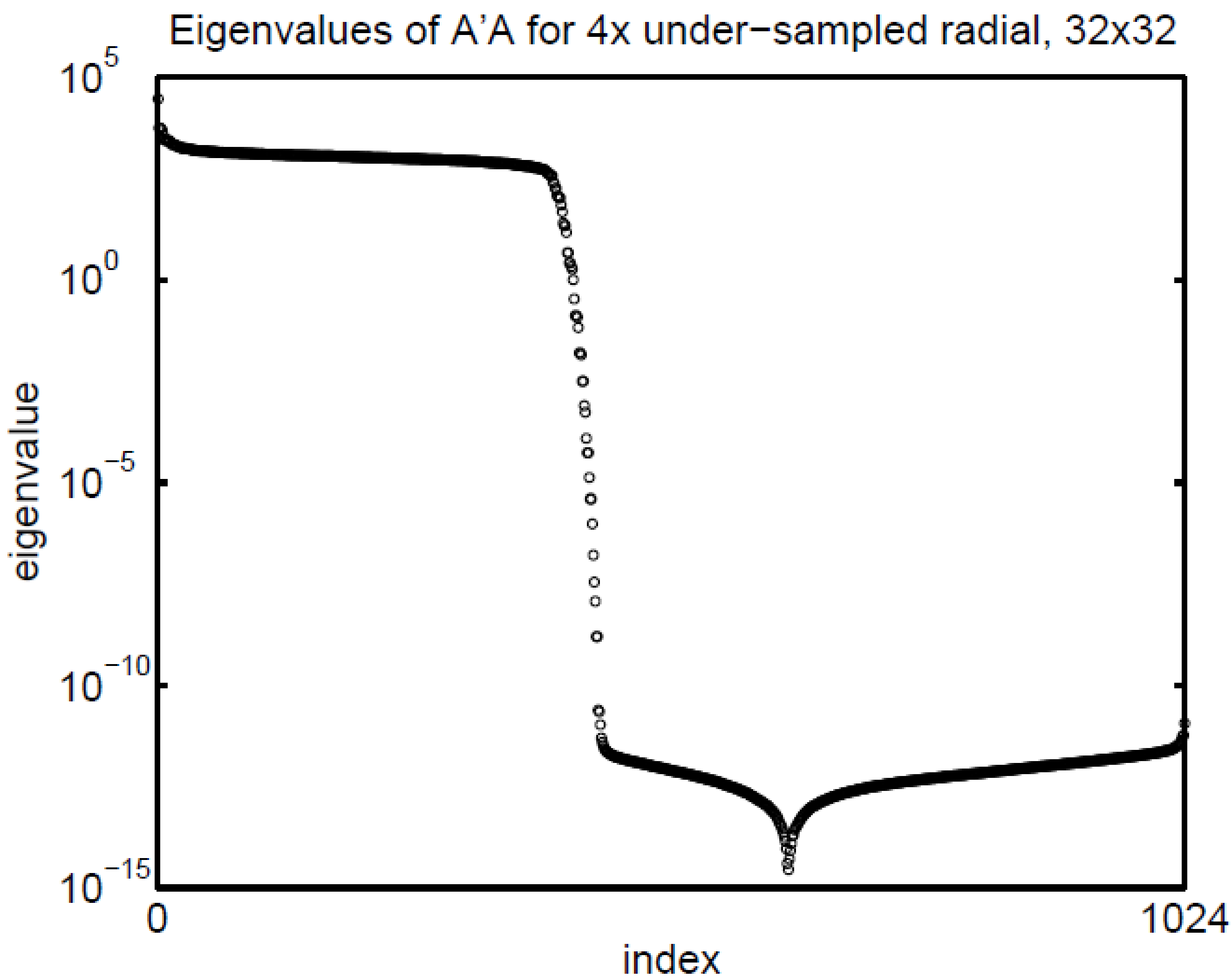

- Bad conditioning i.e. extremely large condition number $\simeq 10^{20}$

REGULARIZED EXAMPLE: IMAGE COMPARISON

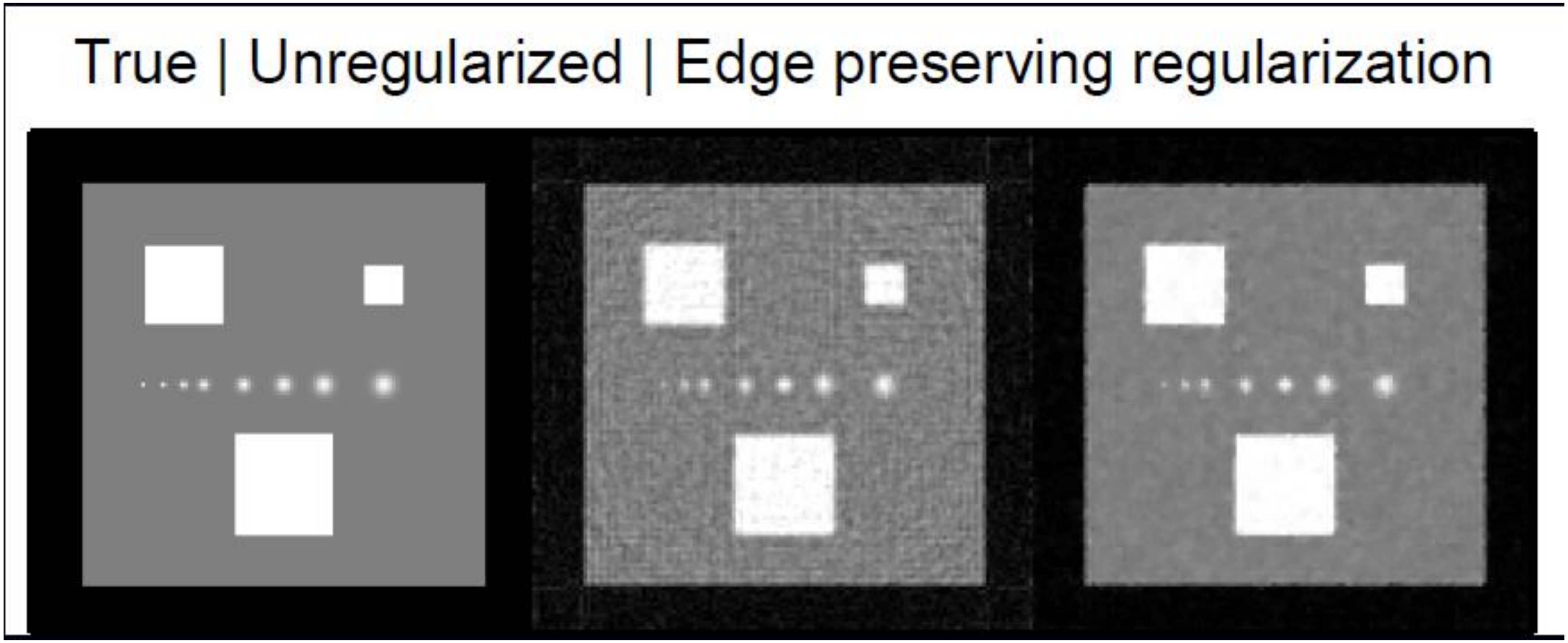

REGULARIZED EXAMPLE: RMS ERROR

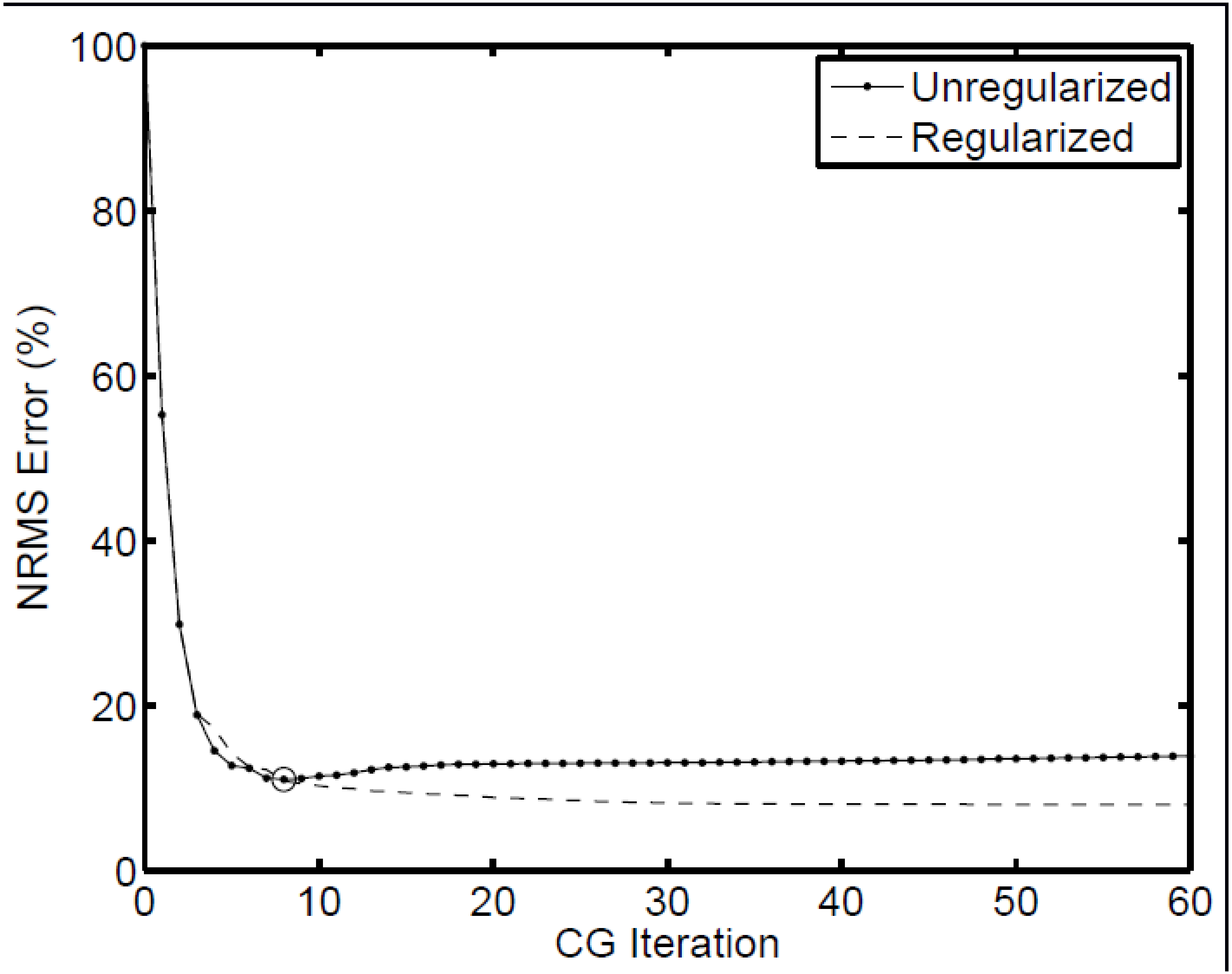

REGULARIZED LEAST SQUARES ESTIMATION

- Estimate object by minimizing a *regularized* criterion:

$$\widehat{\boldsymbol{x}} = \arg\min_{\boldsymbol{x}\in\mathbb{C}^n} \mathcal{J}(\boldsymbol{x}) \quad \mathcal{J}(\boldsymbol{x}) = \|\boldsymbol{y} - \boldsymbol{H}\boldsymbol{x}\|^2 + \alpha\,\mathcal{R}(\boldsymbol{x})$$

  - Data fidelity term $\|\boldsymbol{y} - \boldsymbol{H}\boldsymbol{x}\|^2$
  - Regularizing term $\mathcal{R}(\boldsymbol{x})$ controls noise by penalizing roughness:

$$\mathcal{R}(\boldsymbol{x}) \approx \int \|\nabla \boldsymbol{x}(\vec{r})\|^2 \, d\vec{r}$$

  - Regularization parameter $\alpha > 0$ controls trade-off between spatial resolution and noise
  - Equivalent to Bayesian MAP estimation with prior $\propto e^{-\alpha\mathcal{R}(\boldsymbol{x})}$
- Complexities:
  - Choosing $\mathcal{R}(\boldsymbol{x})$
  - Choosing α
  - Computing minimizer rapidly

QUADRATIC REGULARIZATION

- 1D example: Squared differences between neighboring pixel values:

$$\mathcal{R}(\boldsymbol{x}) = \sum_{j=2}^{n} \frac{1}{2}|x_j - x_{j-1}|^2 = \frac{1}{2}\|\boldsymbol{C}\boldsymbol{x}\|^2$$

$$\boldsymbol{C} = \begin{bmatrix} -1 & 1 & 0 & 0 & \cdots & 0 \\ 0 & -1 & 1 & 0 & \cdots & 0 \\ \vdots & \ddots & \ddots & \ddots & & \\ 0 & \cdots & 0 & 0 & -1 & 1 \end{bmatrix} \quad \boldsymbol{C}\boldsymbol{x} = \begin{bmatrix} x_2 - x_1 \\ \ddots \\ x_n - xx_{n-1} \end{bmatrix}.$$

- For 2D and higher-order differences, modify differencing matrix $\boldsymbol{C}$.
- Closed-form solution:

$$\begin{aligned} \widehat{\boldsymbol{x}} &= \arg\min_{\boldsymbol{x} \in \mathbb{C}^n} \|\boldsymbol{y} - \boldsymbol{H}\boldsymbol{x}\|^2 + \alpha \|\boldsymbol{C}\boldsymbol{x}\|^2 \\ &= \left[\boldsymbol{H}^*\boldsymbol{H} + \alpha \boldsymbol{C}^t\boldsymbol{C}\right]^{-1}\boldsymbol{H}^*\boldsymbol{y} \end{aligned}$$

(A formula of limited practical use for computing $\widehat{\boldsymbol{x}}$).

CHOOSING THE REGULARIZATION PARAMETER

- Spatial resolution analysis [Fessler and Rogers, 1996]:

$$
\begin{aligned}
\mathrm{E}[\hat{\boldsymbol{x}}] &= \left[\boldsymbol{H}^*\boldsymbol{H} + \alpha\, \boldsymbol{C}^t\boldsymbol{C}\right]^{-1}\boldsymbol{H}^*\mathrm{E}[\boldsymbol{y}] \\
&= \left[\boldsymbol{H}^*\boldsymbol{H} + \alpha\, \boldsymbol{C}^t\boldsymbol{C}\right]^{-1}\boldsymbol{H}^*\boldsymbol{H}\boldsymbol{x} \\
&= \underbrace{\left[\boldsymbol{T} + \alpha\, \boldsymbol{C}^t\boldsymbol{C}\right]^{-1}\boldsymbol{T}}_{\text{blur}}\,\boldsymbol{x}
\end{aligned}
$$

- $\boldsymbol{T}$ and $\boldsymbol{C}^t\boldsymbol{C}$ are Toeplitz $\Rightarrow$ blur is approximately shift-invariant.
- Blurring operating in the frequency domain:

$$
L(\omega) = \frac{T(\omega)}{T(\omega) + \alpha R(\omega)}
$$

  - $T(\omega_k) = FFT(\boldsymbol{T}\boldsymbol{e}_j) = FFT(\boldsymbol{H}^*\boldsymbol{H}\boldsymbol{e}_j)$ (low-pass filter)
  - $R(\omega_k) = FFT(\boldsymbol{C}^t\boldsymbol{C}\boldsymbol{e}_j)$ (high-pass filter)
- Adjust α to achieve desired spatial resolution.

SPATIAL RESOLUTION EXAMPLE

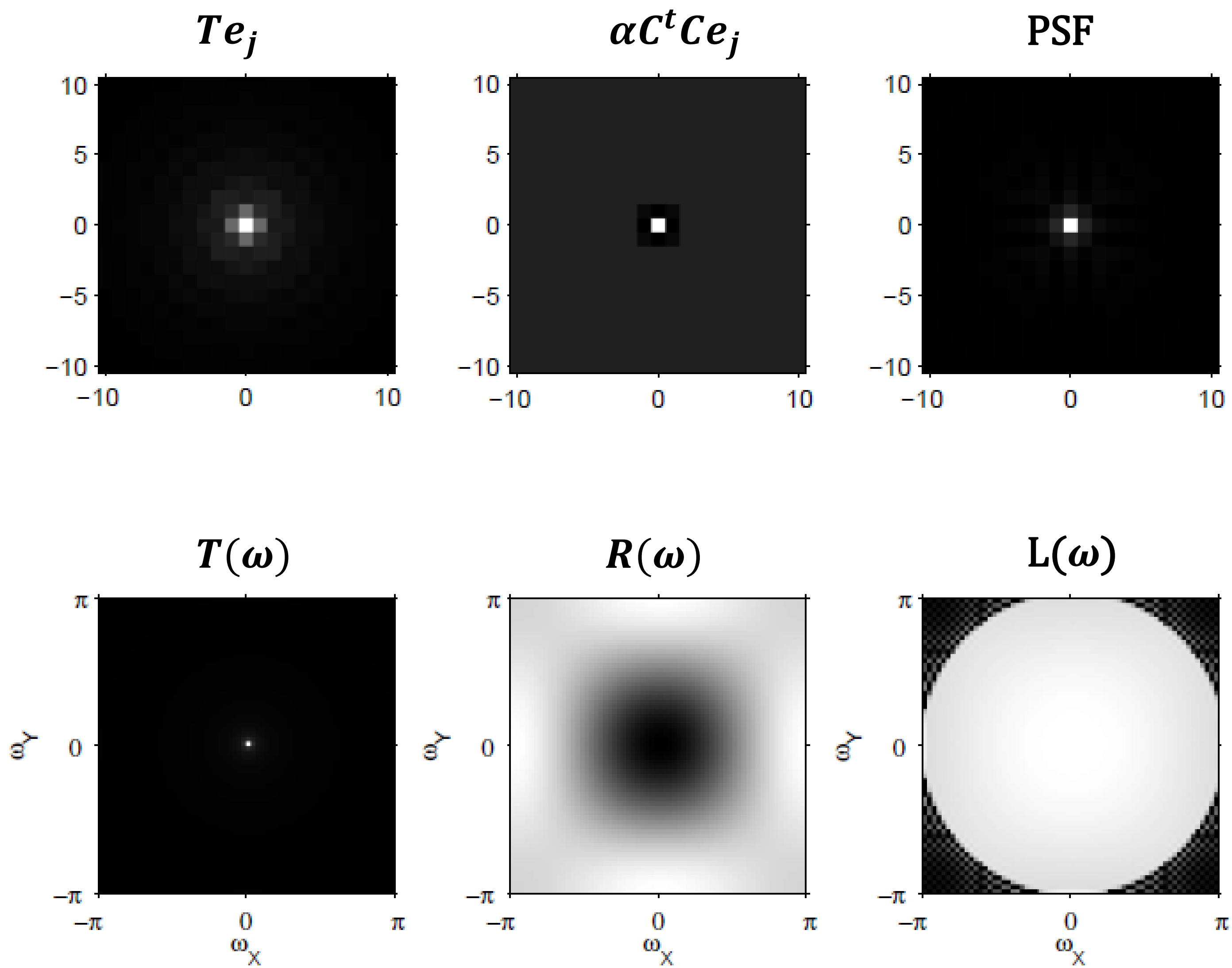

Radial k-space trajectory, FWHM of PSF is 1.2 pixels

SPATIAL RESOLUTION EXAMPLE: PROFILES

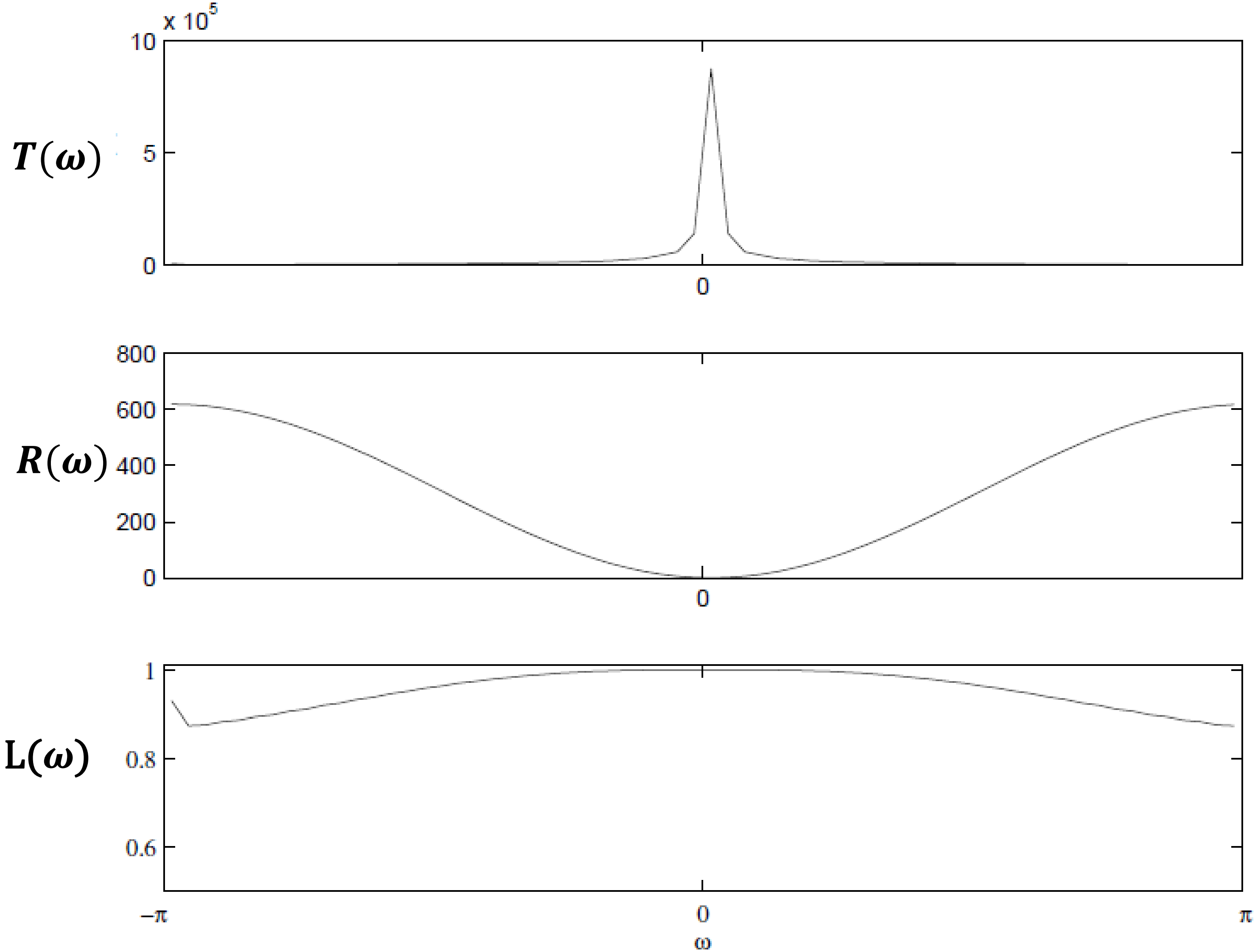

RESOLUTION/NOISE TRADE-OFFS

- Noise analysis:

$$\begin{aligned}\mathrm{Cov}\left[\hat{\boldsymbol{x}}\right] &= \left[\boldsymbol{H}^*\boldsymbol{H} + \alpha\, \boldsymbol{C}^t\boldsymbol{C}\right]^{-1}\boldsymbol{H}^*\mathrm{Cov}\left[\boldsymbol{y}\right]\boldsymbol{H}\left[\boldsymbol{H}^*\boldsymbol{H} + \alpha\, \boldsymbol{C}^t\boldsymbol{C}\right]^{-1} \\ &= \left[\boldsymbol{T} + \alpha\, \boldsymbol{C}^t\boldsymbol{C}\right]^{-1}\boldsymbol{H}^*\mathrm{Cov}\left[\boldsymbol{n}\right]\boldsymbol{H}\left[\boldsymbol{T} + \alpha\, \boldsymbol{C}^t\boldsymbol{C}\right]^{-1}\end{aligned}$$

- Using circulant approximations to $\boldsymbol{T}$ and $\boldsymbol{C}^t\boldsymbol{C}$ yields:

$$\mathrm{var}\left[\hat{x}_j\right] \approx \sigma_n^2 \sum_k \frac{T(\omega_k)}{(T(\omega_k) + \alpha R(\omega_k))^2}$$

  - $T(\omega_k) = \mathit{FFT}(\boldsymbol{T}\boldsymbol{e}_j)$ (low-pass filter)
  - $R(\omega_k) = \mathit{FFT}(\boldsymbol{C}^t\boldsymbol{C}\boldsymbol{e}_j)$ (high-pass filter)

$\Longrightarrow$ Predicting reconstructed image noise requires just 2 FFTs.

- Adjust α to achieve desired spatial resolution/noise trade-off.

RESOLUTION/NOISE TRADE-OFFS EXAMPLE

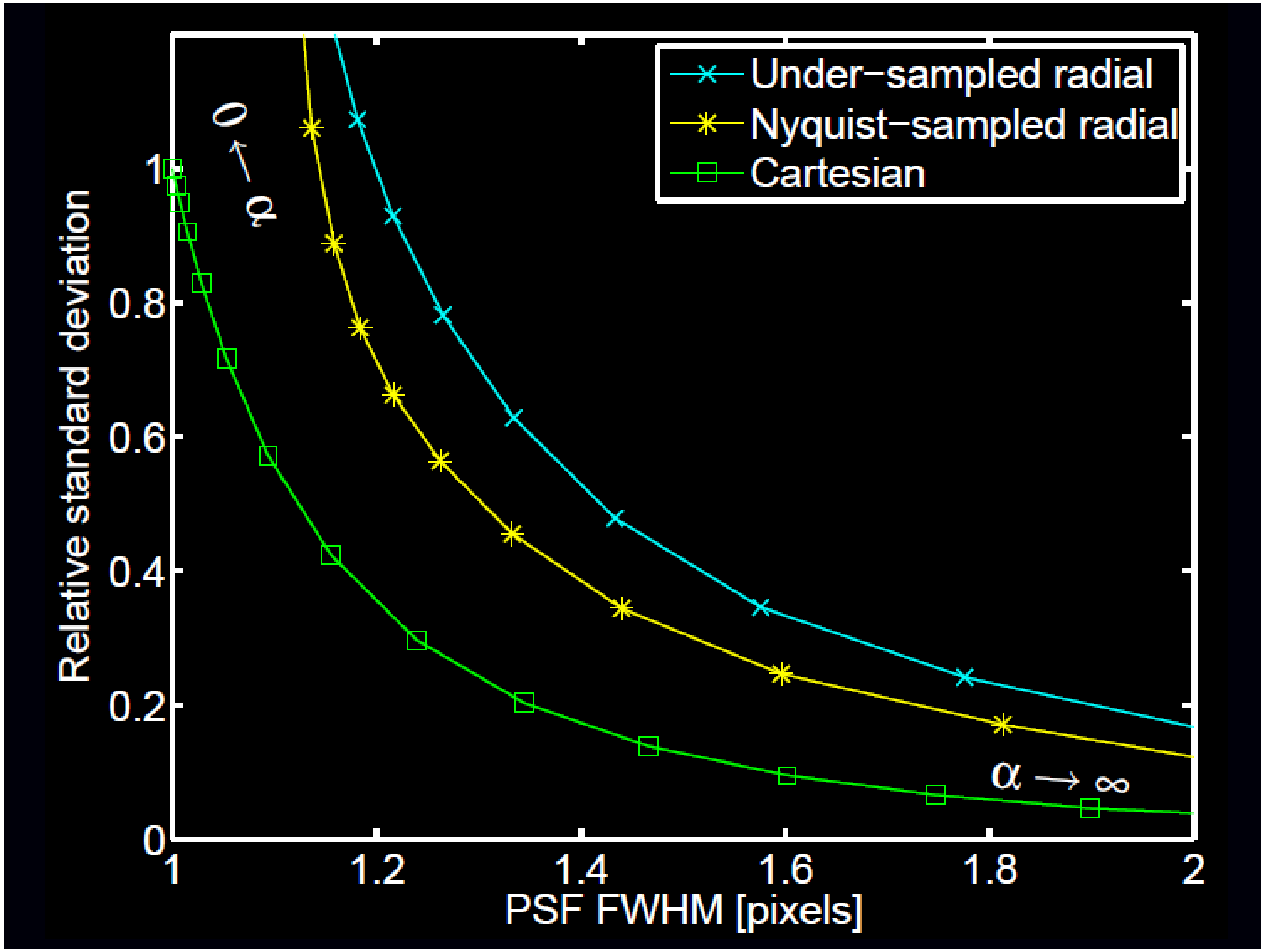

In short: one can choose α rapidly and predictably for quadratic regularization

NON-QUADRATIC REGULARIZATION

- Quadratic regularization is simple and reduces noise but impairs spatial resolution.
- Non-quadratic regularization attempts to circumvent this trade-off
  - Edge-preserving regularization has been intensively investigated for MRI:

$$\mathcal{R}(\boldsymbol{x}) = \sum_{j=1}^{n} \frac{1}{2} \Psi([\boldsymbol{C}\boldsymbol{x}]_j)$$

where Ψ rises less rapidly than a parabola

- Ex. Hyperbola function: $\Psi(t) \triangleq \delta^2(\sqrt{1+(t/\delta)^2} - 1)$. **[Charbonnier et al, IEEE IP 997]**
- Ex. Huber function: $\Psi(t) \triangleq \begin{cases} t^2/2 & |t| \leqslant \delta \\ \delta|t| - \delta^2/2 & |t| > \delta \end{cases}$.

- Challenges
  - Choosing regularization parameter(s)
  - More complicated optimization (essentially solved in the convex case)
  - Analysis/prediction of resolution and noise properties is difficult.

NON-QUADRATIC POTENTIAL FUNCTIONS

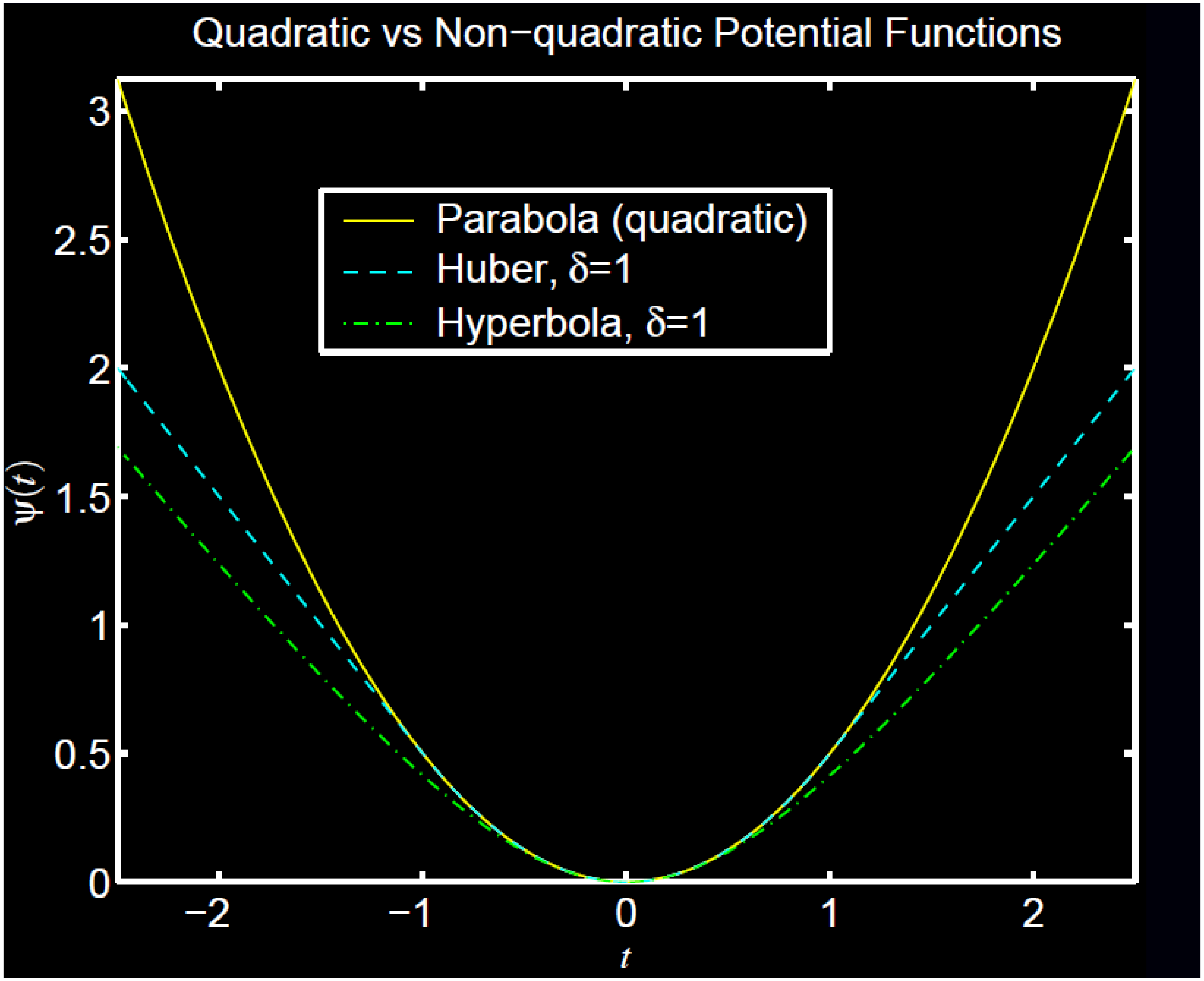

Lower cost for large differences → edge preservation

EDGE-PRESERVING REGULARIZATION EXAMPLE

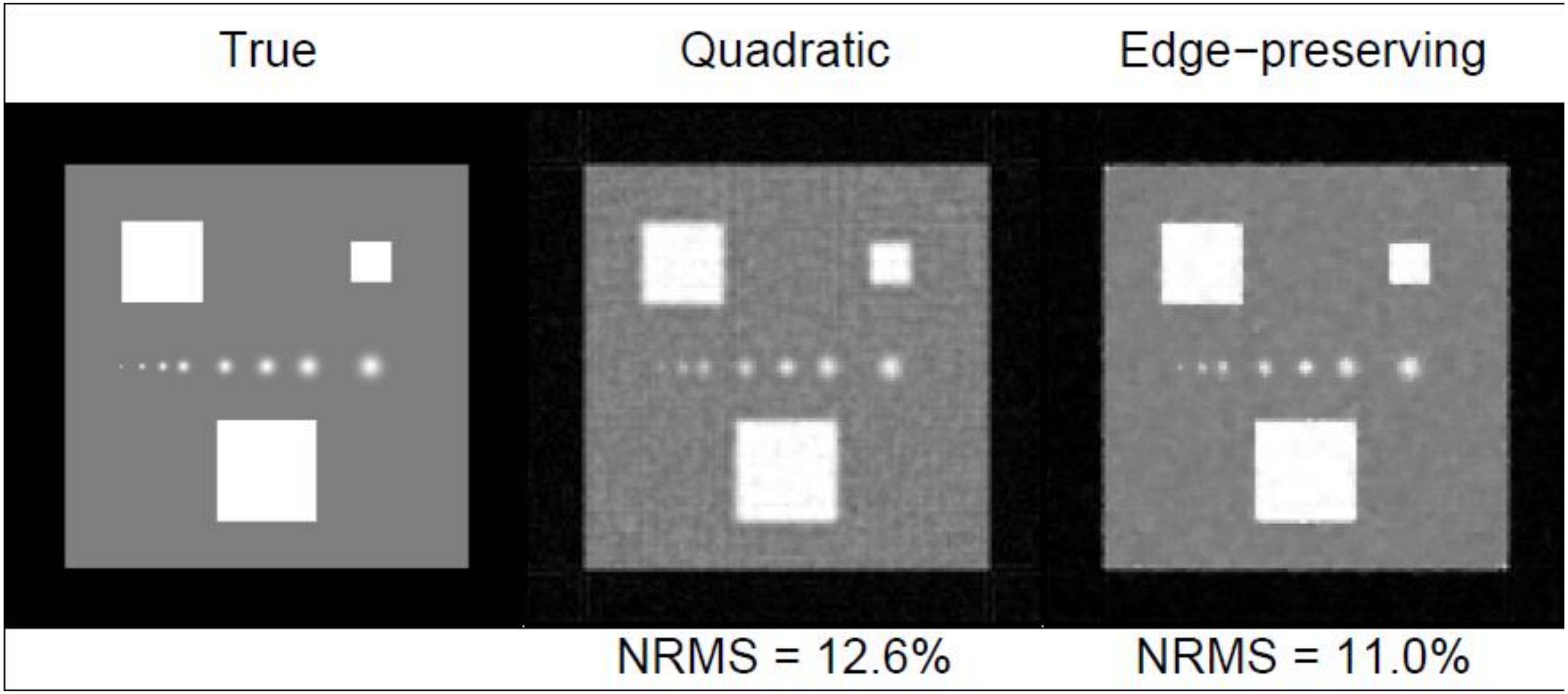

MODE-BASED IMAGE RECONSTRUCTION

- MR signal equation with more complete physics:

$$s(t) = \int x(\vec{r})\, S_{\text{coil}}(\vec{r}) e^{-(\imath\omega(\vec{r})+R_2^*(\vec{r}))t} e^{-2\imath\pi\vec{\kappa}(t)\cdot\vec{r}}\, d\vec{r}$$

$$y_i = s(t_i) + n_i, \quad i =, \ldots, m$$

  - S_{coil}: Receiver coil sensitivity pattern(s) (for SENSE)
  - $\omega(\vec{r})$: Off-resonance frequency map (due to field inhomogeneity/magnetic susceptibility)
  - $R_2^* = 1/T_2^*$: Relaxation map

- Other physical factors:
  - Eddy currents: errors in $\vec{\kappa}(t)$
  - Concomitant gradient terms (cross-talks)
  - Motion
  - ...

Goals?

FIELD INHOMOGENEITY –CORRECTED RECONSTRUCTION

- Key reference [Sutton et al., 2003, Fessler et al., 2005]
- Motivation: Critical for functional MRI in brain regions near air/bone interfaces (e.g., sinus cavities)

$$s(t) = \int x(\vec{r}) S_{\text{coil}}(\vec{r}) e^{-(\imath\omega(\vec{r}) + R_2^*(\vec{r}))t} e^{-2\imath\pi\vec{\kappa}(t)\cdot\vec{r}} \, d\vec{r}$$

- Goal: Reconstruct $x(\vec{r})$ given field map $\omega(\vec{r})$

(Assume all other terms are known or unimportant).

OUTLINE

Part IV: Parallel imaging

BACKGROUND: MRI IS SLOW…

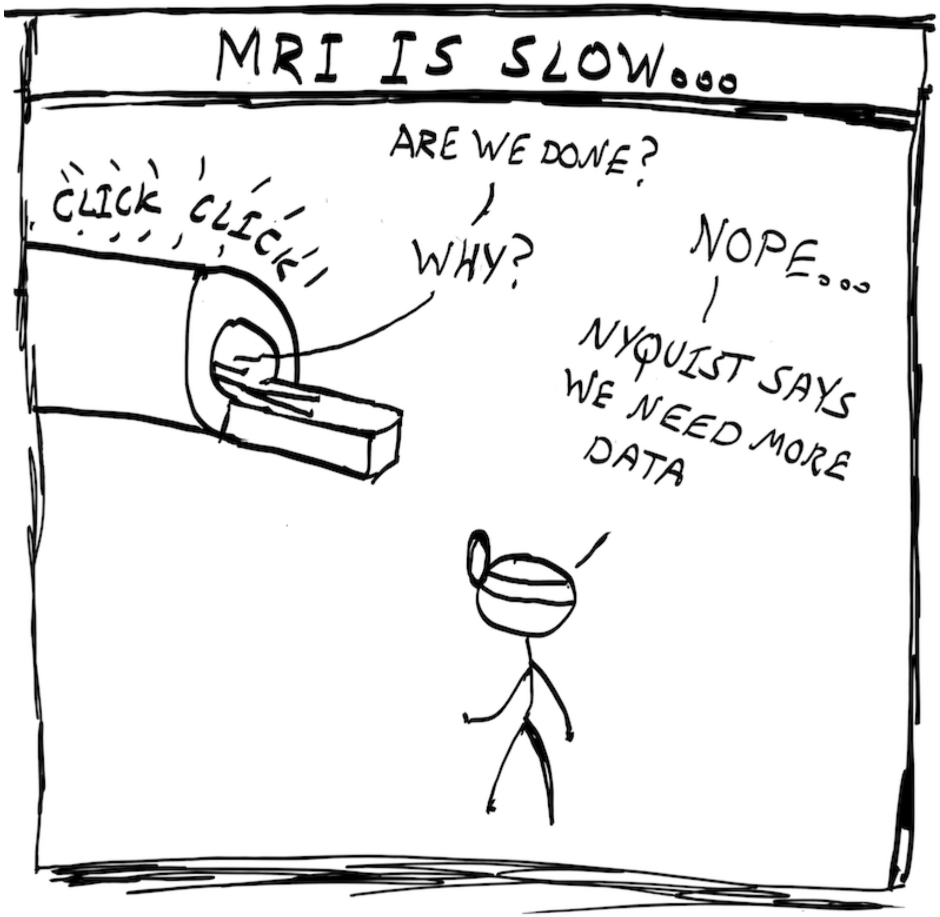

Michael Lustig, http://www.eecs.berkeley.edu/~mlustig/CS.html

BACKGROUND: WHY IS IT SO SLOW?

The sampling frequency should be at least twice the highest frequency contained in the signal

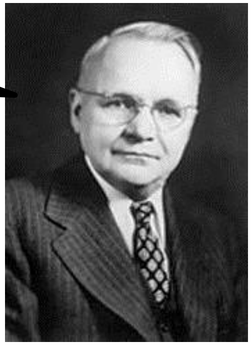

Harry Nyquist

If not...

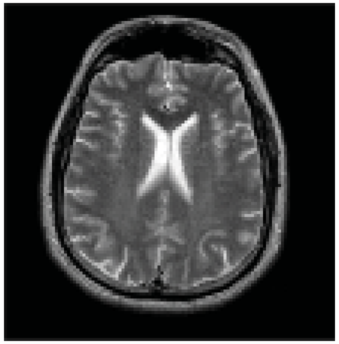

becomes…

Aliasing artifact

(Zhang et al. 2013)

EXAMPLE: 3D-image of Baboon whole Brain T2* at high resolution iso-200μm

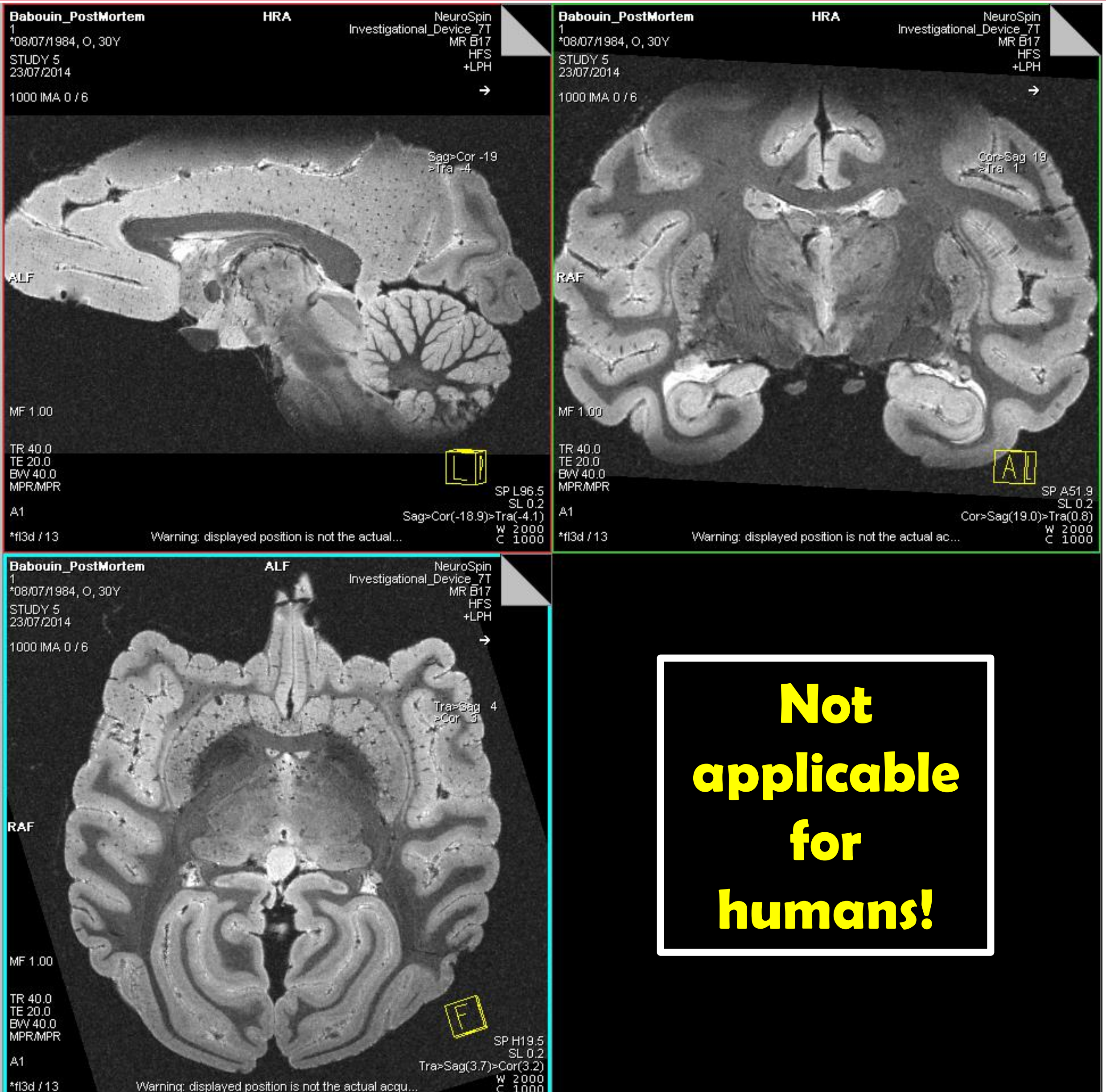

Nova Medical 1Tx/32Rx

Natif SNR~7.6 (WM)
FOV 205x205x52mm3

Matrix: 1024x1024x256
~270 million samples!!
1 average only!

Displayed Reco:
0.2x0.2x0.2mm3

TA~2h54min

Raw data size: 137GB
Dicom data size: 1.0GB

(Courtesy of A. Vignaud & S. Mériaux)

UNDERSAMPLING TO REDUCE ACQUISITION TIME

- Can we reduce the acquisition time by measuring fewer samples and still be able to reconstruct nice images?

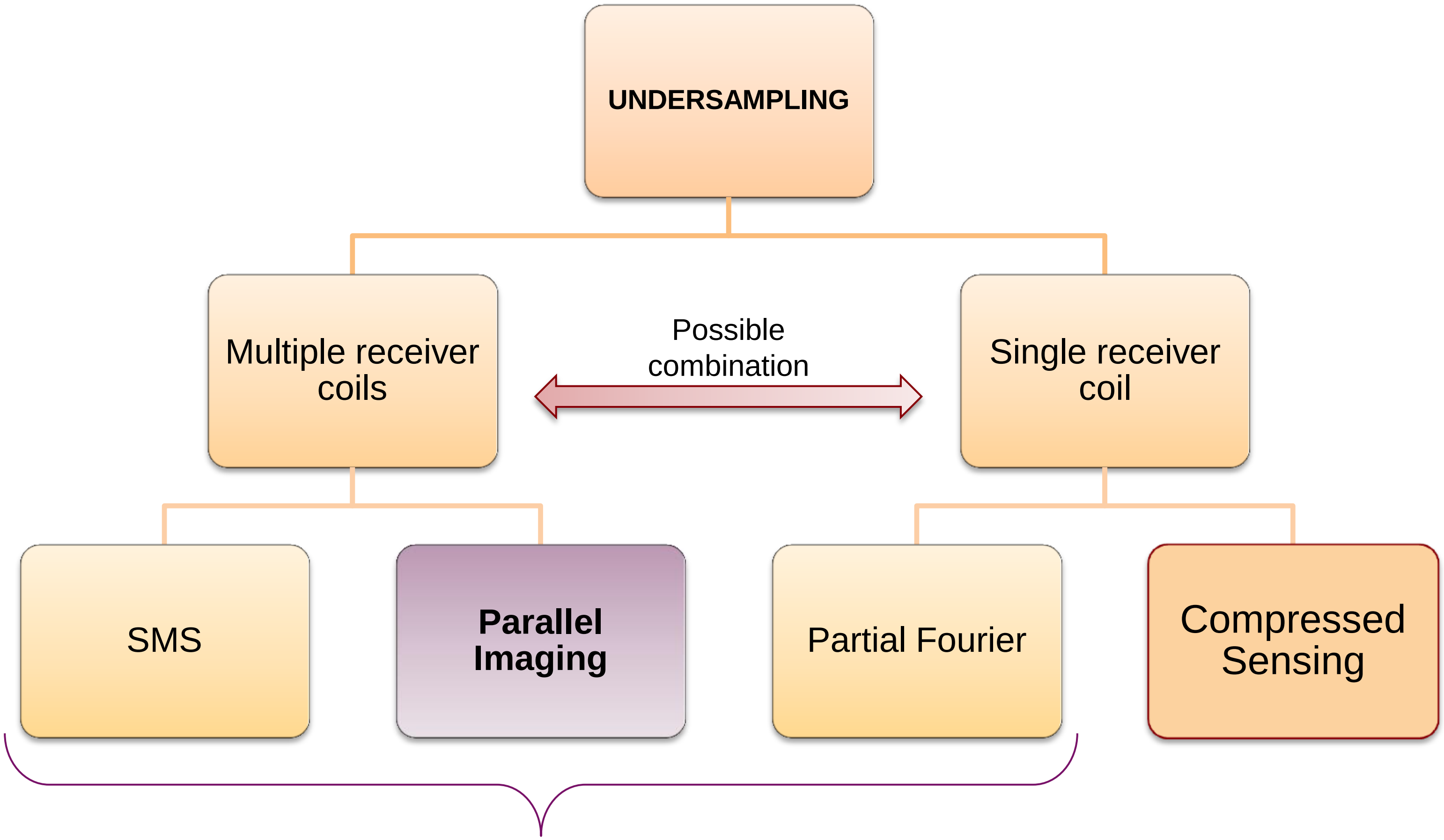

Limitations: - R = acceleration factor ≤ 6
- SNR drops rapidly with R

OBJECTIVES OF PARALLEL IMAGING (PMRI)

Combining the signal of multiple coils

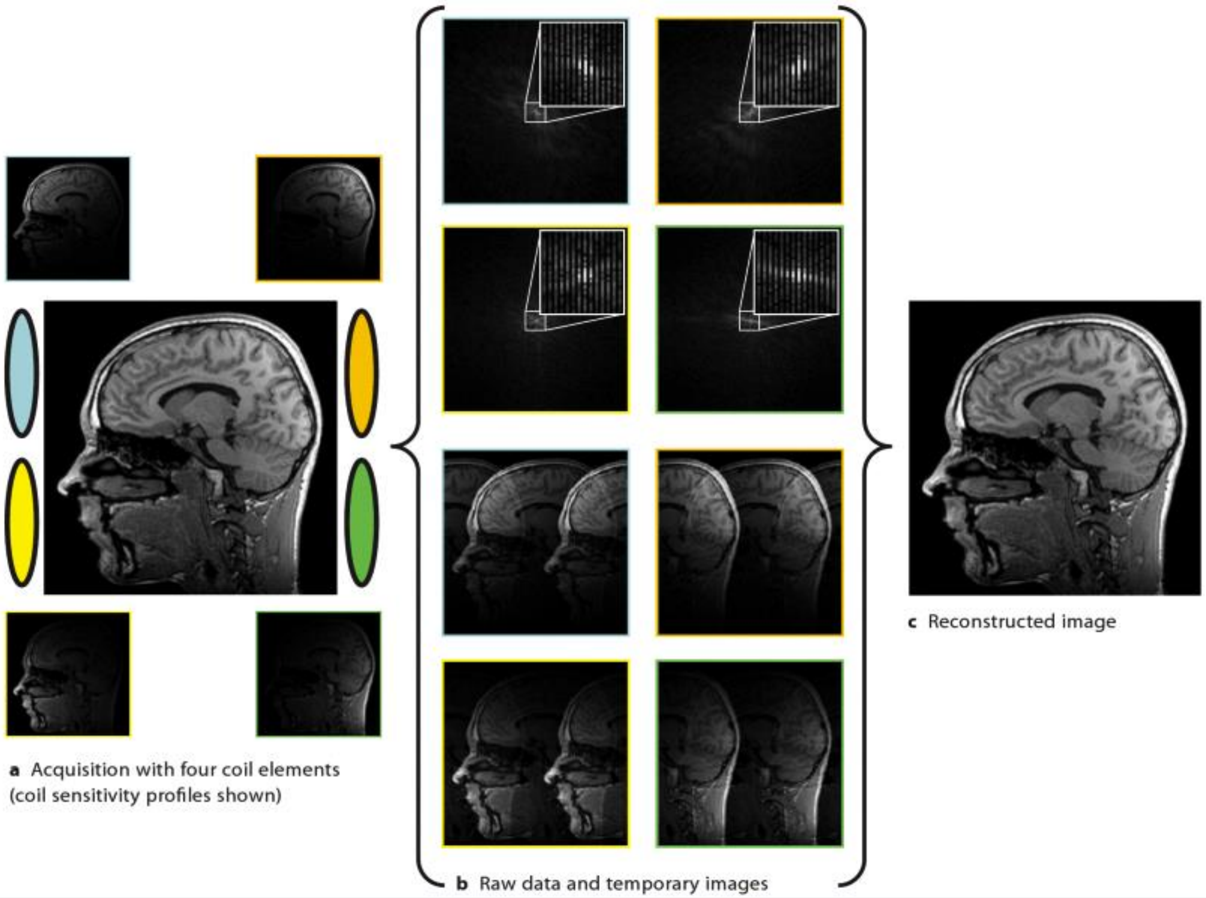

a Acquisition with four coil elements (coil sensitivity profiles shown)

b Raw data and temporary images

- ✓ Reduce scan time
- ✓ Improve spatial / temporal resolution
- ✓ Limit geometric distorsions

- ✗ Decrease the SNR
- ✗ Non-homogeneous coils

EXAMPLE IN ANATOMICAL MRI

Reduce scanning time at fixed spatial resolution

$1 \times 1 \times 1.1$ mm^3 — 9'14"

Standard acquisition

$R = 2$—$1 \times 1 \times 1.1$ mm^3 — 5'03"

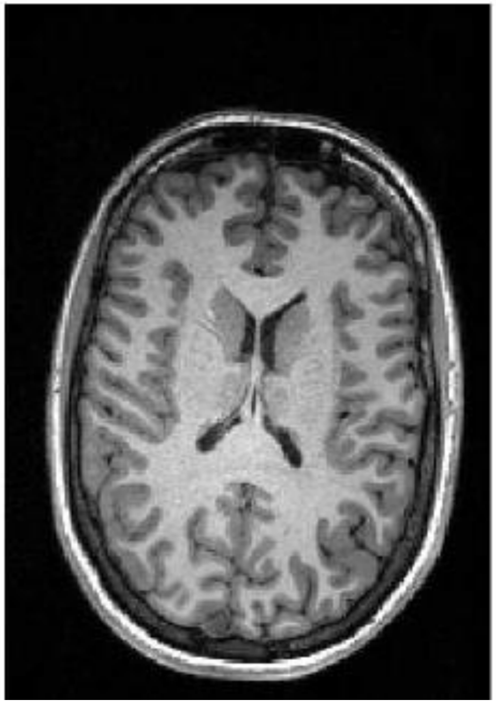

Parallel acquisition

$R = 4$—$1 \times 1 \times 1.1$ mm^3 — 2'59"

Parallel acquisition

EXAMPLE IN FUNCTIONAL MRI (EPI SEQUENCE)

Improve spatial resolution at fixed TR

$3 \times 3 \times 3$ mm^3 — 5'14"

Standard acquisition

$R = 2$ — $2 \times 2 \times 3$ mm^3 — 5'14"

Parallel acquisition

$R = 4$ — $2 \times 2 \times 3$ mm^3 — 5'22"

Parallel acquisition

PARALLEL MRI PRINCIPLE

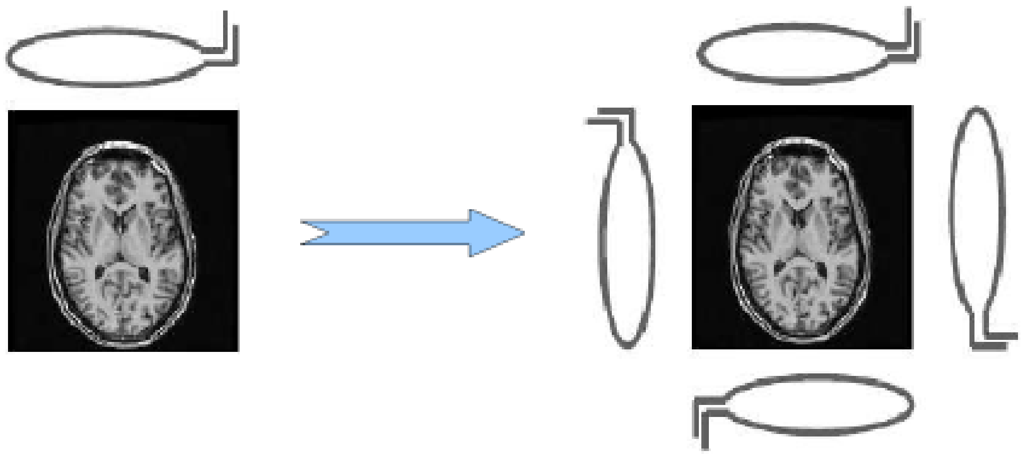

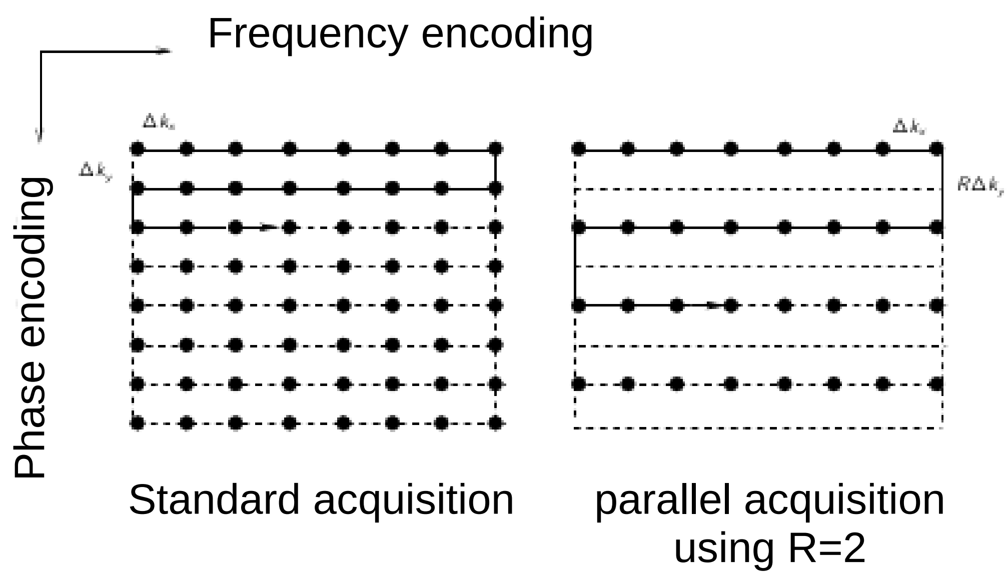

SPATIAL COIL SENSITIVITIES

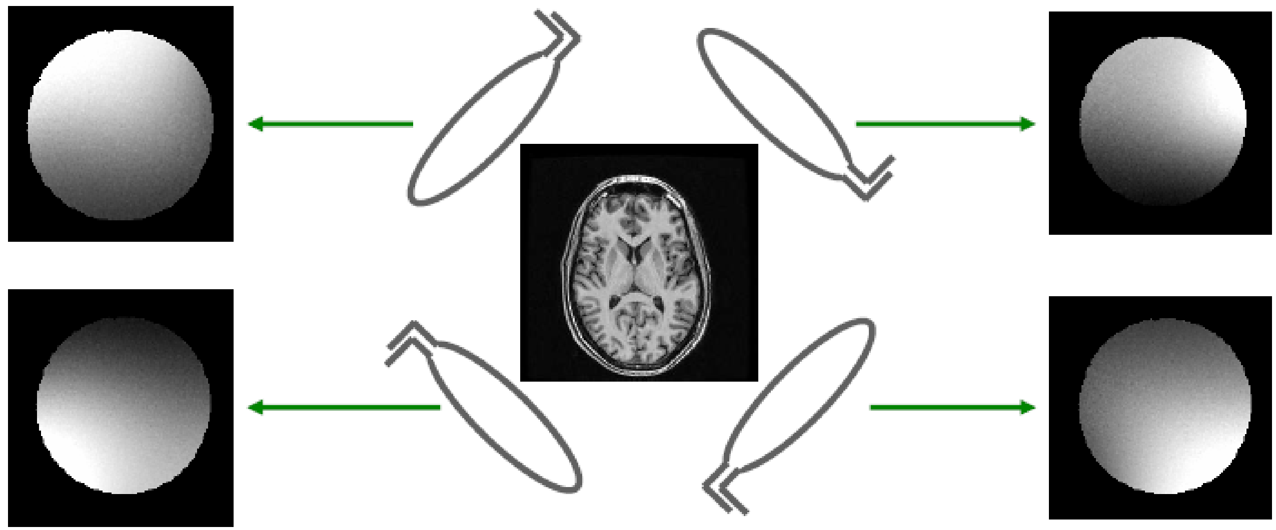

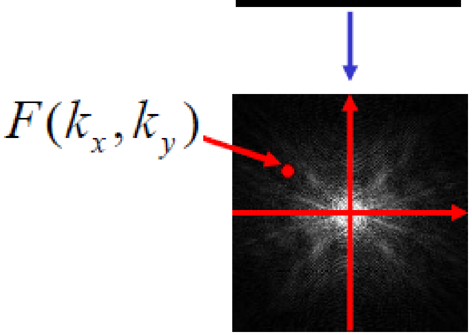

$$s_\ell(t) = \int x(\vec{r})\, S_\ell(\vec{r}) e^{-2\imath\pi\vec{\kappa}(t)\cdot\vec{r}}\, d\vec{r}, \quad \ell = 1, \ldots, L$$

$$y_{i,\ell} = s_\ell(t_i) + n_{i,\ell}, \quad i =, \ldots, m$$

PARALLEL MRI RECONSTRUCTION TECHNIQUES

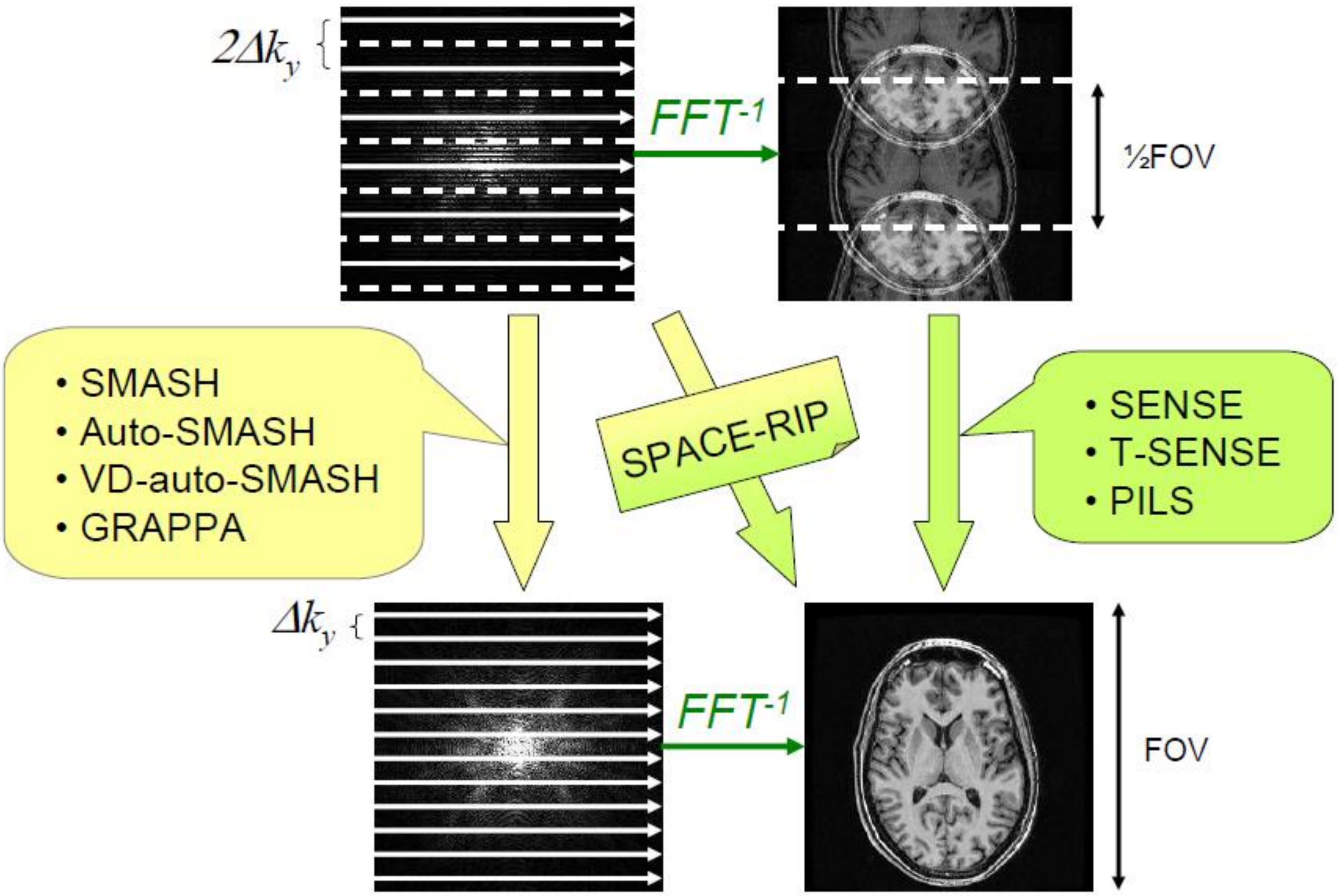

K-SPACE ACQUISITION

Full k-space sampling

k-space
Under-sampling
(R=2)

Acceleration factor

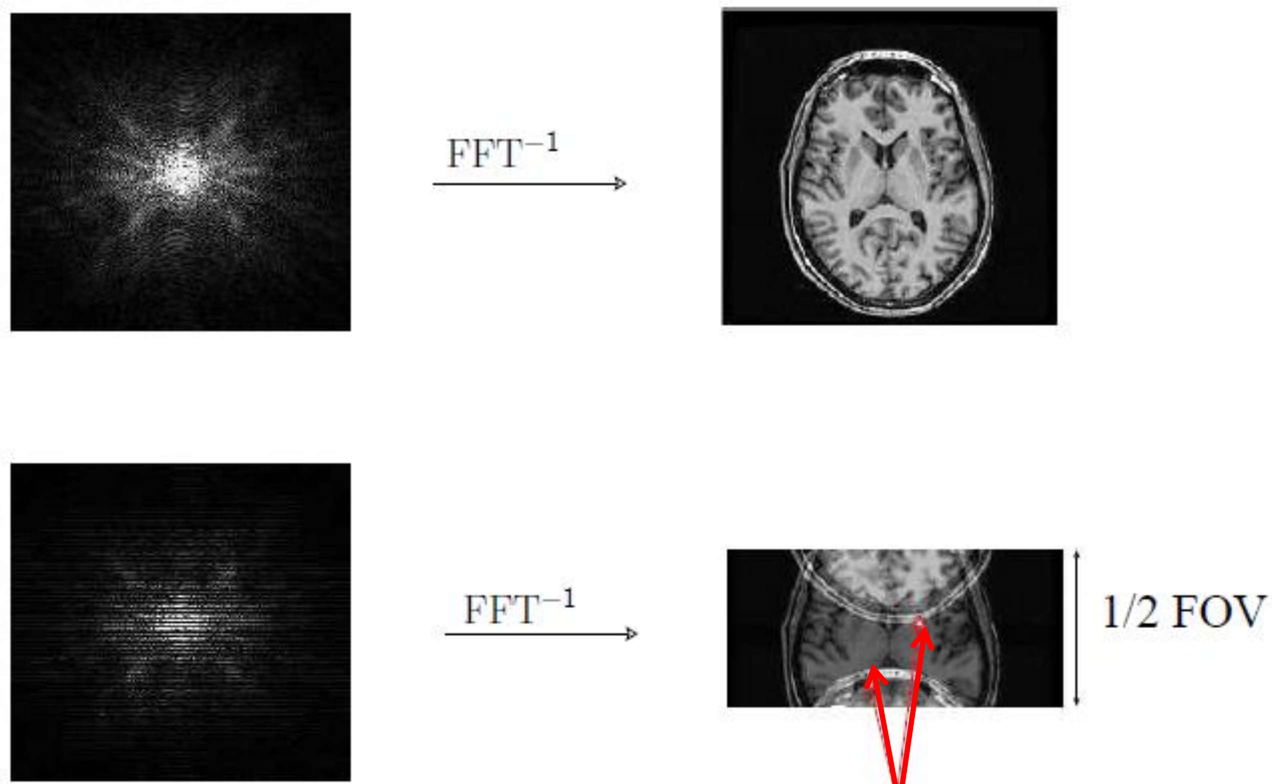

Aliasing artifacts

K-SPACE ACQUISITION

Full k-space sampling

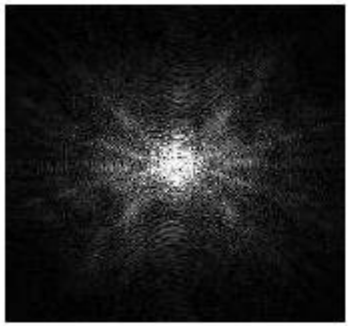

$\xrightarrow{\mathrm{FFT}^{-1}}$

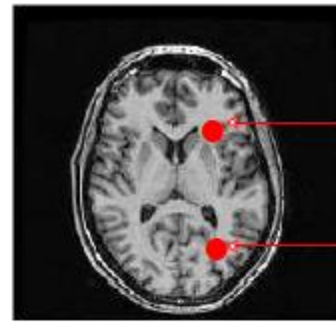

$x(r_1)$

$x(r_2)$

k-space
Under-sampling
(R=2)

Acceleration factor

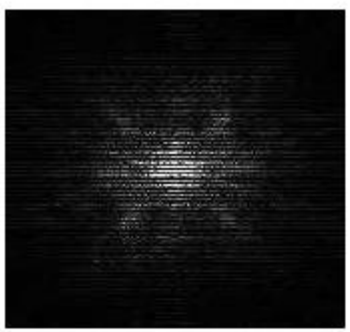

$\xrightarrow{\mathrm{FFT}^{-1}}$

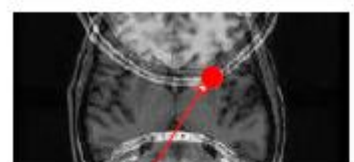

1/2 FOV

$$y(r) = x(r_1) + x(r_2)$$

SENSITIVITY ENCODING IMAGING

2 coils
R=2

[Pruessman et al, MRM 1999]

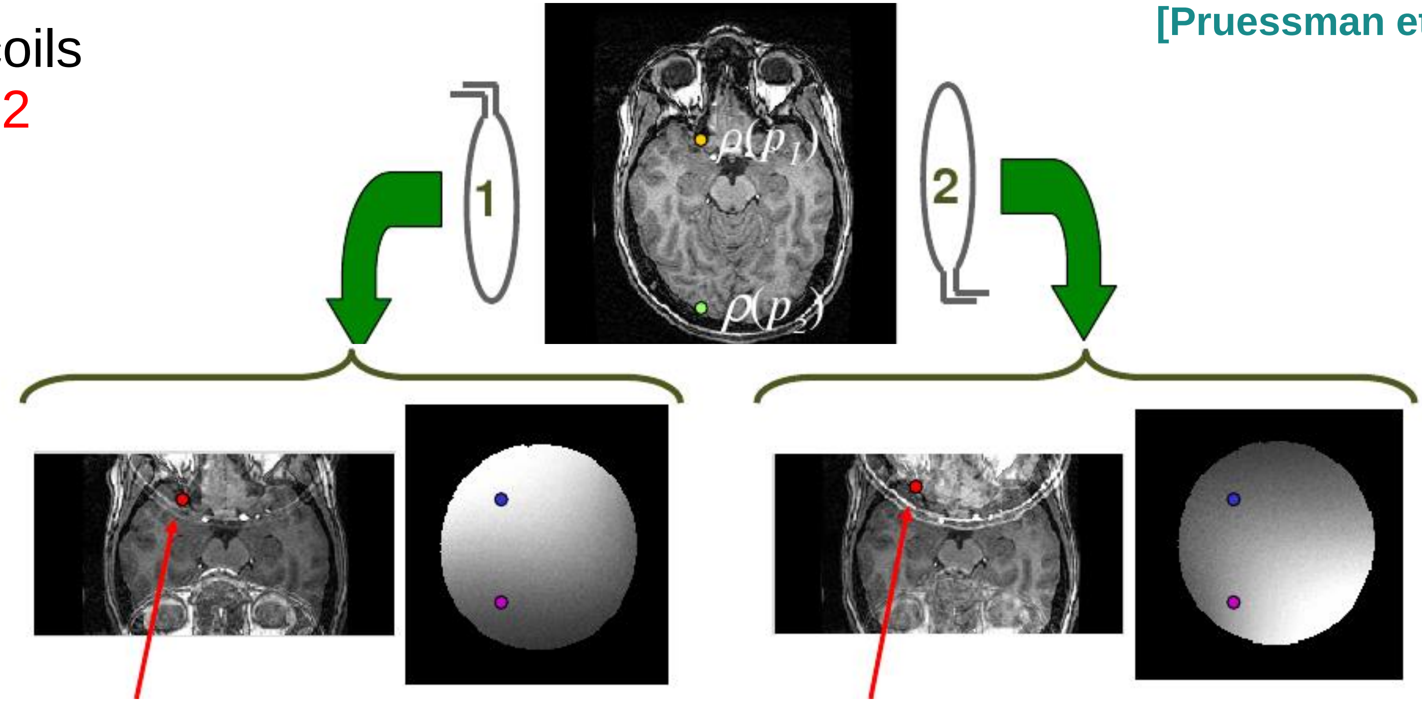

$$y_1(\vec{r}) = S_1(\vec{r}_1)x(\vec{r}_1) + S_1(\vec{r}_2)x(\vec{r}_2) + n_1(\vec{r})$$

$$y(\vec{r}) = S_2(\vec{r}_1)x(\vec{r}_1) + S_2(\vec{r}_2)x(\vec{r}_2) + n_2(\vec{r})$$

$$\vec{r}_1 = \vec{r}$$

$$\vec{r}_2 = \vec{r} + \frac{FOV_y}{2}$$

$$\begin{bmatrix} y_1(\vec{r}) \\ y_2(\vec{r}) \end{bmatrix} = \begin{bmatrix} S_1(\vec{r}_1) & S_1(\vec{r}_2) \\ S_2(\vec{r}_1) & S_2(\vec{r}_2) \end{bmatrix} \begin{bmatrix} x(\vec{r}_1) \\ x(\vec{r}_2) \end{bmatrix} + \begin{bmatrix} n_1(\vec{r}) \\ n_2(\vec{r}) \end{bmatrix}$$

SENSITIVITY ENCODING IMAGING

[Pruessman et al, MRM 1999]

L coils
R acceleration factor

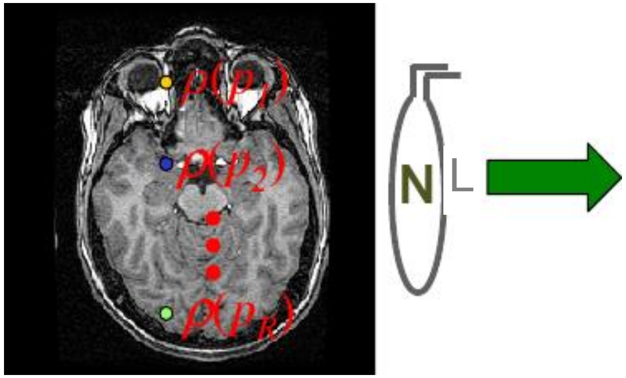

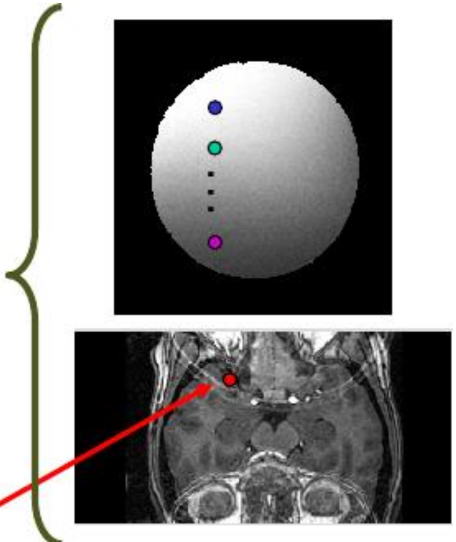

$$y_L(\vec{r}) = S_L(\vec{r}_1)x(\vec{r}_1) + S_L(\vec{r}_2)x(\vec{r}_2) + \ldots + S_L(\vec{r}_R)x(\vec{r}_R) + n_L(\vec{r})$$

$$\begin{bmatrix} y_1(\vec{r}) \\ y_2(\vec{r}) \\ \vdots \\ y_L(\vec{r}) \end{bmatrix} = \begin{bmatrix} S_1(\vec{r}_1) & \ldots & S_1(\vec{r}_R) \\ S_2(\vec{r}_1) & \ldots & S_2(\vec{r}_R) \\ \vdots & \ddots & \vdots \\ S_L(\vec{r}_1) & \ldots & S_L(\vec{r}_R) \end{bmatrix} \begin{bmatrix} x(\vec{r}_1) \\ x(\vec{r}_2) \\ \vdots \\ x(\vec{r}_R) \end{bmatrix} + \begin{bmatrix} n_1(\vec{r}) \\ n_2(\vec{r}) \\ \vdots \\ n_L(\vec{r}) \end{bmatrix}$$

$$\vec{r}_j = \vec{r} + j\,\frac{FOV_y}{R}$$

$$\Rightarrow \quad \mathbf{y}(\vec{\boldsymbol{r}}) = \boldsymbol{S}(\vec{\boldsymbol{r}})\,\boldsymbol{x}(\vec{\boldsymbol{r}}) + \boldsymbol{n}(\vec{\boldsymbol{r}})$$

Simultaneous reconstruction of R pixels of the full FOV image

COMPLEX-VALUED DATA

Subscript $\cdot_R$: real part $\Re\{\cdot\}$ of the data.

Subscript $\cdot_I$: imaginary part $\Im\{\cdot\}$

$$\begin{bmatrix} y_R(\vec{r}) \\ y_I(\vec{r}) \end{bmatrix} = \begin{bmatrix} S_R(\vec{r}) & -S_I(\vec{r}) \\ S_I(\vec{r}) & S_I(\vec{r}) \end{bmatrix} \begin{bmatrix} x_R(\vec{r}) \\ x_I(\vec{r}) \end{bmatrix} + \begin{bmatrix} n_R(\vec{r}) \\ n_I(\vec{r}) \end{bmatrix}$$

$$\Rightarrow \quad \boldsymbol{y_C}(\vec{\boldsymbol{r}}) = \boldsymbol{S_C}\,(\vec{\boldsymbol{r}})\,\boldsymbol{x_C}\,(\vec{\boldsymbol{r}}) + \boldsymbol{n_C}(\vec{\boldsymbol{r}})$$

SENSE RECONSTRUCTION

- SENSE reconstruction: Least squares formulation
  - Complex circular noise vector corrupting all channels: $\boldsymbol{n}(\vec{r})$
  - Noise covariance: $\mathrm{Cov}\left[\boldsymbol{n}_\mathrm{C}(\vec{r})\boldsymbol{n}_\mathrm{C}(\vec{r'})\right] = \boldsymbol{\Psi}\delta(\vec{r}-\vec{r'})$
  - Iterate over positions $\vec{r}$:

$$\widehat{\boldsymbol{x}}_\mathrm{C}(\vec{r}) = \underset{\boldsymbol{x}_\mathrm{C}\in\mathbb{C}^L}{\arg\min} \|\boldsymbol{y}_\mathrm{C}(\vec{r}) - \boldsymbol{S}_\mathrm{C}(\vec{r})\boldsymbol{x}_\mathrm{C}(\vec{r})\|^2_{\boldsymbol{\Psi}^{-1}}$$

$$\widehat{\boldsymbol{x}}_\mathrm{C}(\vec{r}) = \left[\boldsymbol{S}_\mathrm{C}(\vec{r})^\mathrm{H}\boldsymbol{\Psi}^{-1}\boldsymbol{S}_\mathrm{C}(\vec{r})\right]^{-1}\boldsymbol{S}_\mathrm{C}(\vec{r})^\mathrm{H}\boldsymbol{\Psi}^{-1}\boldsymbol{y}_\mathrm{C}(\vec{r})$$

  - Or more globally:

$$\widehat{\boldsymbol{x}}_\mathrm{C} = \underset{\boldsymbol{x}_\mathrm{C}\in\mathbb{C}^n}{\arg\min} \sum_{\vec{r}\in\mathrm{FOV}} \|\boldsymbol{y}_\mathrm{C}(\vec{r}) - \boldsymbol{S}_\mathrm{C}(\vec{r})\boldsymbol{x}_\mathrm{C}(\vec{r})\|^2_{\boldsymbol{\Psi}^{-1}}$$

RESULTS AT 1.5 TESLA

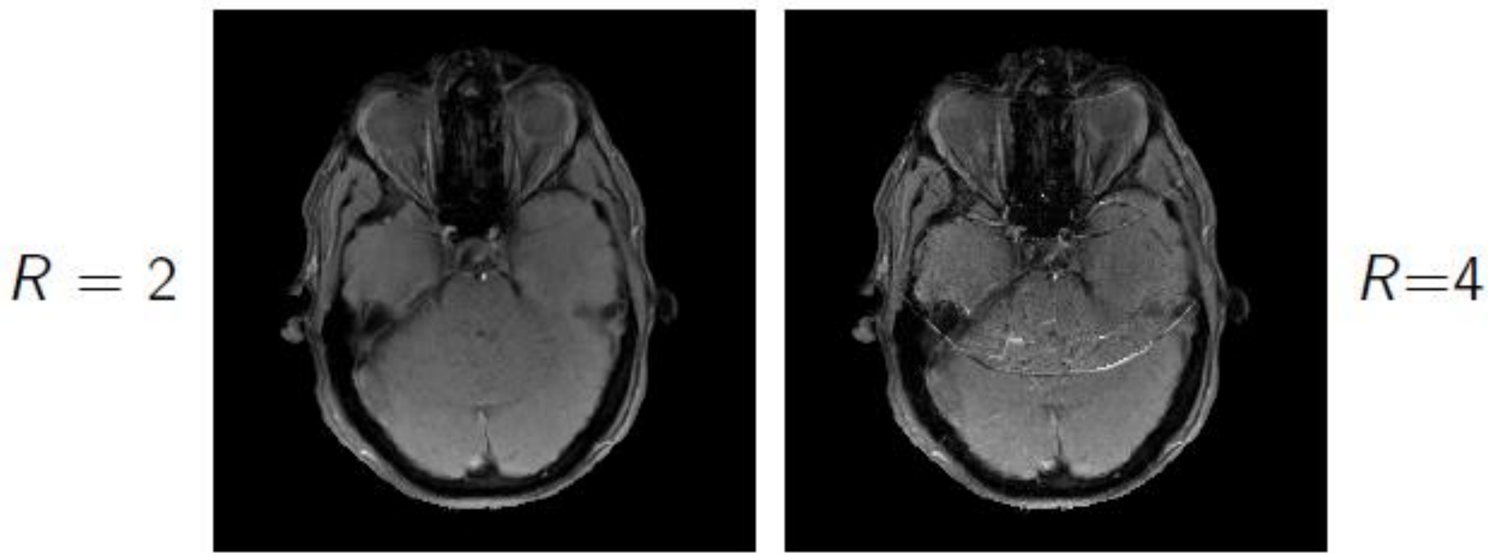

- Artifacts appear for large values of R

RESULTS AT 3 TESLA FOR R=4

- Coronal slice: same effect in the FOV center

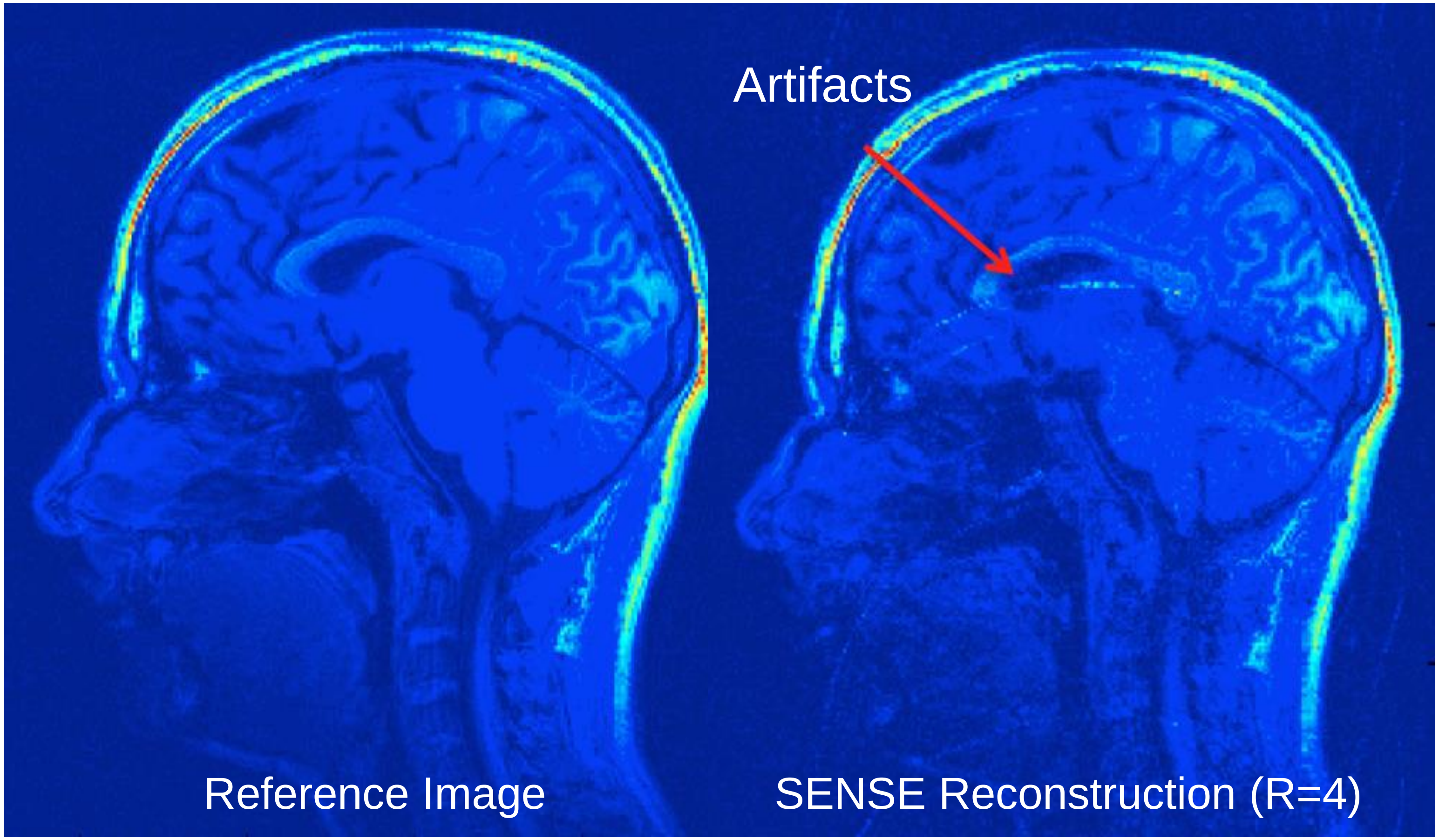

REGULARIZED SENSE RECONSTRUCTION

- Tikhonov regularization
  - In case of reference image $\boldsymbol{x}_{\mathrm{ref}}$ ...

$$\widehat{\boldsymbol{x}}_{\mathrm{C}} = \underset{\boldsymbol{x}_{\mathrm{C}} \in \mathbb{C}^n}{\arg\min} \left[\sum_{\vec{r} \in \mathrm{FOV}} \left\| \boldsymbol{y}_{\mathrm{C}}(\vec{r}) - \boldsymbol{S}_{\mathrm{C}}(\vec{r}) \boldsymbol{x}_{\mathrm{C}}(\vec{r}) \right\|^2_{\boldsymbol{\Psi}^{-1}} + \lambda \left\| \boldsymbol{x}_{\mathrm{C}}(\vec{r}) - \boldsymbol{x}_{\mathrm{ref}}(\vec{r}) \right\|^2 \right]$$

$R{=}2$

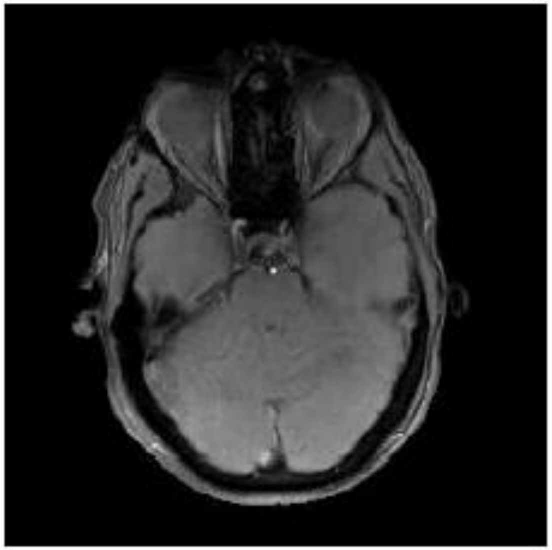

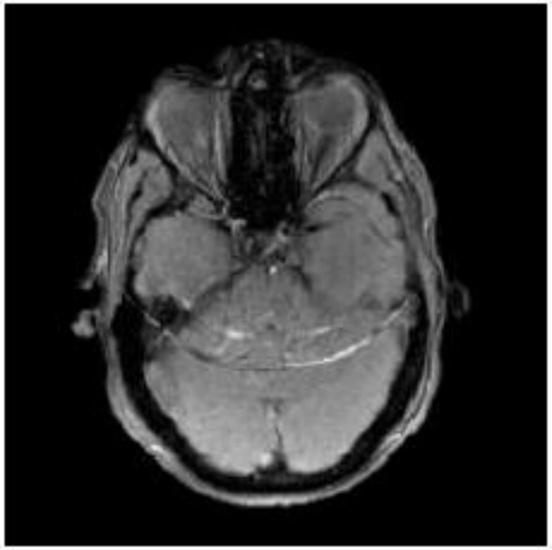

$R{=}4$

REGULARIZED SENSE RECONSTRUCTION

- Total variation regularization

$$\widehat{\boldsymbol{x}}_{\mathrm{C}} = \arg\min_{\boldsymbol{x}_{\mathrm{C}} \in \mathbb{C}^n} \left[\sum_{\vec{r} \in \mathrm{FOV}} \left\| \boldsymbol{y}_{\mathrm{C}}(\vec{r}) - \boldsymbol{S}_{\mathrm{C}}(\vec{r}) \boldsymbol{x}_{\mathrm{C}}(\vec{r}) \right\|^2_{\Psi^{-1}} \right] + \lambda \left\| \nabla \boldsymbol{x}_{\mathrm{C}} \right\|_1$$

with $\lambda > 0$ a regularization parameter.

$R = 4$

λ=0.001

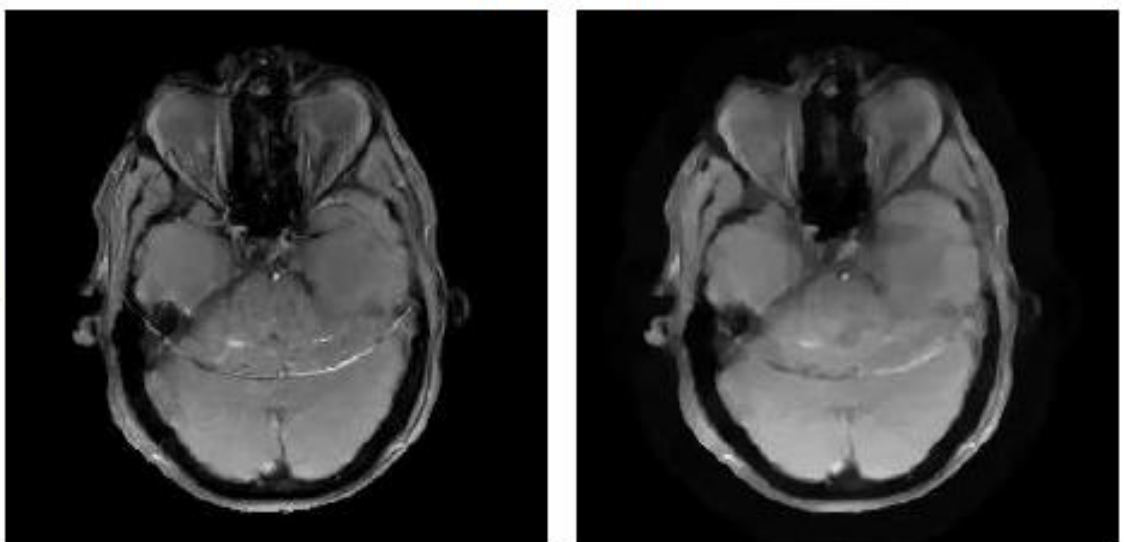

λ=1

WAVELETS ENTER INTO THE GAME …

MR images: sparse in the wavelet domain

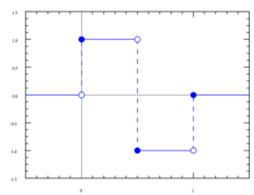

Haar's
1D-wavelet

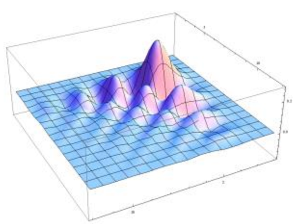

Daubechies'
2D-wavelet

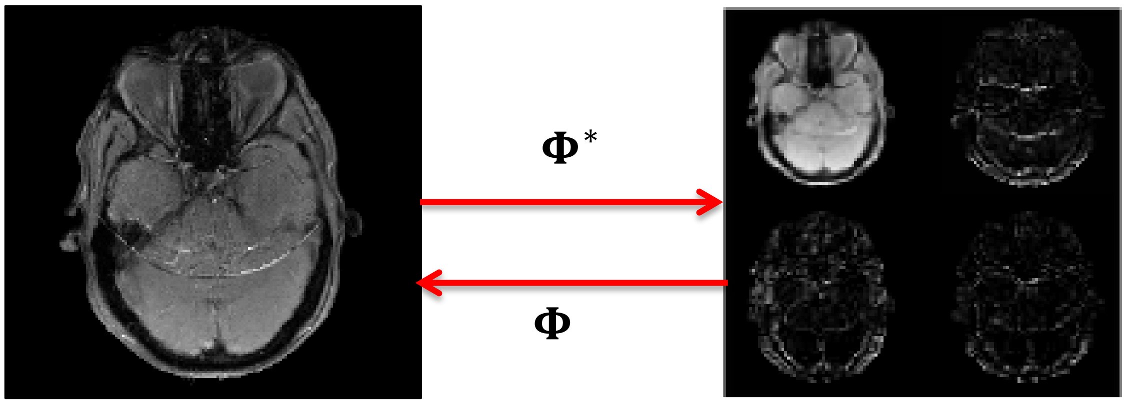

Spatial domain

Wavelet domain

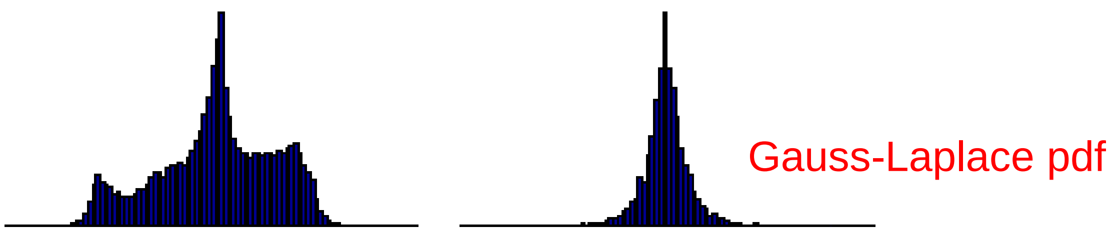

Image histogram

Wavelet subband histogram

- Improved spatial and frequency artifact localization
- Simple and accurate statistical model in the wavelet space

WAVELETS ENTER INTO THE GAME …

- Wavelet-based (synthesis approach) regularization:

$$\widehat{\boldsymbol{x}}_{\mathrm{C}} = \boldsymbol{T}\widehat{\alpha} \quad \text{and} \quad \widehat{\alpha} = \arg\min_{\alpha \in \mathbb{C}^n} \mathcal{J}(\alpha)$$

$$\mathcal{J}(\alpha) = \mathcal{J}_1(\alpha) + \mathcal{J}_2(\alpha)$$

- Data fidelity term reformulation in the Fourier domain:

$$\mathcal{J}_1(\alpha) = \mathcal{J}_1(\boldsymbol{T}\alpha) = \sum_{\vec{r} \in \mathrm{FOV}} \|\boldsymbol{y}_{\mathrm{C}}(\vec{r}) - \boldsymbol{S}_{\mathrm{C}}(\vec{r})\boldsymbol{x}_{\mathrm{C}}(\vec{r})\|^2_{\boldsymbol{\Psi}^{-1}}$$

$$= \sum_{\ell=1}^{L} \|\boldsymbol{y}_\ell - \boldsymbol{F}^*_{\Omega}\boldsymbol{S}_\ell \boldsymbol{T}\alpha\|^2_{\boldsymbol{\Lambda}_\ell^{-1}}$$

- Wavelet-based or synthesis penalization:

$$\mathcal{J}_2(\alpha) = \sum_m \Phi_a(\alpha_{a,m}) + \sum_{j=1}^{j_{\max}} \sum_{o \in \{h,v,d\}} \sum_m \Phi_{o,j}(\alpha_{o,j,m})$$

- proximal operator of $f : \mathbf{R}^n \to \mathbf{R} \cup \{+\infty\}$ is

$$v\|_2^2)$$

with parame

- f may be no .
- evaluating p :ion problem
- can evaluate ry often has an
analytical sc gorithm

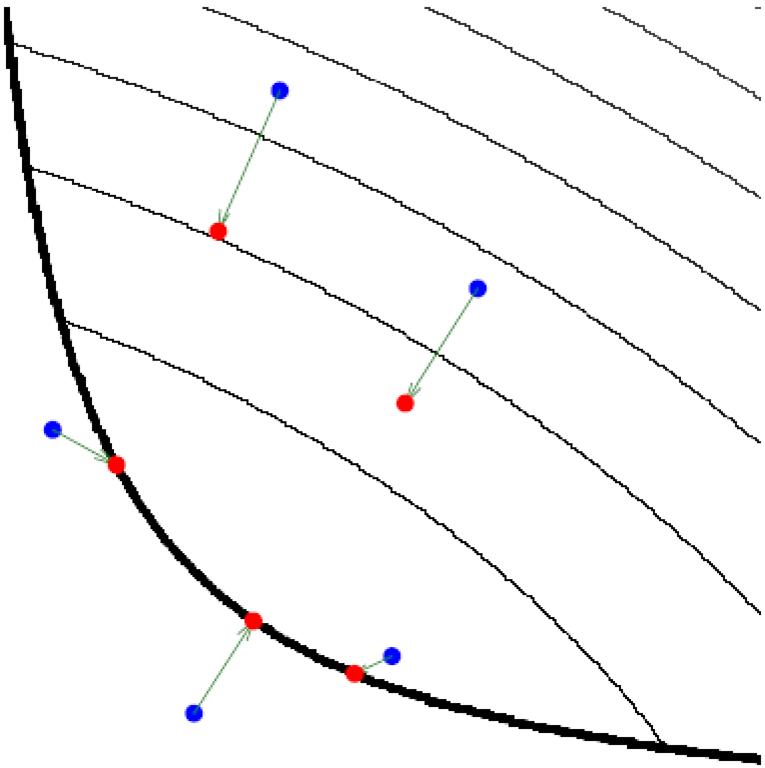

PROX. OPERATOR: GENERALIZED PROJECTION (2/3)

- proximal operator of an indicator function of a convex set is projection:

$$\mathbf{prox}_{\lambda I_{\mathcal{C}}}(v) = \Pi_{\mathcal{C}}(v) = \underset{x \in \mathcal{C}}{\operatorname{argmin}} \|x - v\|_2$$

- many properties carry over

- **example**: projection onto box $\mathcal{C} = \{x \mid l \preceq x \preceq u\}$ given by

$$(\Pi_{\mathcal{C}}(v))_k = \begin{cases} l_k & v_k \leq l_k \\ v_k & l_k \leq v_k \leq u_k \\ u_k & v_k \geq u_k \end{cases}$$

PROX. OPERATOR: SEPARABLE SUM (3/3)

- if f is block separable, so $f(x) = \sum_{i=1}^{N} f_i(x_i)$, then

$$(\mathbf{prox}_f(v))_i = \mathbf{prox}_{f_i}(v_i), \quad i = 1, \ldots, N$$

- key to parallel/distributed proximal algorithms

- **example**: if $f = \|\cdot\|_1$, then

$$\mathbf{prox}_{\lambda f}(v) = (v-\lambda)_+ - (-v-\lambda)_+ = \begin{cases} v_i - \lambda & v_i \geq \lambda \\ 0 & |v_i| \leq \lambda \\ v_i + \lambda & v_i \leq -\lambda \end{cases}$$

- **in general**: if $f = \|\cdot\|$ and $\mathcal{B}$ is unit ball of dual norm, then

$$\mathbf{prox}_{\lambda f}(v) = v - \lambda \Pi_{\mathcal{B}}(v/\lambda)$$

PROXIMAL GRADIENT ALGORITHM

$$\text{minimize} \quad f(x) + g(x)$$

f is smooth

$g : \mathbf{R}^n \to \mathbf{R} \cup \{+\infty\}$ is closed proper convex

- method:

$$x^{k+1} := \mathbf{prox}_{\lambda^k g}(x^k - \lambda^k \nabla f(x^k))$$

- converges with rate $O(1/k)$ when ∇f is Lipschitz continuous with constant L and step sizes are $\lambda^k = \lambda \in (0, 1/L]$

- special case: projected gradient method (take $g = I_C$)

- traces back to Bruck, Lions, Mercier (1970s)

FORWARD BACKWARD OPTIMIZATION

Algorithm:

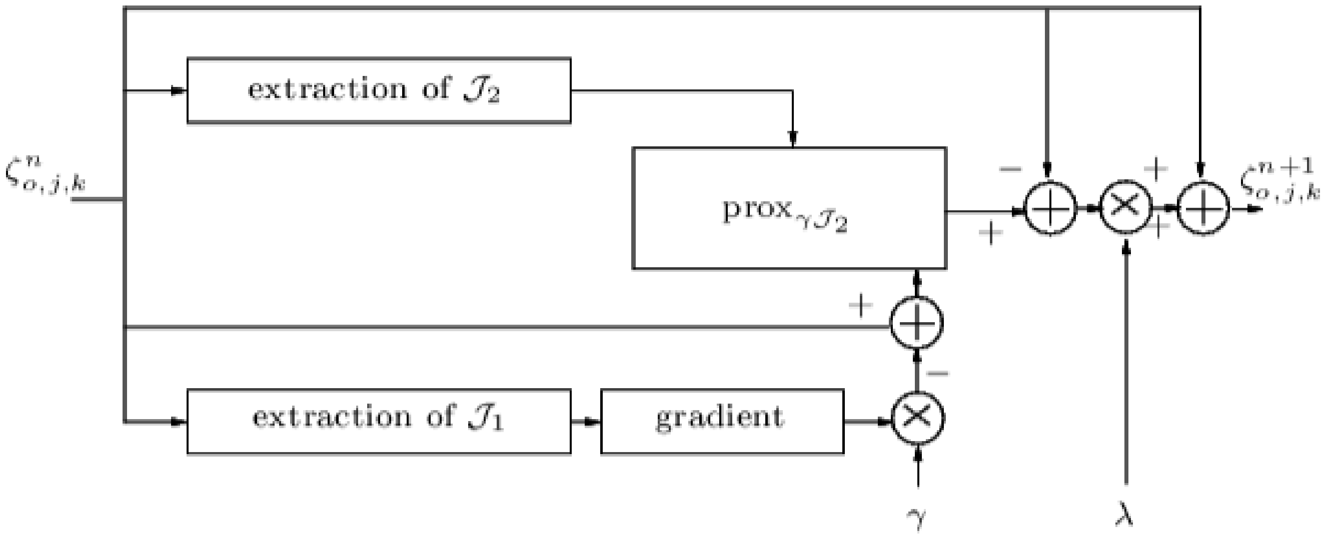

$$\alpha^{(n+1)}_{o,j,m} = \alpha^{(n)}_{o,j,m} + \lambda\Big(\text{prox}_{\gamma\Phi_{o,j}}\big(\alpha^{(n)}_{o,j,m} - \gamma[\nabla\mathcal{J}_1(\alpha^{(n)})]_{o,j,m}\big) - \alpha^{(n)}_{o,j,m}\Big)$$

$* \;\; [\nabla\mathcal{J}_1]_{o,j,m} = \dfrac{\partial\mathcal{J}_1}{\partial\text{Re}(\alpha_{o,j,m})} + \imath.\dfrac{\partial\mathcal{J}_1}{\partial\text{Im}(\alpha_{o,j,m})}$

$* \;\; \lambda \in]0,1]$: relaxation parameter

$* \;\; \gamma \in]0,\gamma_{\max}[$: step-size parameter

$$\Phi : \mathbb{R} \to \mathbb{R} \quad \Longrightarrow \quad \text{prox}_\Phi : \mathbb{R} \to \mathbb{R}$$

$$\xi \mapsto \alpha|\xi| + \beta\xi^2 \qquad\qquad \xi \mapsto \frac{\text{sign}(\xi)}{2\beta+1}\max\{|\xi|-\alpha, 0\}$$

WAVELET-BASED RESULTS

$R = 4$

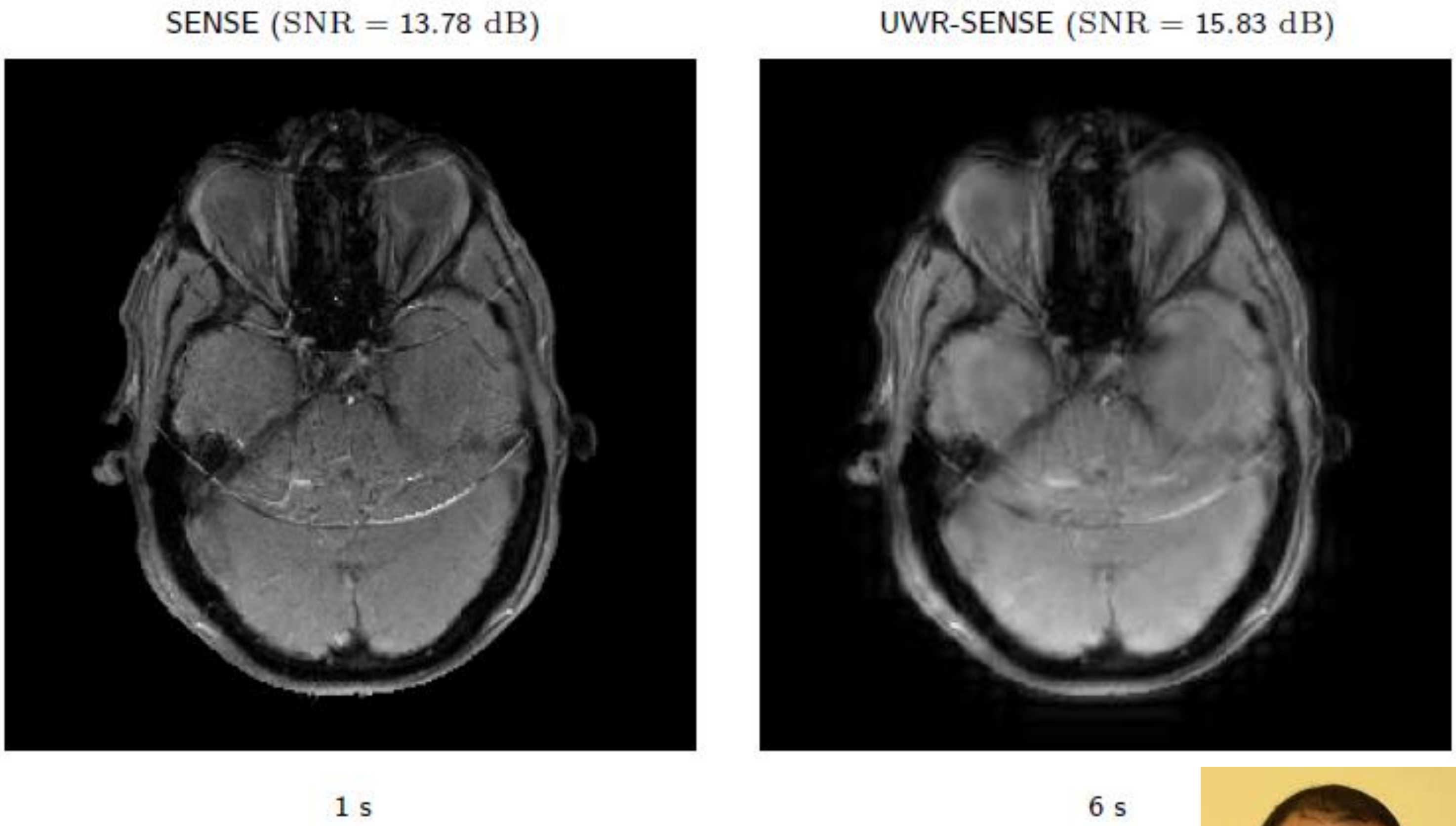

[Chaari et al, IEEE ISBI 2008]

CONSTRAINED REGULARIZATION

- Constrained Problem

$$\text{Find } \min_{\boldsymbol{\alpha}\in\mathbb{C}^K} \mathcal{J}_1 + \mathcal{J}_2$$

$$\Downarrow$$

$$\text{Find } \min_{\boldsymbol{\alpha}\in C} \mathcal{J}_1 + \mathcal{J}_2$$

where C is a nonempty closed convex subset of $\mathbb{C}^K$

$$\Longleftrightarrow \text{Find } \min_{\boldsymbol{\alpha}\in\mathbb{C}^K} \mathcal{J}_1 + \mathcal{J}_2 + \imath_C$$

$$\text{where } \forall \vec{r} \in \mathbb{C},\ \imath_C(\vec{r}) = \begin{cases} 0, & \text{if } \vec{r} \in C \\ +\infty, & \text{otherwise} \end{cases}$$

[Chaari et al, MedIA 2011]

CONSTRAINED CONVEX OPTIMIZATION

In practice:

$$C = \left\{\boldsymbol{\alpha} \in \mathbb{C}^K \;\middle|\; \forall \vec{r} \in \mathbb{D},\ \mathrm{Re}((\boldsymbol{T}\boldsymbol{\alpha})(\vec{r})) \in \mathbb{I}_{\vec{r}}^{\mathrm{Re}}\ , \mathrm{Im}((\boldsymbol{T}\boldsymbol{\alpha})(\vec{r})) \in \mathbb{I}_{\vec{r}}^{\mathrm{Im}}\right\}$$

where $\mathbb{I}_{\vec{r}}^{\mathrm{Re}} = [\mathrm{I}_{\min}^{\mathrm{Re}}(\vec{r}), \mathrm{I}_{\max}^{\mathrm{Re}}(\vec{r})]$, $\mathbb{I}_{\vec{r}}^{\mathrm{Im}} = [\mathrm{I}_{\min}^{\mathrm{Im}}(\vec{r}), \mathrm{I}_{\max}^{\mathrm{Im}}(\vec{r})]$ and $\mathbb{D}$ corresponds to the artifact areas.

Algorithm:

$$\boldsymbol{\alpha}^{(n+1)} = \boldsymbol{\alpha}^{(n)} + \lambda\Big(\mathrm{prox}_{\imath_C + \gamma \mathcal{J}_2}(\boldsymbol{\alpha}^{(n)} - \gamma \nabla \mathcal{J}_1(\boldsymbol{\alpha}^{(n)})) - \boldsymbol{\alpha}^{(n)}\Big)$$

We use a Douglas-Rachford algorithm to iteratively compute $\mathrm{prox}_{\imath_C + \gamma \mathcal{J}_2}$ [Pustelnik et al. , EUSIPCO 08].

[Chaari et al, MedIA 2011]

CONSTRAINED WAVELET-BASED RESULTS

$R = 4$

UWR-SENSE (SNR = 15.83 dB) CWR-SENSE (SNR = 16.04 dB)

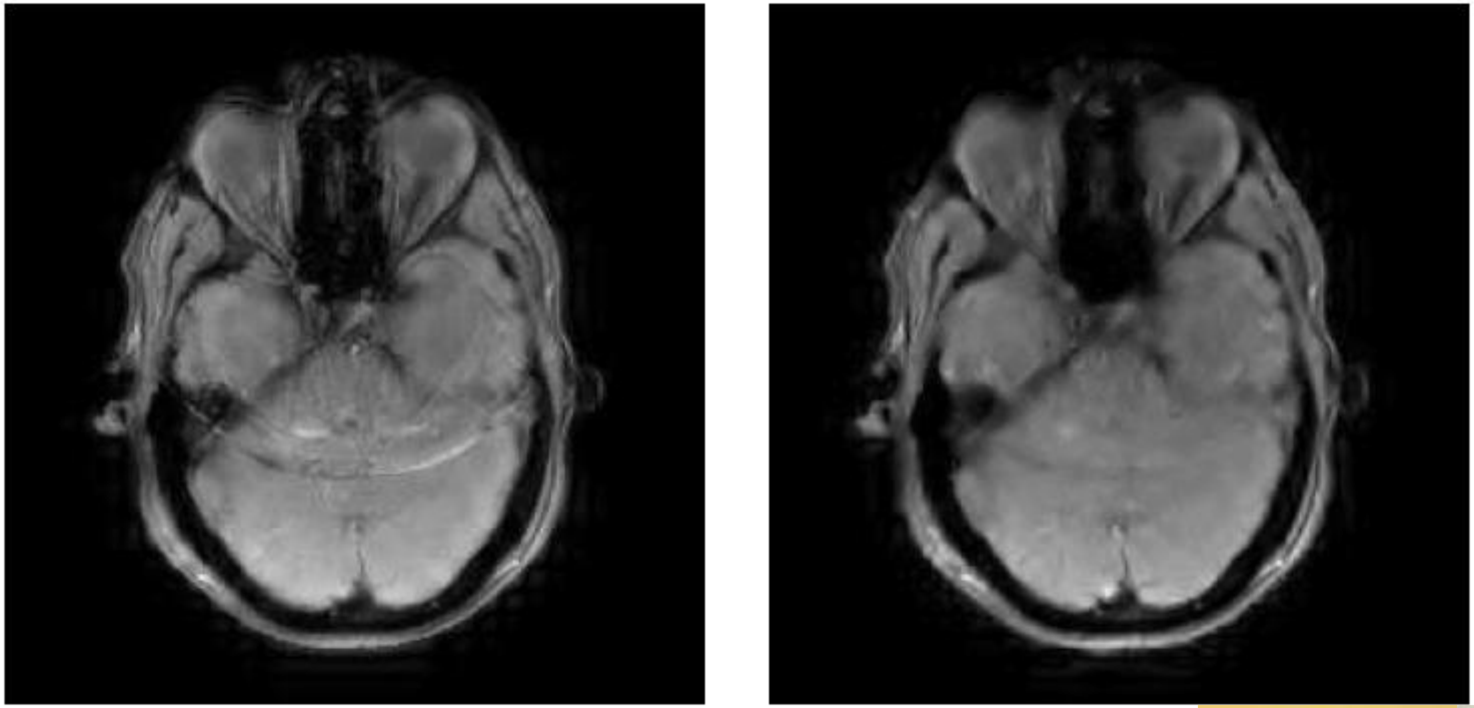

6 s 9 s

[Chaari et al, MedIA 2011]

ANALYSIS & SYNTHESIS REGULARIZED RESULTS

TV-SENSE (SNR = 13.39 dB)

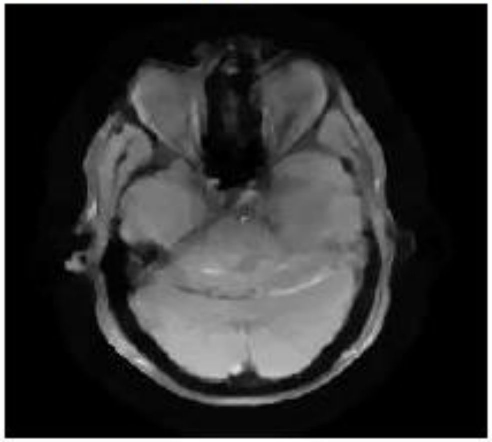

4 s

CWR-SENSE (SNR = 16.04 dB)

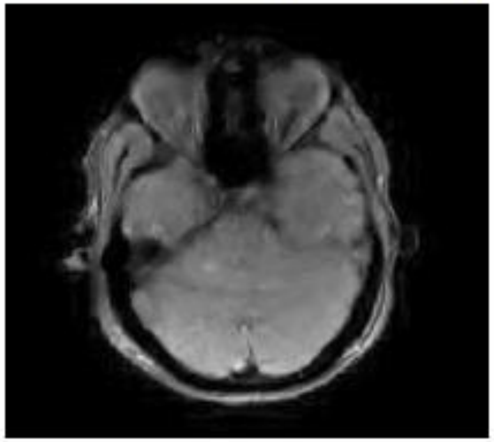

9 s

W-TV-SENSE (SNR = 16.37 dB)

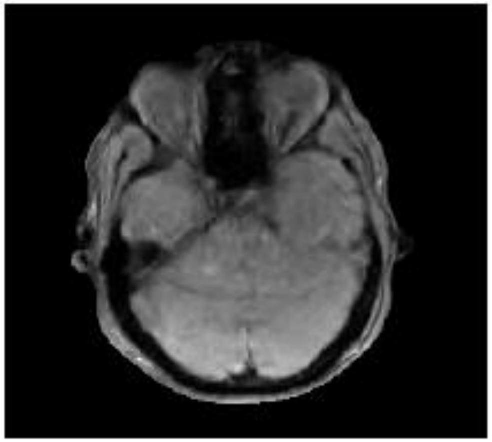

8 s

[Chaari et al, MedIA 2011]

ZOOMING

TV-SENSE (SNR = 13.39 dB)

4 s

CWR-SENSE (SNR = 16.04 dB)

9 s

W-TV-SENSE (SNR = 16.37 dB)

8 s

[Chaari et al, MedIA 2011]

3D REGULARIZATION & RECONSTRUCTION

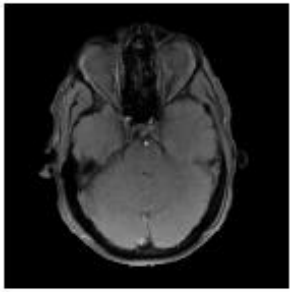

2D

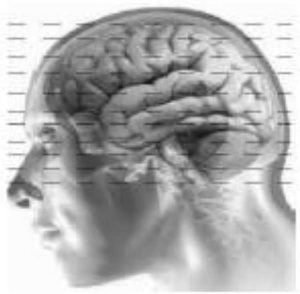

3D

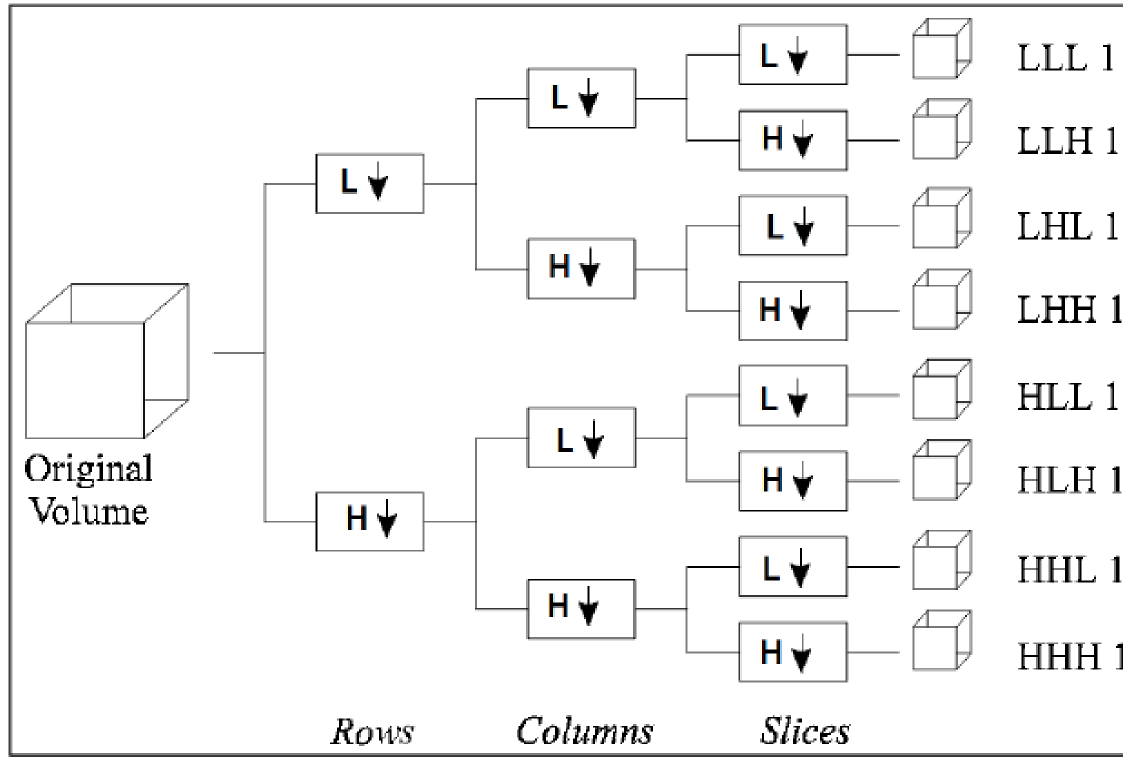

[Chaari et al, IEEE ISBI 2011]

$$\text{Trouver } \min_{\zeta \in \mathbb{C}^K} \mathcal{J}_1(\zeta) + \mathcal{J}_2(\zeta) + \iota_C(\zeta)$$

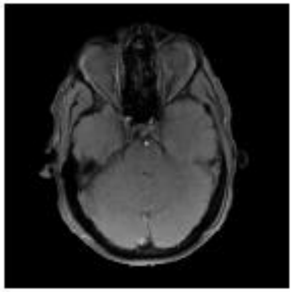

2D

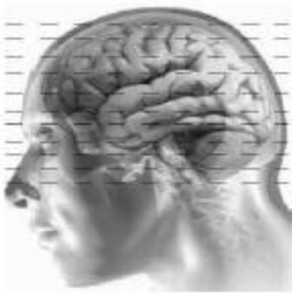

3D

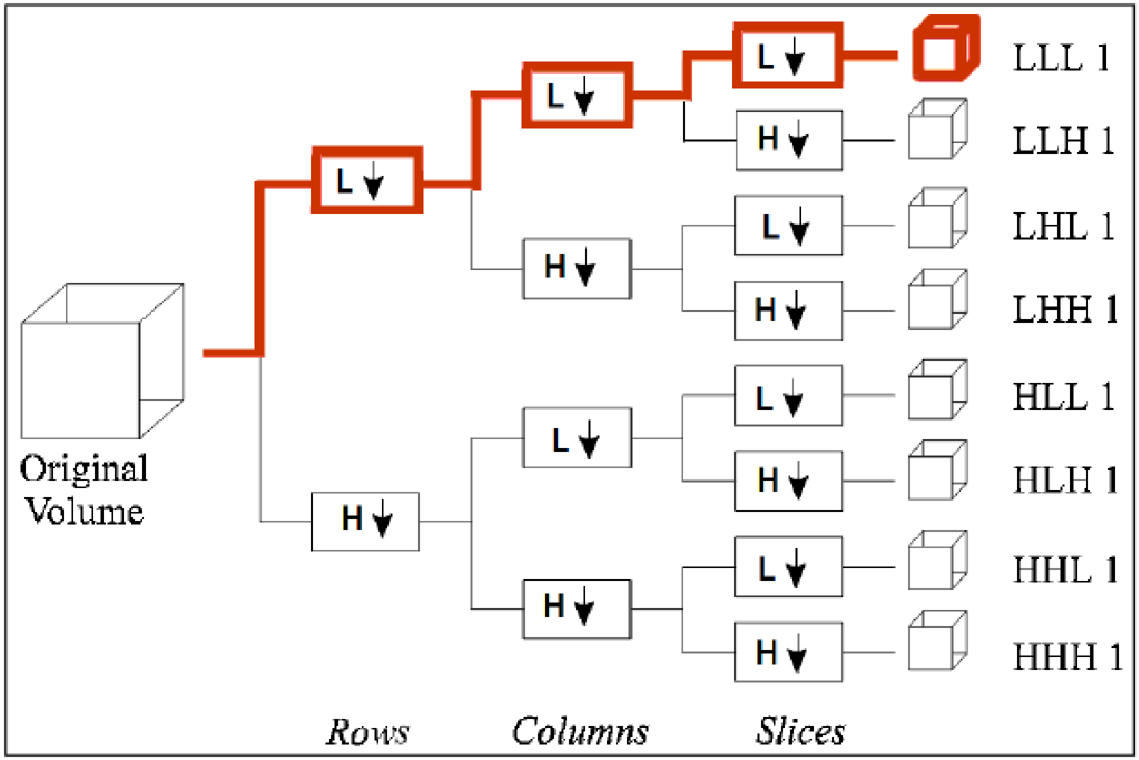

[Chaari et al, IEEE ISBI 2011]

- $\Phi_1(T\rho_C) = \sum_k \Phi_a((T\rho_C)_{a,k}) + \sum_o \sum_j \sum_k \Phi_{o,j}((T\rho_C)_{o,j,k})$

  where $\mathbb{O} = \{LLL, LLH, LHL, LHH, HLL, HLH, HHL, HHH\}$

  and

$$\begin{aligned}\forall o \in \mathbb{O},\ \Phi_{o,j}(\xi) =& \Phi^{\mathrm{Re}}_{o,j}(\xi) + \Phi^{\mathrm{Im}}_{o,j}(\xi)\\ =& (\omega^{\mathrm{Re}}_{o,j}|\mathrm{Re}(\xi)|)^{\beta^{\mathrm{Re}}_{o,j}} + (\omega^{\mathrm{Im}}_{o,j}|\mathrm{Im}(\xi)|)^{\beta^{\mathrm{Im}}_{o,j}}\end{aligned}$$

3D UWR-SENSE SEGMENTATION RESULTS

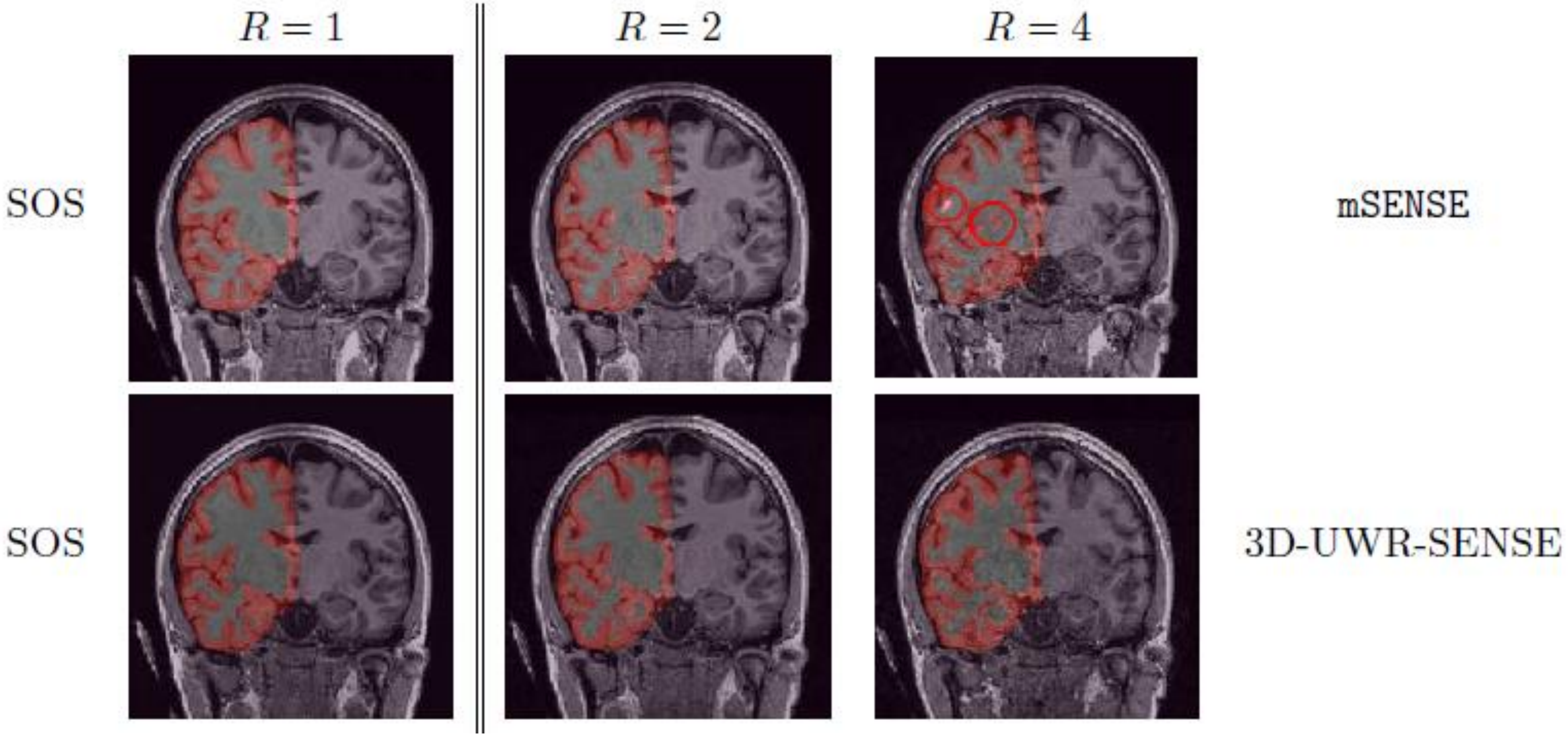

[Chaari et al, MAGMA 2014]

OUTLINE

Nicolas Chauffert
CEA/NeuroSpin

Carole Lazarus
CEA/NeuroSpin

Alexandre Viggnaud
CEA/NeuroSpin

Part V: Compressed Sensing in MRI

Pierre Weiss
CNRS/ITAV

Claire Boyer
IMT, U. Toulouse

Jonas Kahn
CNRS/IMT

COMPRESSED SENSING CONCERN: WHEN IMAGE ACQUISITION MEETS IMAGE RECONSTRUCTION

Reducing scanning time in MRI

- Improve patient comfort
- Reduce distortions due to patient movement
- Reducing scanning costs
- Improve either spatial, temporal or angular resolution (MRI/fMRI/dw-MRI)

Let $\boldsymbol{x} : [0,1]^d \to \mathbb{C}$ be an image and $\mathring{\boldsymbol{x}}$ denote its Fourier transform.

Our objective: reconstruct $\widehat{\boldsymbol{x}}$ such that $\|\widehat{\boldsymbol{x}} - \boldsymbol{x}\|_2 \leq \epsilon$

Minimize T_ϵ under the constraint that there exists $g : [0, T_\epsilon] \to \mathbb{R}^d$ s.t.

- $\vec{G}$ and $\dot{\vec{G}}$ are uniformly bounded.
- Sampling the curve $\vec{\kappa}(t)$ generates a set

$$y(\vec{\kappa}) = \{\mathring{\boldsymbol{x}}(\vec{\kappa}(k\Delta t))\}_{k \in \{0, \ldots, T_\epsilon/(\Delta t)\}}$$

that allows reconstructing $\widehat{\boldsymbol{x}}$ with precision ϵ.

COMPRESSED SENSING CONCERN: WHEN IMAGE ACQUISITION MEETS IMAGE RECONSTRUCTION

Let $\boldsymbol{x} : [0,1]^d \to \mathbb{C}$ be an image and $\mathring{\boldsymbol{x}}$ denote its Fourier transform.

Our objective: reconstruct $\widehat{\boldsymbol{x}}$ such that $\|\widehat{\boldsymbol{x}} - \boldsymbol{x}\|_2 \leq \epsilon$

Minimize T_ϵ under the constraint that there exists $g : [0, T_\epsilon] \to \mathbb{R}^d$ s.t.

- $\vec{G}$ and $\dot{\vec{G}}$ are uniformly bounded.
- Sampling the curve $\vec{\kappa}(t)$ generates a set

$$y(\vec{\kappa}) = \{\mathring{\boldsymbol{x}}(\vec{\kappa}(k\Delta t))\}_{k \in \{0,\dots,T_\epsilon/(\Delta t)\}}$$

  that allows reconstructing $\widehat{\boldsymbol{x}}$ with precision ϵ.

Questions...

- How to choose the measurements (or locations in k-space)?
- How to find $\vec{\kappa}(t)$?
- How to reconstruct $\widehat{\boldsymbol{x}}$ knowing $y(\vec{\kappa})$?

COMPRESSED SENSING IN MRI

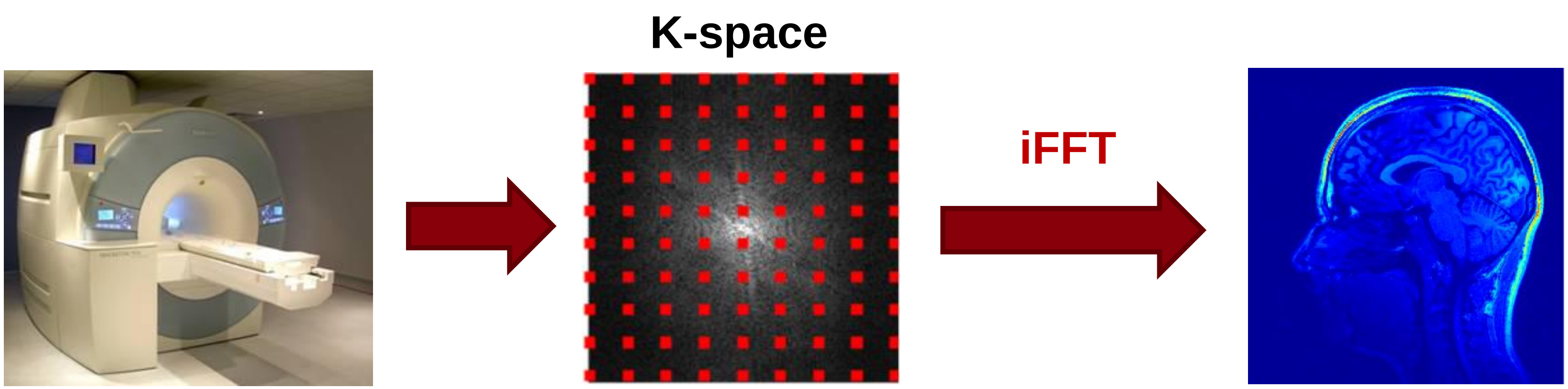

COMPRESSED SENSING IN IRM

K-space

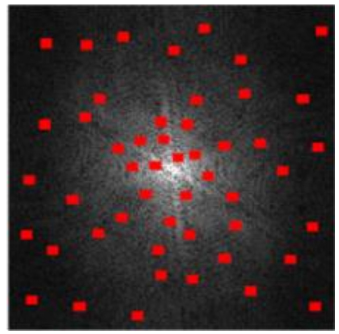

??

??

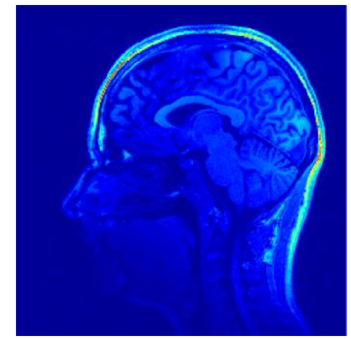

??

- What images?
- What samples?
- What reconstruction technique?

[Lustig et al, MRM 2007]

COMPRESSED SENSING RECIPE

Data is sparse, compressible, redundant…
Sense the compressed information directly!

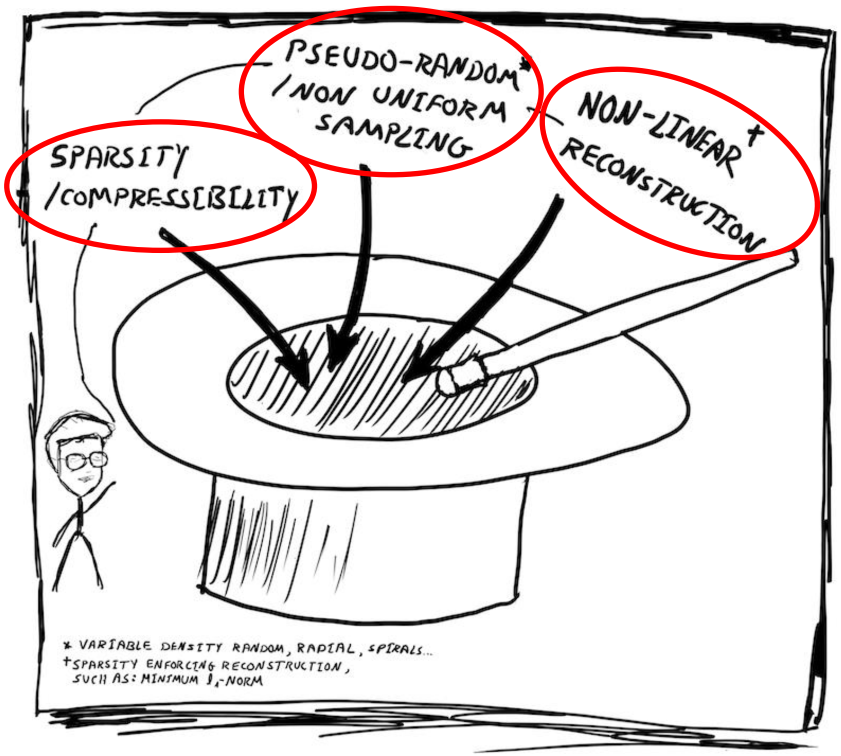

Michael Lustig, http://www.eecs.berkeley.edu/~mlustig/CS.html

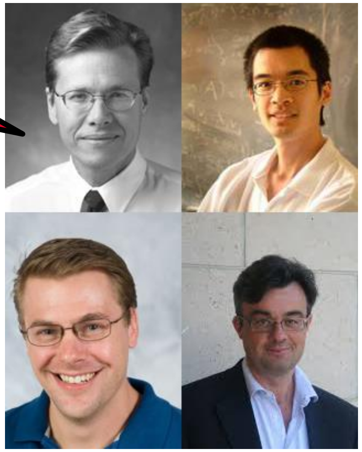

Donoho, Tao,
Romberg, Candes

WHAT SPARSITY AND COMPRESSIBILITY MEAN?

1. Sparsity/Compressibility

Sparse
(spärs),
adj. **spars•er, spars•est.**
1. Thinly scattered or distributed; not thick or dense.
2. Scanty; meager.
(http://www.thefreedictionary.com/sparse)

Compressible
1. There exists a basis where the representation has just a few large coefficients and many small coefficients.
2. Compressible signals are well approximated by sparse representations

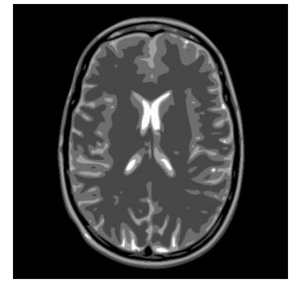

is not sparse…
… but compressible!

Wavelet Represensation… is sparse!

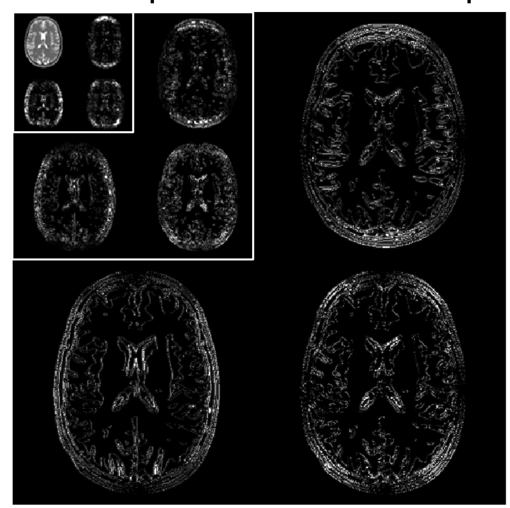

3 levels of decomposition

COMPRESSED SENSING RECIPE (1/3)

- Increase sparsity by changing the image decomposition

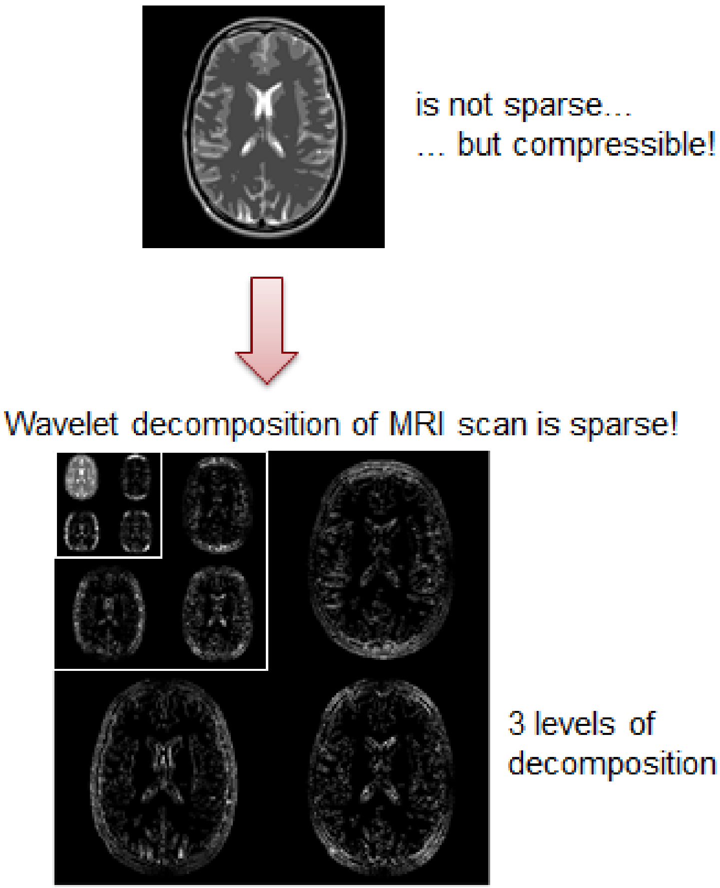

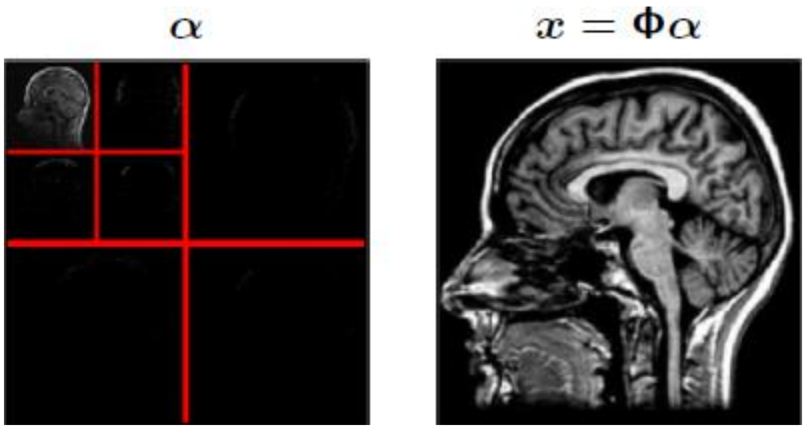

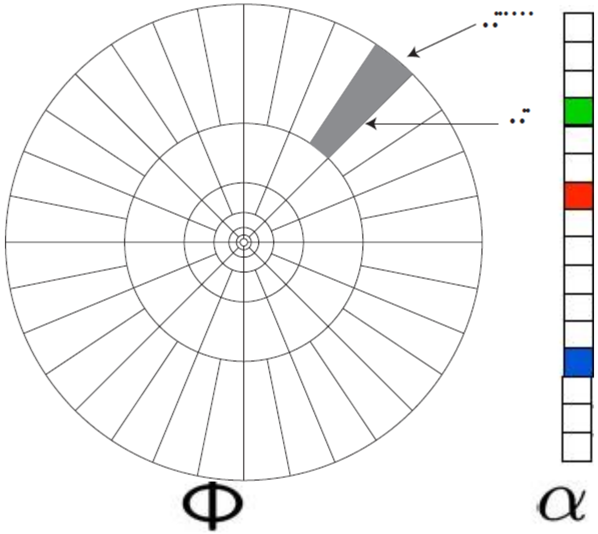

Redundant transforms
$\boldsymbol{\Phi}$ induces sparser decompositions $\boldsymbol{\alpha}$

Curvelets
Starlets, shearlets

COMPRESSED SENSING THEORY (1/4)

Compressed sensing theory:

- x is sparse in a given basis (e.g. wavelets): $x = \Phi\alpha$, where $\alpha \in \mathbb{C}^n$ is s-sparse.
- Acquisition matrix: $\boldsymbol{H} = \boldsymbol{F}^*\boldsymbol{\Phi}$.

Let $\Gamma \subseteq \{1, \cdots, n\}$ and $\boldsymbol{H}_\Gamma = (h_i^*)_{i\in\Gamma}$. We acquire a measurement vector:

$$y = \boldsymbol{H}_\Gamma \alpha + b.$$

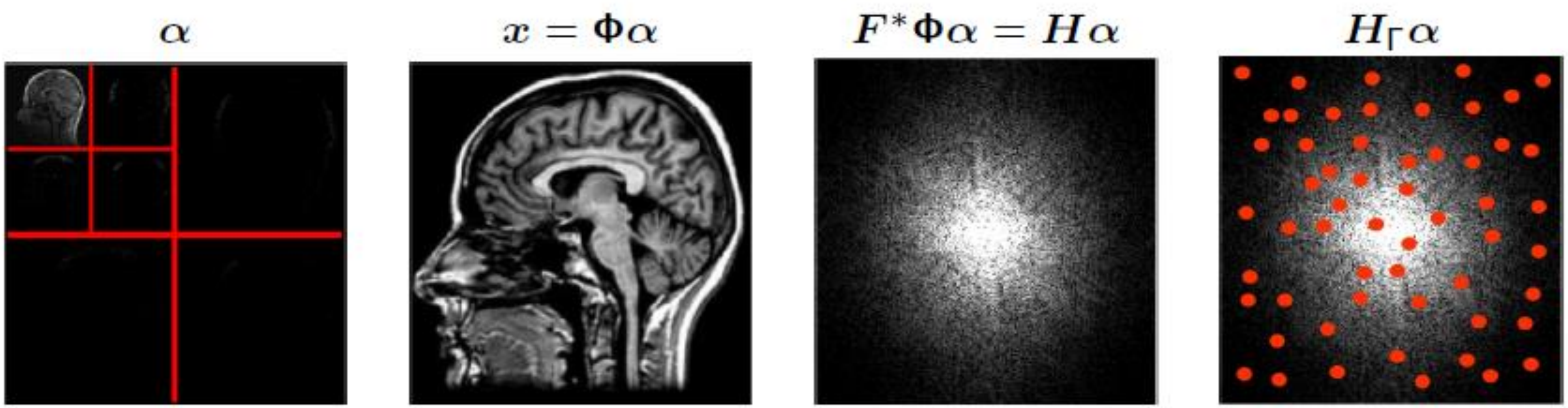

COMPRESSED SENSING THEORY (2/4)

Compressed sensing theory:

- x is sparse in a given basis (e.g. wavelets): $x = \Phi\alpha$, where $\alpha \in \mathbb{C}^n$ is s-sparse.
- Acquisition matrix: $H = F^*\Phi$.

Let $\Gamma \subseteq \{1, \cdots, n\}$ and $H_\Gamma = (h_i^*)_{i\in\Gamma}$. We acquire a measurement vector:

$$y = H_\Gamma \alpha + b.$$

α | $x = \Phi\alpha$ | $F^*\Phi\alpha = H\alpha$ | $H_\Gamma\alpha$

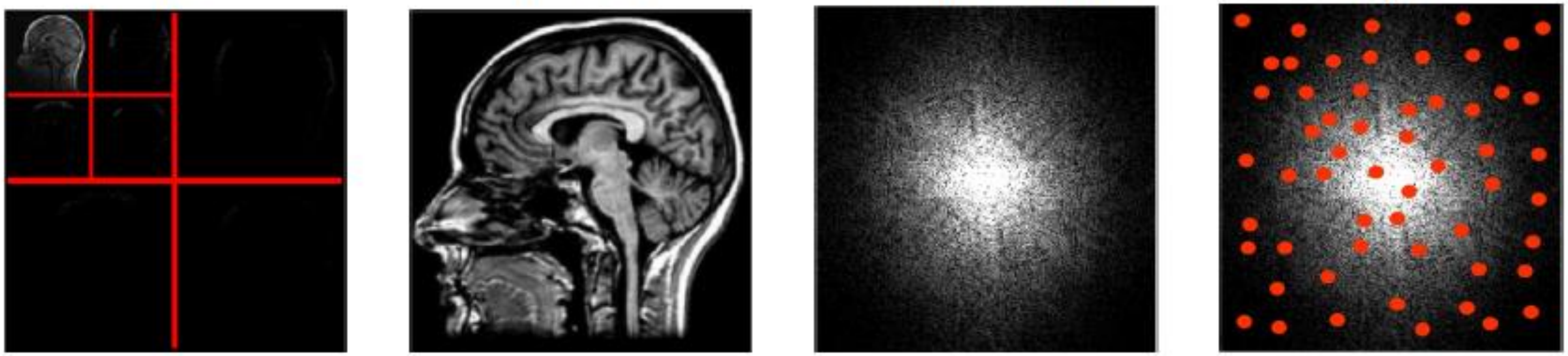

ℓ_1 reconstruction (promoting sparsity)

$$\min_{z\in\mathbb{C}^n, H_\Gamma z = y} \|z\|_1.$$

COMPRESSED SENSING THEORY (3/4)

Compressed sensing theory:

- $\boldsymbol{x}$ is sparse in a given basis (e.g. wavelets): $\boldsymbol{x} = \boldsymbol{\Phi}\boldsymbol{\alpha}$, where $\boldsymbol{\alpha} \in \mathbb{C}^n$ is s-sparse.
- Acquisition matrix: $\boldsymbol{H} = \boldsymbol{F}^*\boldsymbol{\Phi}$.

Let $\Gamma \subseteq \{1, \cdots, n\}$ and $\boldsymbol{H}_\Gamma = (\boldsymbol{h}_i^*)_{i\in\Gamma}$. We acquire a measurement vector:

$$\boldsymbol{y} = \boldsymbol{H}_\Gamma\boldsymbol{\alpha} + \boldsymbol{b}.$$

$\boldsymbol{\alpha}$ | $\boldsymbol{x} = \boldsymbol{\Phi}\boldsymbol{\alpha}$ | $\boldsymbol{F}^*\boldsymbol{\Phi}\boldsymbol{\alpha} = \boldsymbol{H}\boldsymbol{\alpha}$ | $\boldsymbol{H}_\Gamma\boldsymbol{\alpha}$

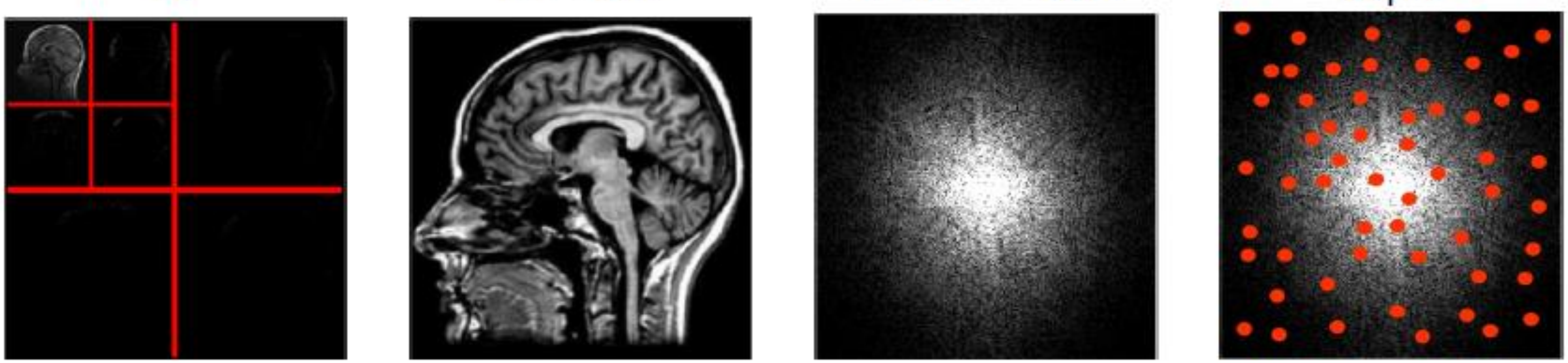

or in case of noise (Synthesis formulation):

$$\widehat{\boldsymbol{\alpha}} = \operatorname*{Arg\,min}_{\boldsymbol{z}\in\mathbb{C}^n} \|\boldsymbol{y} - \boldsymbol{H}_\Gamma\boldsymbol{z}\|_2^2 + \lambda\|\boldsymbol{z}\|_1$$

(FISTA algorithm)

COMPRESSED SENSING THEORY (4/4)

Compressed sensing theory:

- x is sparse in a given basis (e.g. wavelets): $x = \Phi\alpha$, where $\alpha \in \mathbb{C}^n$ is s-sparse.
- Acquisition matrix: $H = F^* \Phi$.

Let $\Gamma \subseteq \{1, \cdots, n\}$ and $H_\Gamma = (h_i^*)_{i \in \Gamma}$. We acquire a measurement vector:

$$y = H_\Gamma \alpha + b.$$

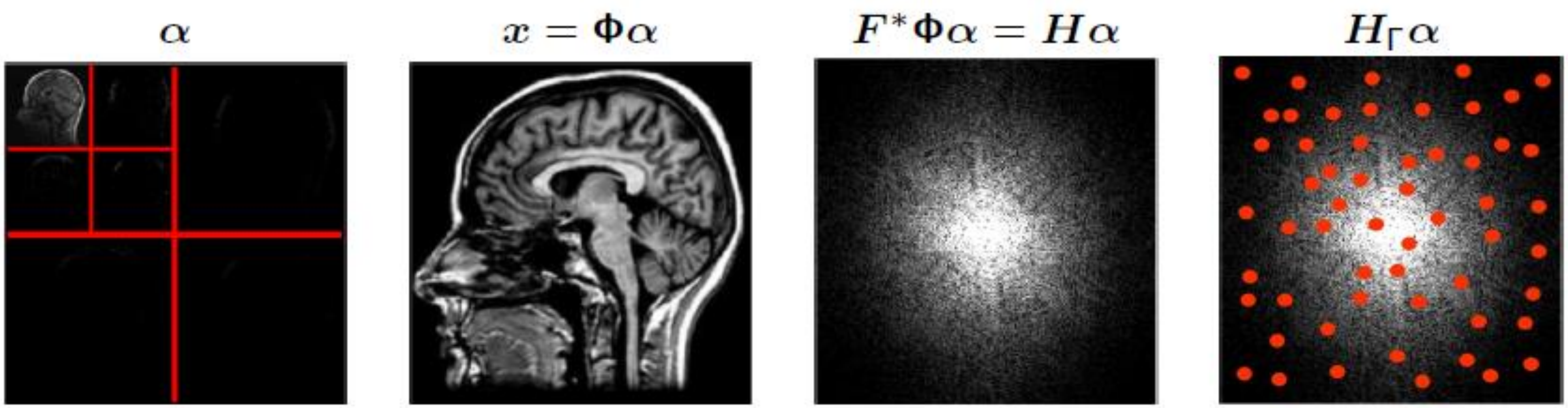

or in case of noise (Analysis formulation):

$$\widehat{x} = \underset{x \in \mathbb{C}^n}{\operatorname{Arg\,min}} \|y - F^* x\|_2^2 + \lambda \|\Phi^* x\|_1$$ (ADMM algorithm)

THEORETICAL RESULTS (1/2)

A first CS theorem [Candès and Plan, 2011]

Theorem

Construct Γ by **uniform** *and i.i.d. drawing the lines of* $\boldsymbol{H}$.
Let $\boldsymbol{x}$ *be a sparse vector, containing* s *non-zero entries. Assume that:*

$$m \geqslant C \cdot s \cdot \left(n \cdot \max_{1 \leqslant k \leqslant n} \|\boldsymbol{h}_k\|_\infty^2 \right) \cdot \log\left(\frac{n}{\eta}\right) \tag{1}$$

where C *is a universal constant. Then, with probability* $1-\eta$, $\boldsymbol{x}$ *is the unique solution of:*

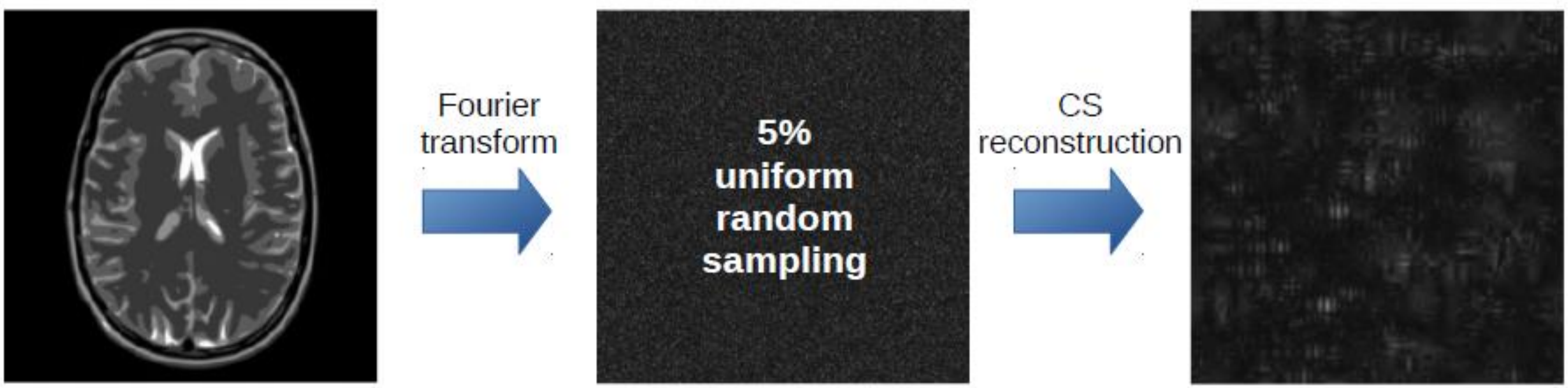

2. Pseudo-random sampling

- Non-uniform sampling

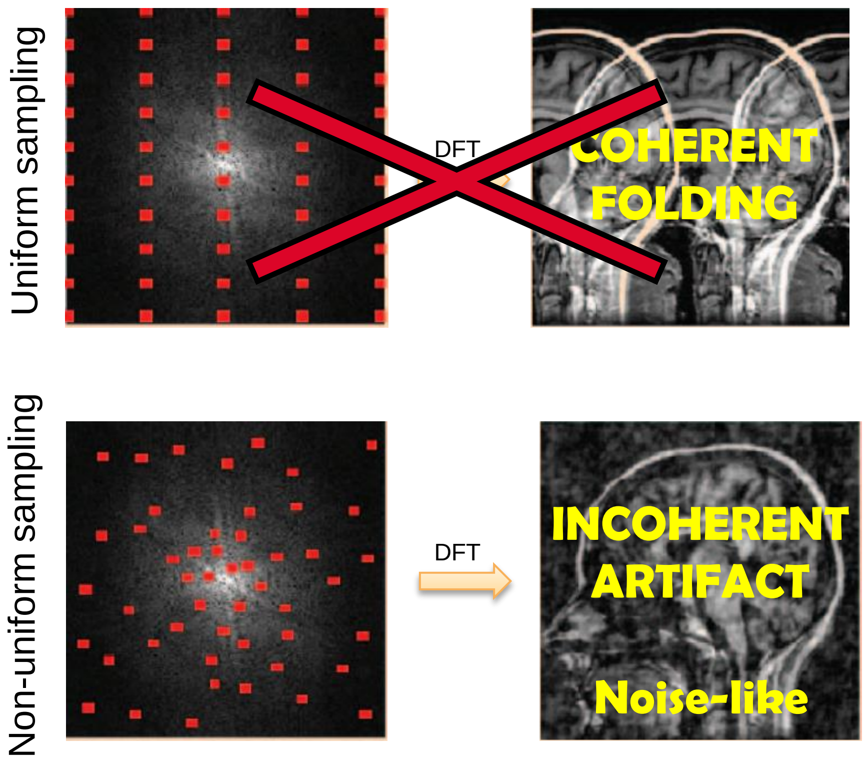

- Variable Density Sampling

(Lustig et al. 2007, Chauffert et al. 2013, Puy et al. 2011)

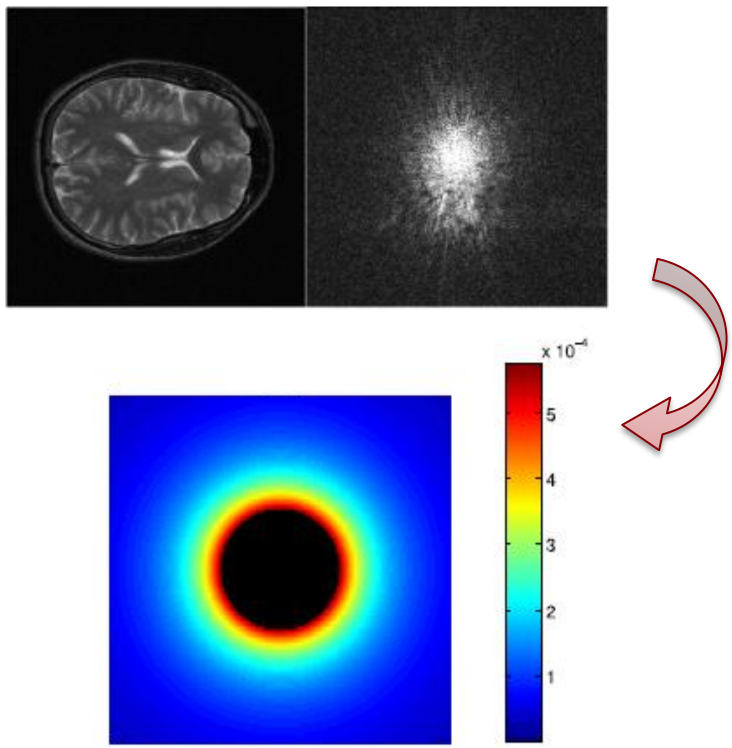

Lustig et al. 2008

THEORETICAL RESULTS (2/2)

Theorem [Chauffert et al., 2013]

Let $\boldsymbol{x}$ be an arbitrary s-sparse vector. Let $(J_k)_{k\in\{1,\ldots,m\}}$ denote a sequence of i.i.d. random variables taking value $i \in \{1,\ldots,n\}$ with probability p_i. Generate a random set $\Gamma = \{J_1,\ldots,J_m\}$ and measure $\boldsymbol{y} = \boldsymbol{H}_\Gamma \boldsymbol{x}$. Take $\eta \in]0,1[$ and assume that:

$$m \geqslant C \cdot s \cdot \max_{k\in\{1,\ldots,n\}} \frac{\|\boldsymbol{h}_k\|_\infty^2}{p_k} \ln\left(\frac{n}{\eta}\right)$$

where C is a universal constant. Then with probability $1-\eta$ vector x is the unique solution of the following problem:

$$\min_{\boldsymbol{z}\in\mathbb{C}^n, \boldsymbol{H}_\Gamma \boldsymbol{z}=\boldsymbol{y}} \|\boldsymbol{z}\|_1 .$$

Optimal distribution $\pi_k \propto \|\boldsymbol{h}_k\|_\infty^2$.

Coherence is now $\displaystyle\max_{k\in\{1,\ldots,n\}} \frac{\|\boldsymbol{h}_k\|_\infty^2}{p_k} = \sum_k \|\boldsymbol{h}_k\|_\infty^2 = O(\log(n))$ in MRI.

ILLUSTRATION OF VARIABLE DENSITY SAMPLING

Illustration of optimal sampling strategy for $\boldsymbol{H} = \boldsymbol{F}^*\boldsymbol{\Psi}$ (MRI)

Shannon
Wavelets

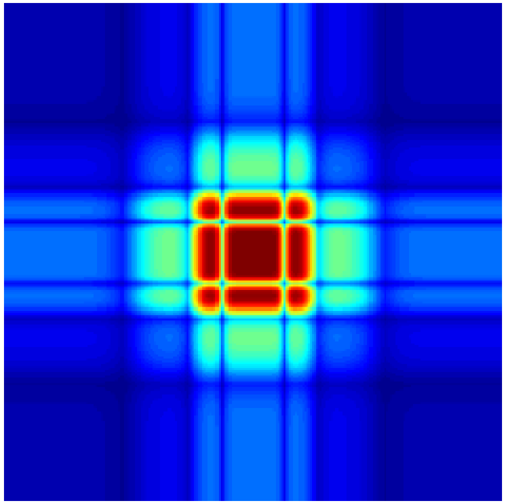

π in 2D

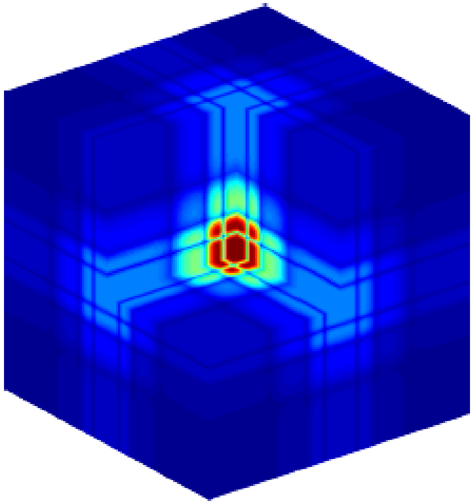

π in 3D

Example of sampling pattern obtained in 2D :

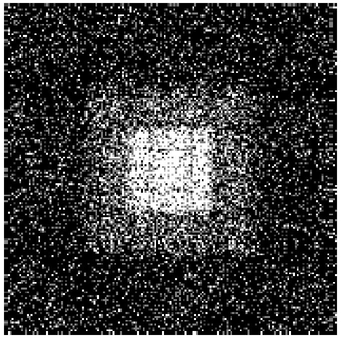

FROM THEORY TO PRACTICE

- ***From the traditionnal CS theory...***

➔ To faithfully recover a signal with s on-zero entries:

number of required measurements: $m = \cancel{O(s}\, log(n))$ where n=#pixels

➔ Noisy case: still holds but a larger error

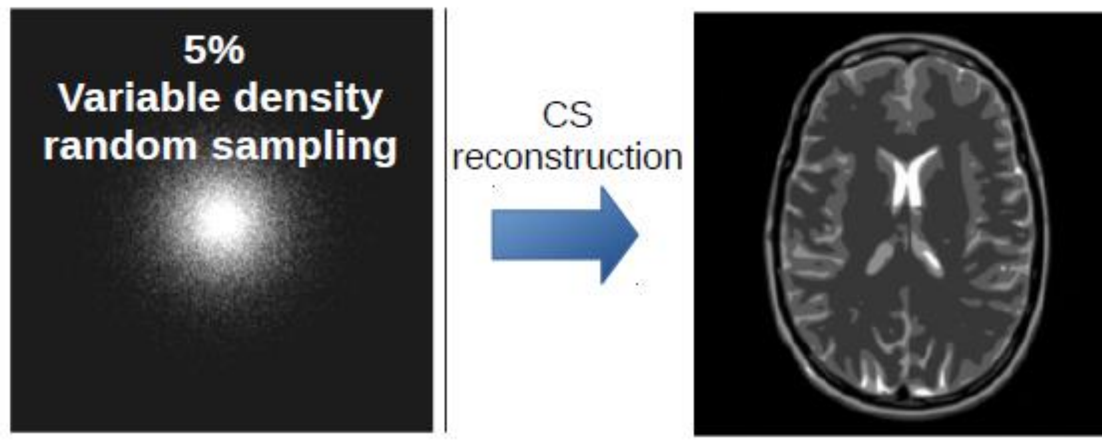

- ***... to a CS adapted to MRI***

- **CSMRI** [Lustig et al. 2008]
- **V**ariable **D**ensity **S**ampling [Puy et al. 2011]
- *Breaking the coherence barrier: A new theory for Compressed Sensing* [Adcock et al. 2013]

« The success of compressed sensing is resolution dependent »

CS-MRI AND EXISTING RESULTS

- CS must comply with MR hardware constraints

7T MRI

$$\vec{\kappa}(t) = \vec{\kappa}(0) + \gamma \int_0^t \vec{G}(u)du$$

$$\boxed{\begin{array}{c} \|G\| < G_{max} \approx 50\ mTm^{-1} \\ \|\dot{G}\| < \dot{G}_{max} \approx 333\ Tm^{-1}s^{-1} \end{array}}$$

➢ Regular trajectories

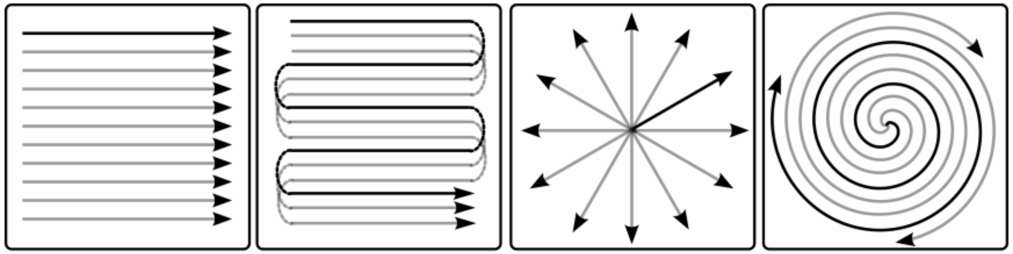

Lustig et al. 2008

- Easy implementation: undersampling standard MR trajectories!
  - Radial for cardiac cine MR imaging (Winkelmann et al. 2007)
  - Spiral or noisy spirals (Lustig et al. 2005)
  - Poisson disk sampling (Vasanawala et al. 2011)

CS-MRI AND EXISTING RESULTS

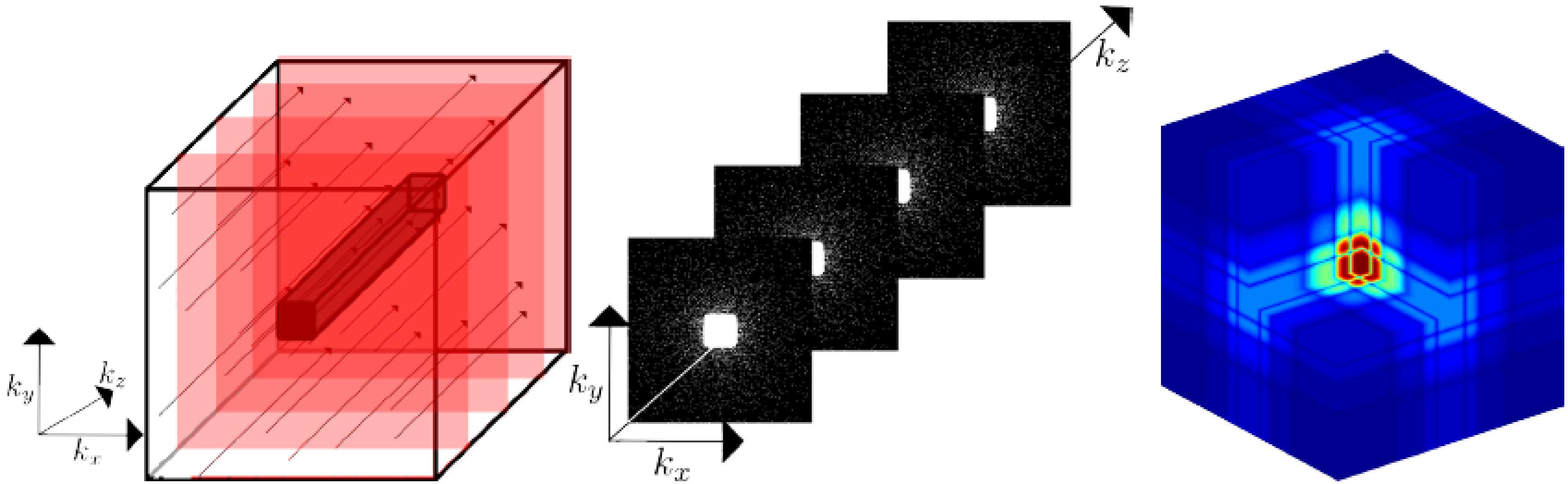

CS-MRI is sub-optimal! [Lustig et al., 2007]

- ➢ CS is not used to its full potential!
- Hindered randomness
- Variable density sampling not fulfilled
- K-space not well covered or oversampled in one direction

- ➢ Undersampling factor generally limited to : $\boxed{R \leq 10}$

NEED OF NEW MR UNDERSAMPLING SCHEMES

➢ New trajectories developed by Nicolas Chauffert during his PhD

- Projection of an image on a measure set of… points (image halftoning)

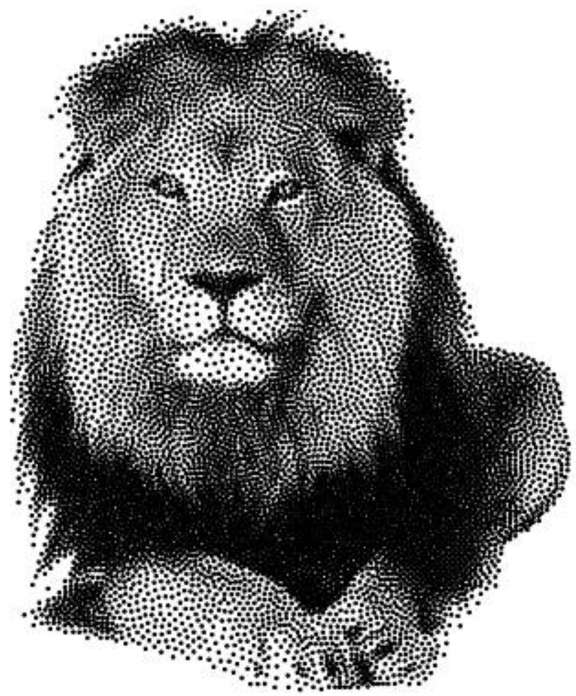

« Repulsion sampling »

✓ Target probability density

✓ Cinematic constraints

✓ Coverage speed

NEED OF NEW MR UNDERSAMPLING SCHEMES

➢ New image approximation techniques
[Chauffert et al, Construct. Approx., 2016]

- Projection of an image on a measure set of… curves (image stippling)

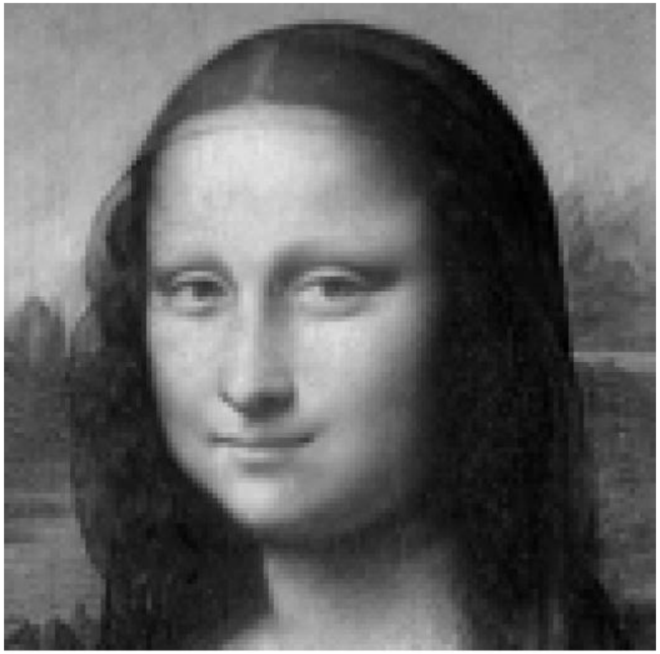

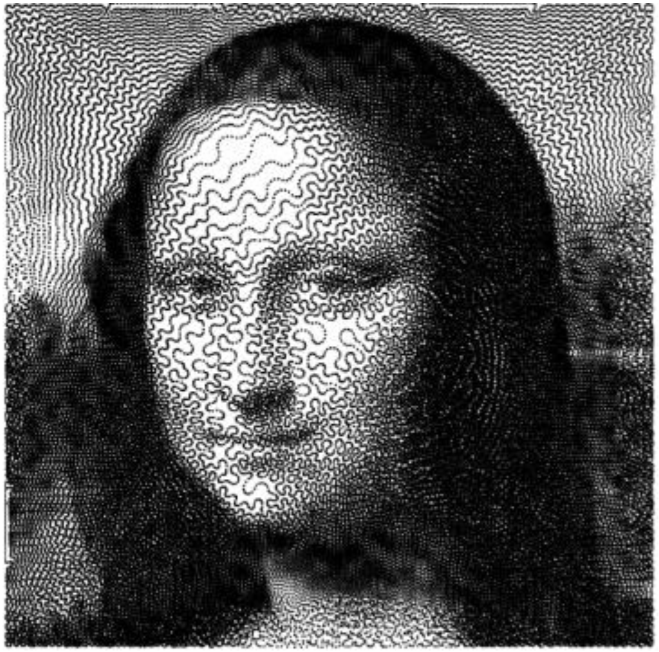

- ✓ Target probability density
- ✓ Cinematic constraints
- ✓ Coverage speed

NEED OF NEW MR UNDERSAMPLING SCHEMES

- Application to design of k-space trajectories

[Chauffert et al, IEEE TMI 2016; Chauffert et al, SIAM Imaging Sci 2016]

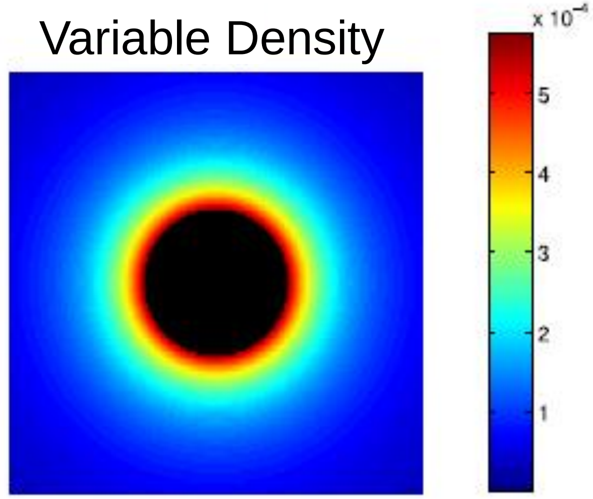

+

$$\|G\| < G_{max} \approx 50\ mTm^{-1}$$
$$\|\dot{G}\| < \dot{G}_{max} \approx 333\ Tm^{-1}s^{-1}$$

- ✓ Target probability density
- ✓ Gradient constraints
- ✓ Coverage speed

NEED OF NEW MR UNDERSAMPLING SCHEMES

➢ Application to design of k-space trajectories

[Chauffert et al, IEEE TMI 2016; Chauffert et al, SIAM Imaging Sci 2016]

- Projection of a target density on a measure set of… admissible curves for MRI

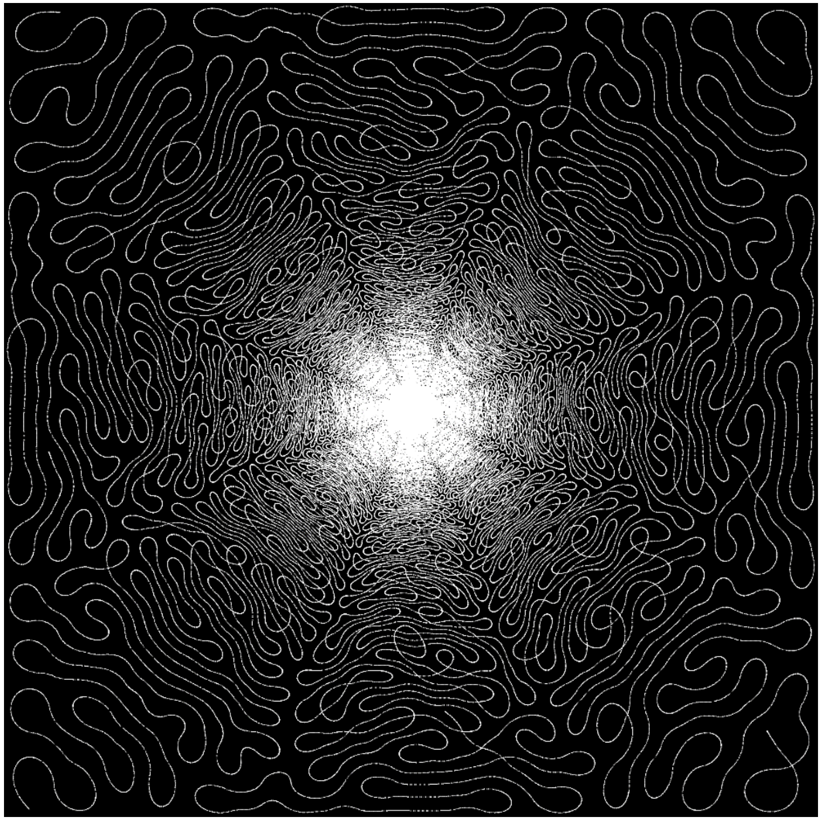

✓ Target probability density

✓ Gradient constraints

✓ Coverage speed

VERY HIGH RESOLUTION IMAGING: SIMULATION SETUP

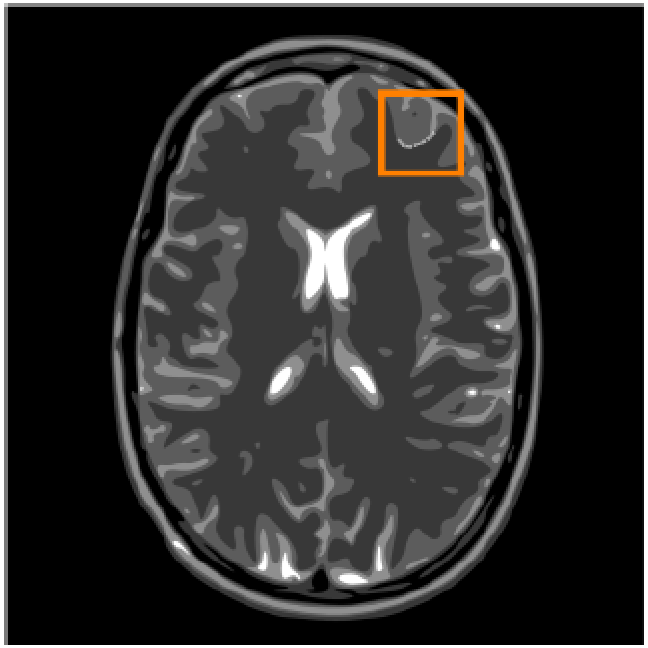

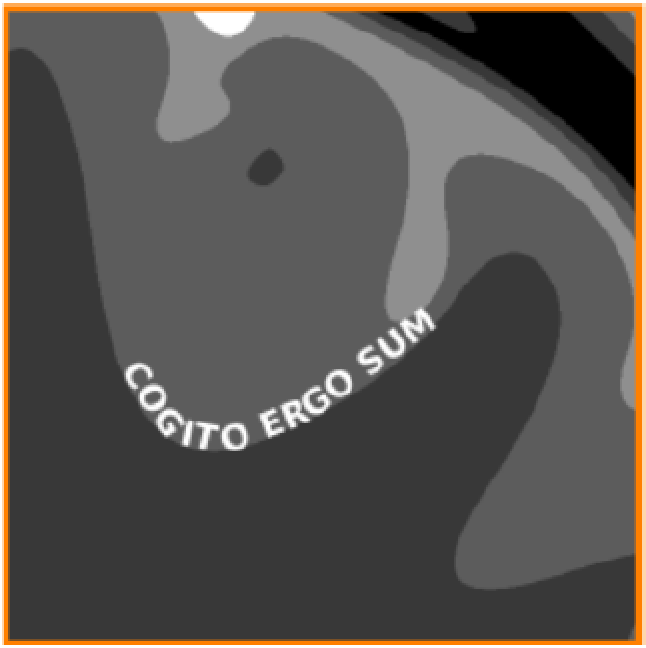

Parameters:

Image size: $n = 2048 \times 2048$ ($100\ \mu$m isotropic). $m = 0.048n$ decomposed in:

- 196 radial lines of 1, 024 equispaced samples
- 8 rotated versions of the same spiral made up by 25,000 samples
- 8 curves of 25,000 samples each

VERY HIGH RESOLUTION IMAGING: SIMULATION SETUP

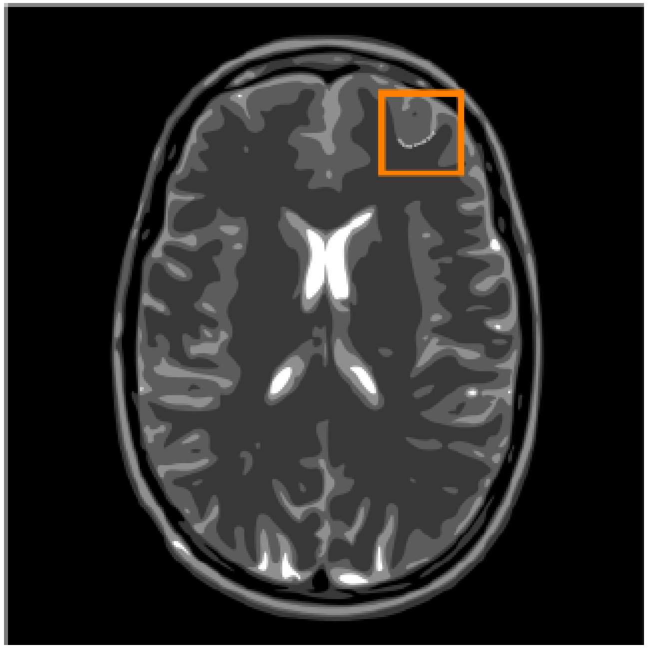

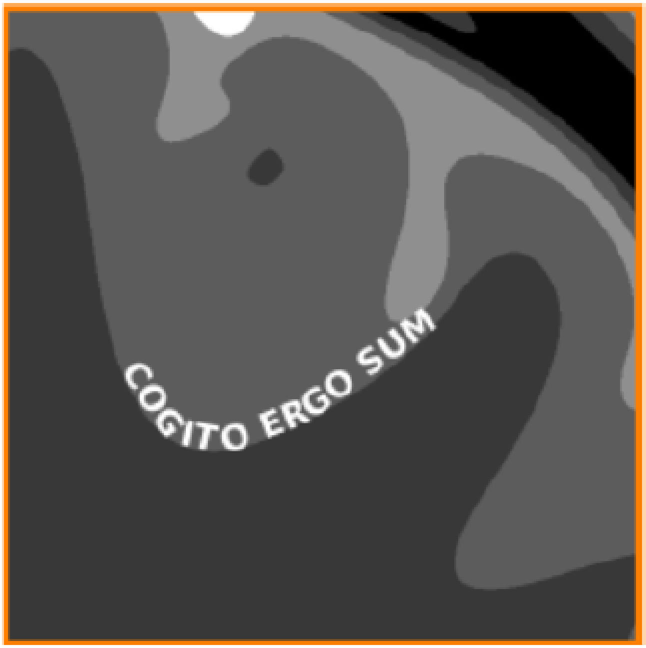

MRI hardware constraints:

- $G_{\text{max}} = 40\,\text{mT.m}^{-1}$ and $S_{\text{max}} = 150\,\text{mT.m}^{-1}.\text{ms}^{-1}$.
- For proton imaging, $\gamma = 42.57\,\text{MHz.T}^{-1} \implies \alpha = 1,703\,\text{m}^{-1}.\text{ms}^{-1}$ and $\beta = 6,386\,\text{m}^{-1}.\text{ms}^{-2}$.

VERY HIGH RESOLUTION IMAGING: COMPETING TRAJECTORIES (1/2)

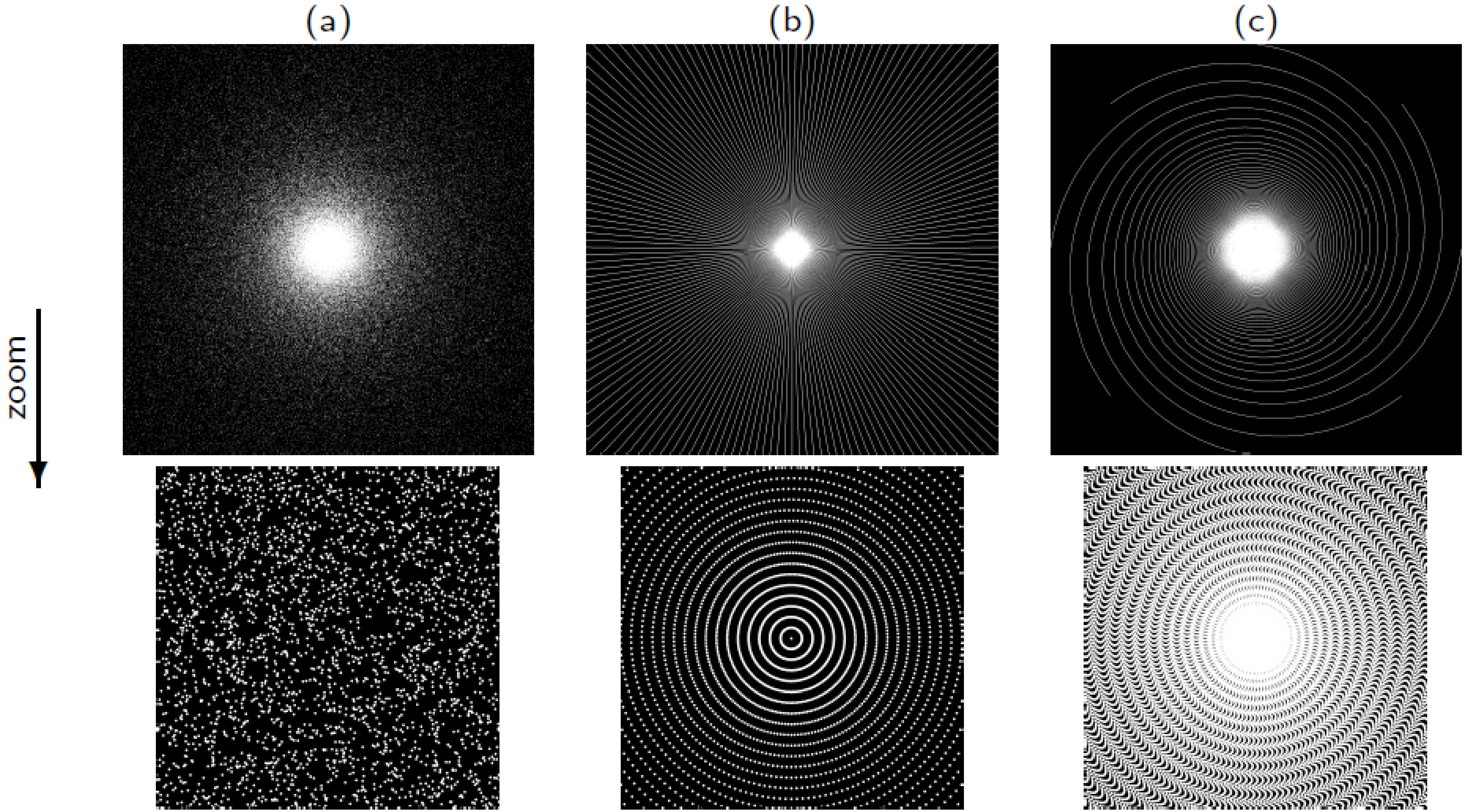

Figure : Standard sampling schemes composed of 200,000 samples. (a): i.i.d. drawings. (b): Radial lines; (c): 8 interleaved spirals.

VERY HIGH RESOLUTION IMAGING: COMPETING TRAJECTORIES (2/2)

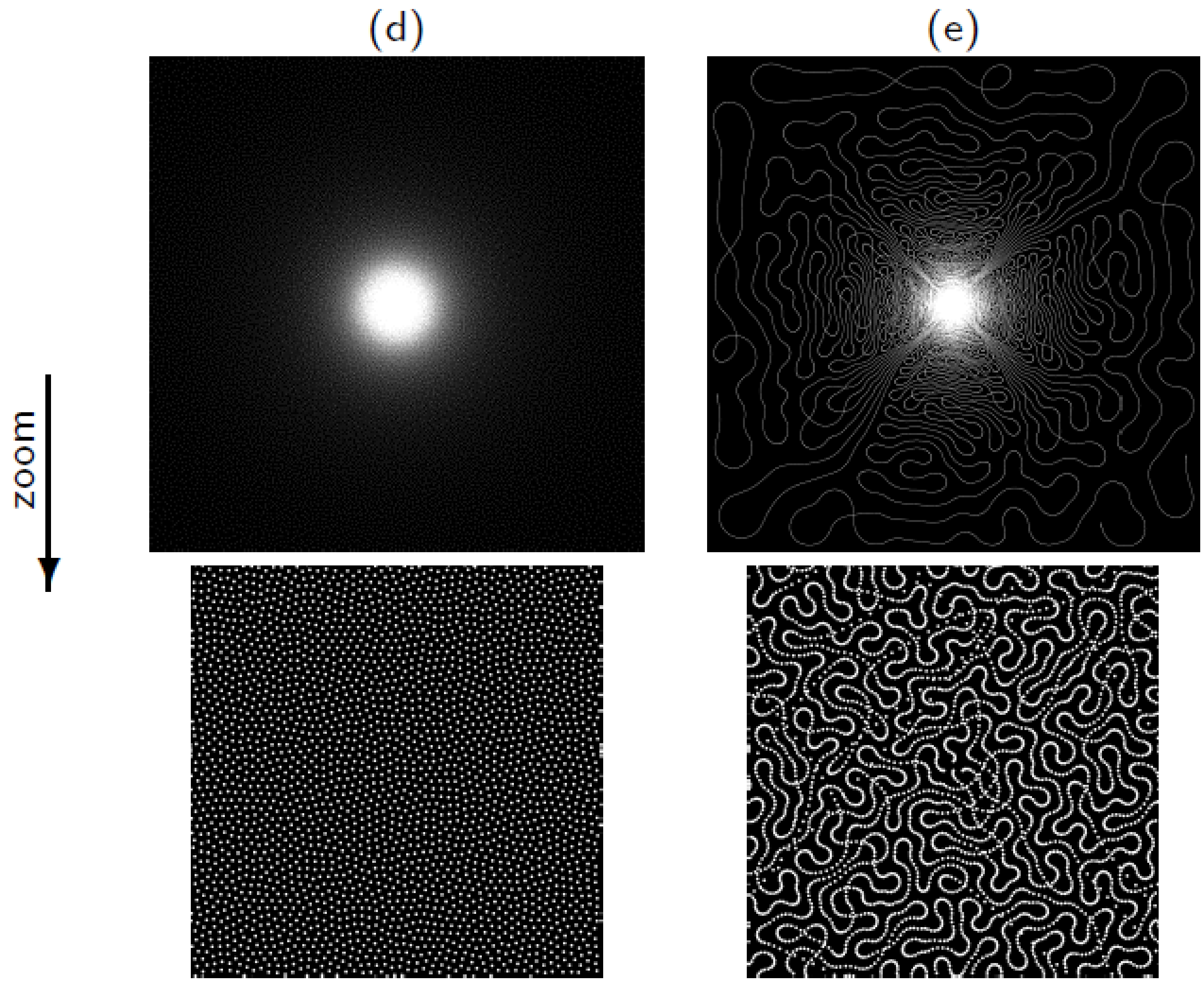

Figure : Sampling schemes yielded by our algorithm and composed of 200,000 samples. (d): isolated points with repulsion; (e): 8 feasible curves in MRI.

VERY HIGH RESOLUTION IMAGING CS RESULTS (1/2)

(a) SNR=26.7 dB (b) SNR=20.6 dB (c) SNR=21.0 dB

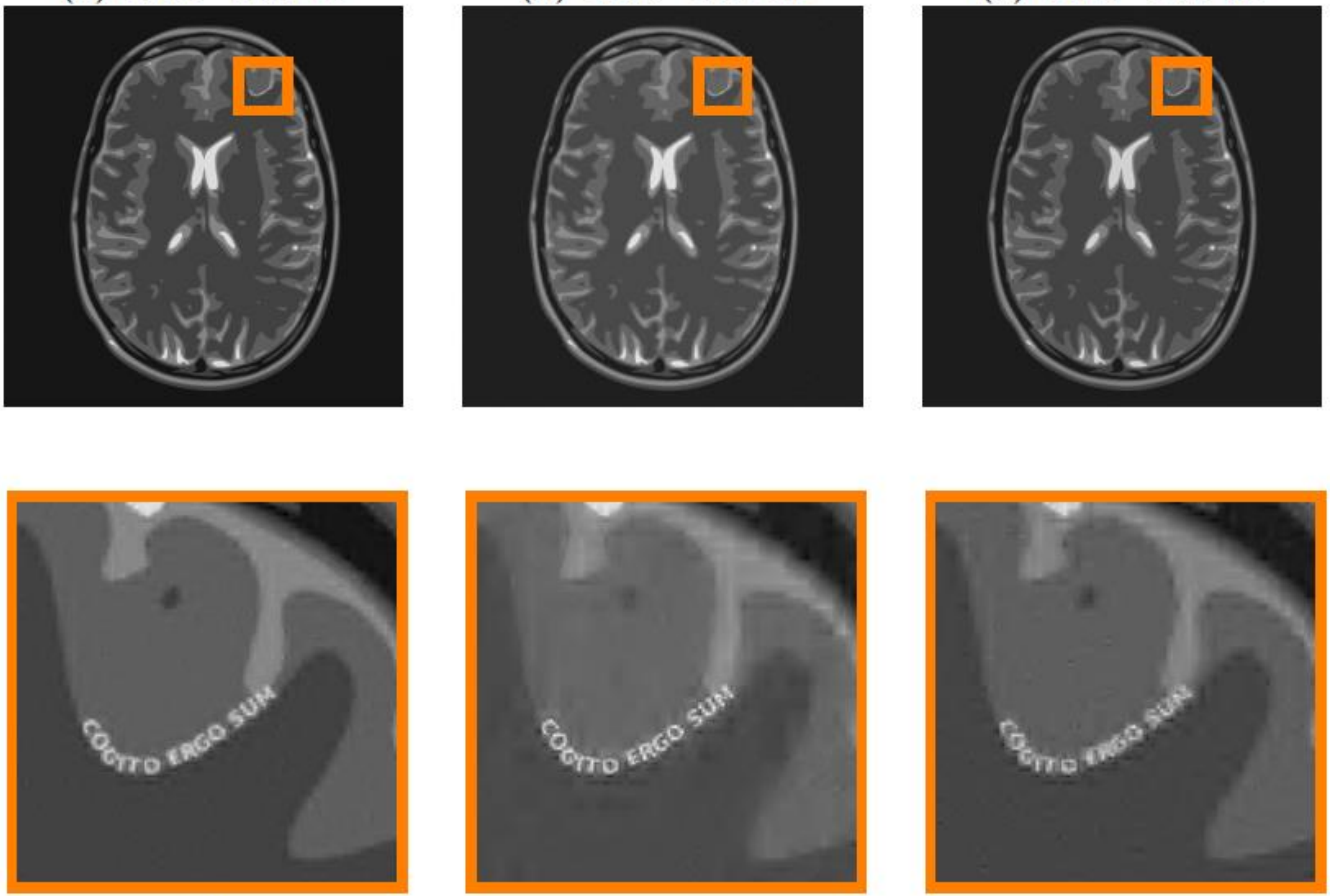

(i.i.d.) (radial) (spiral)

VERY HIGH RESOLUTION IMAGING CS RESULTS (2/2)

(d) SNR=27.0 dB　　(e) SNR=23.5 dB

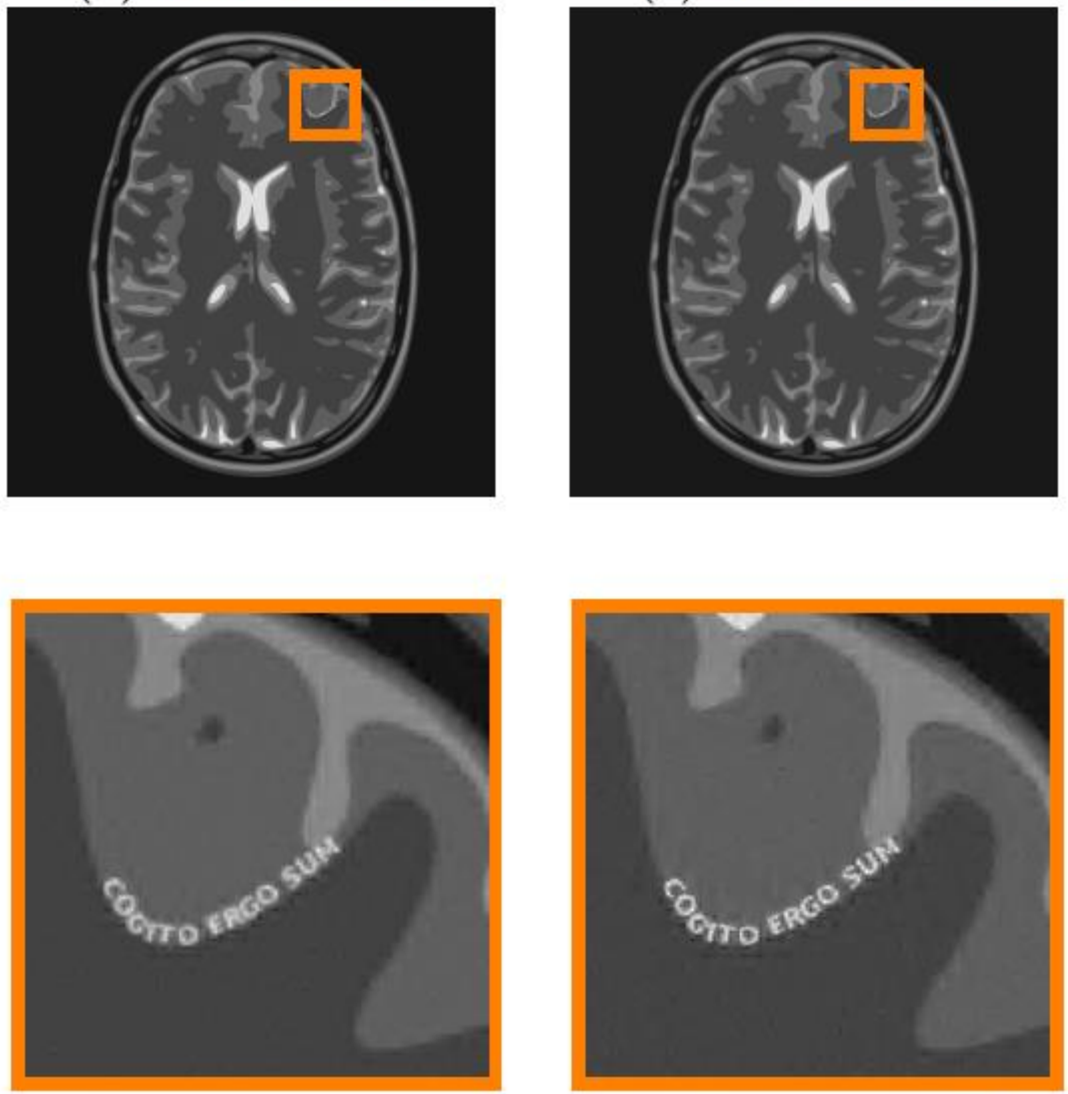

(m-points measure)　　(admissible curve for MRI)

CS SUMMARY

- Higher undersampling factor achievable at higher resolution: 20-fold acceleration/undersampling
- Better performance achieved in terms of image quality (SNR, pSNR, SSIM) using isolated points (projection on m-points measure)
- Projection on admissible curves for MRI outperforms radial and spiral sampling schemes